

# **HOST RESPONSES TO MICROGEL-BASED BIOMATERIAL INTERFACES**

A Dissertation  
Presented to  
The Academic Faculty

by

**Amanda Walls Bridges**

In Partial Fulfillment  
of the Requirements for the Degree  
Doctor of Philosophy in the  
Wallace H. Coulter Department of Biomedical Engineering

Georgia Institute of Technology  
Emory University  
December 2008

# HOST RESPONSES TO MICROGEL-BASED BIOMATERIAL INTERFACES

Approved by:

Dr. Andrés J. García, Advisor  
School of Mechanical Engineering  
*Georgia Institute of Technology*

Dr. Julia E. Babensee  
Department of Biomedical Engineering  
*Georgia Institute of Technology*

Dr. Ravi V. Bellamkonda  
Department of Biomedical Engineering  
*Georgia Institute of Technology*

Dr. Johnna S. Temenoff  
Department of Biomedical Engineering  
*Georgia Institute of Technology*

Dr. L. Andrew Lyon  
School of Chemistry and Biochemistry  
*Georgia Institute of Technology*

Date Approved: August 19, 2008

To my family, who teaches me love, humor, wisdom, strength, courage, and humility.

## ACKNOWLEDGEMENTS

First and foremost, I have to admit that obtaining a Ph.D. has been anything but easy, as the most challenging years of my life have surrounded its attainment. However, this journey has helped me grow not only as an engineer and researcher, but also as a person. I have met some great friends and had a lot of fun along the way.

I'd like to acknowledge everyone who played a role in this accomplishment, starting with my advisor, Dr. Andrés García. When I first met Andrés, he seemed quite calm and approachable. Over the years, however, I have heard countless hilarious anecdotes and witnessed the boisterous personality that is the man, the legend – Andrés. Somehow I have managed to eke out a Ph.D. without an embarrassing proper lab nickname. For that, I thank you Andrés. I realize that students frequently profess their respect for their advisors, but I truly admire mine for being a wonderful mentor. He has guided me through many difficult situations over the years, and I don't think I could ask for a more understanding leader.

I'd also like to thank my thesis committee members: Drs. Julia Babensee, Ravi Bellamkonda, Andrew Lyon, and Johnna Temenoff. They have given me great input and advice over the years, and my project has been strengthened because of them. In particular, our collaboration with Dr. Lyon has significantly improved my knowledge of all things chemistry, and I appreciate his willingness to attend our many last-minute meetings. In addition, I need to thank a few of Dr. Lyon's students, Dr. Neetu Singh and Toni Bonhivert, for their efforts with the infamous microgel coatings. Neetu piloted the material functionalization process, and Toni has recently taken over the project

seamlessly. I truly appreciate their accommodating nature, mass-producing samples for me in record time.

I can honestly say that life in the García lab has never been boring. Even the driest scientific content can be spruced up with just the right amount of quirkiness, which is found in any of the past or current lab members. Second only to Andrés in pure decibels, Kellie Burns is quite possibly the funniest and most competent lab manager Tech has ever seen. She can process reagent orders with lightning speed, keep the entire lab spotless, and brighten your day with hilarious commentary in Buffalo-meets-Reno 911 style. I've never met anyone with more Tech pride, owing to her hundreds of authentic GT t-shirts and paraphernalia. Among other things, I will remember Kellie for her love of lab lunch outings, her inability to handle sangria, the “phosphorylation” dating ad on Craigslist, and assisting with animal studies while singing Afroman.

I also have to thank some of the 1<sup>st</sup> Generation García lab members who impacted the initial stages of my research. Although my interactions with them were limited, Nate Gallant and Jeff Capadona are some of the nicest guys I've met. They also do quite well on the golf course. Kristin and Catherine cordially dealt with my nagging microscope questions and invited me for afternoon Starbucks runs to de-stress. As our former “lab mother,” Kristin always remembered our birthdays, and we also owe the ingenious design of the current García lab t-shirts to her. I will remember Charlie for his love of zinc fingers, his impressive laugh, and his will to succeed at everything. Ben K (a.k.a. Professor Keselowsky) will always be remembered for his keen eye of critical research-related details, including (but not limited to) trypsinization time, cell passaging over long weekends, Western blot voltage, and surgical suturing technique. Thank you, Ben, for

mentoring me in my first year and inviting me on the revered Taco Bell and gas station slushy runs in the pimp mobile. Joe Charest made some pretty amazing cell patterns, including the infamous bowtie, and I hear he's quite the Salsa dancer. Ms. Phillips (or Jenny Jenn as I affectionately call her and she affectionately hates) mentored me during my lab rotation, giving me insight into the late night research opportunities available in the García lab. From Jenn, I learned how to do Western blots, PCR, sterile culture of excessive cell numbers, extreme ambition, and the distinguished rule of science – nothing less than  $n = 100$  is acceptable! Jenn was my GRC roomie and fellow urbandictionary.com enthusiast.

The current García lab members (i.e. 2<sup>nd</sup> and 3<sup>rd</sup> Generation) keep me entertained on a daily basis. Tim Petrie (a.k.a. Mr. Fantastic) is, by far, the most unique scientist I've ever met. His traits include multi-tasking dozens of projects, pulling all-nighters by choice, romancing expensive lab equipment (Ms. Centrifuge and Ms. SPR), playing at least three intramural sports at a time, and leaving a Polaner's All Fruit strawberry jelly trail wherever he goes. Thank you, Tim, for all the wonderful mid-afternoon smells of tuna salad, bagels, and protein shakes emanating from your desk to mine. Sean is our resident Mr. International researcher, having done a cell patterning stint in Switzerland. Although he seems very sophisticated upon first glance, I believe there's a mad scientist within him. He continues to remind me that I act like one of the guys. I appreciate the small artifacts tossed from the infamous 1<sup>st</sup> Row dwellers, Sean and Dave, as a reminder that I'll never be quite as cool as them. Dave (a.k.a. D-train) is our resident lab Ginger, stated with utmost affection, and he is also the Spinning Disk Master. Dave is one of the hardest working students in the lab, and he always has excellent scientific input. Thank

you, Dave, for listening to all my stories over the years and giving me advice when needed. Abbey is the García lab Information Technologist, by choice of course. Abbey has been a good friend since recruitment weekend, and we've shared many a drink over the years. I thank you, Abbey, for always being in a good mood and cheering me up or giving me advice when needed, and thanks for not getting annoyed by my childish shoulder tapping. Ed, Rachel, Nduka, and Asha are the newest lab members. Thank you, Ed and Nduka, for helping me with hydrogels and SAMs during my crunch-time. Thank you, Rachel, for all your research assistance, and I appreciate our lively discussions of microgels, dogs, and last names. I hereby dub Asha (a.k.a. Shaw-tay) as the feistiest member of the García lab. Thank you, Asha, for keeping the 1<sup>st</sup> Row boys on their toes.

I also have to thank my fellow BMEs for all the 40<sup>+</sup> hr weekend study sessions over takeout food and caffeine. Since I had to spend 2 more years of my life taking classes, I am grateful to have done so with you all. I appreciated our Quals prep nights, which forced me to think on my feet. Thank you, Victoria, for encouraging us all to run a Half Marathon. I can't say it was easy (or necessarily fun), but I'm glad I experienced it with great friends. I thank Brock Wester for opening my eyes to Rocky Mountain Pizza trivia and showing us the ropes as newbies in Atlanta. Thank you, Priya, for your lovely vodka and brownies contributions to our parties. I have to especially thank Carolyn Sargent and Jesica McLane for their friendship. As stressful as weddings are, I'm glad the three of us went through it all together. Thanks for being wonderful bridesmaids and also throwing me one sweet bachelorette party (details not included). In particular, Carolyn has always given me a place to stay during my crazy traveling schedule, and I feel like part of her family. We have many common interests, including our love of good

wine and sweet dogs. We've also started many traditions including Champagne Monday (you should all try it), which always makes the week a little easier.

I'd like to thank other members of Wing 2D, as well. Maya and Reyhan have been my good friends for years, and we've had a lot of fun. Reyhan almost let me out-bowl him once – such a nice guy. Maya has become my outdoor companion, and we've shared many photography endeavors around Atlanta. She's a world traveler and an all-around great person. She even turned me into a Beer Snob (you must try the “banana beer” at Gordon Birsch).

Finally, I have to thank my family for all their encouragement throughout the years. I thank my husband infinitely for unexpectedly dealing with an extra-long distance relationship for 75% of my graduate career, and for trying to give me encouragement over the phone no matter how much it hurt to be apart. Thank you for allowing me to make school a priority, too. It's been extremely tough on both of us, but I hope we're stronger for enduring it. I have to thank my younger brother for reminding me in an affectionate way that I'm a big nerd and he got a real job before I did. My parents have always been there for me, and grad school has been no different. On many days, my mom has prescribed me a good glass of wine to relax and lent an ear to listen. She has always been my role model, and she is probably the strongest and most resilient person I know. I also have to thank my new family of in-laws. My younger brother-in-law and niece constantly remind me that life is amazing and the simple things are really important. I thank my mother-in-law for countless words of wisdom over the years, including “you better finish that degree!” She is sadly missed, and I wish that she could have seen me finish this degree.



**To all – I hope that, at some point over the years, I have made you laugh.  
Life is too short to be serious constantly. Learn something every day, and enjoy  
those around you. Simple advice.**

## TABLE OF CONTENTS

	Page
ACKNOWLEDGEMENTS	iv
LIST OF TABLES	xiv
LIST OF FIGURES	xv
LIST OF ABBREVIATIONS	xvii
SUMMARY	xx
<u>CHAPTER</u>	
1 INTRODUCTION	1
2 LITERATURE REVIEW: INFLAMMATORY RESPONSES TO BIOMATERIALS	6
Host foreign body response	6
Chemical mediators of inflammation	8
Protein adsorption and cell adhesion	11
Integrins in inflammation	12
Macrophage as central regulator of inflammation	15
Hydrogel materials for biomedical and biotechnological applications	17
3 LITERATURE REVIEW: ANTI-INFLAMMATORY POLYMERIC COATINGS FOR IN VIVO SENSORS	19
Inflammation and device performance	19
Anti-inflammatory coating strategies	20
I. <i>Passive strategies: non-fouling surface treatments</i>	20
II. <i>Microgel-based implant coatings</i>	23
III. <i>Active strategies: delivery of anti-inflammatory agents</i>	26
Existing considerations and future prospects	30

4	ROLE OF PLASMA FIBRONECTIN IN THE FOREIGN BODY RESPONSE TO BIOMATERIALS	32
	Introduction	32
	Materials and Methods	34
	<i>pFN conditional knockout mice</i>	34
	<i>Biomaterial implantation and analysis</i>	35
	<i>Statistical analysis</i>	35
	Results	36
	Discussion	43
	Conclusion	45
5	REDUCED ACUTE INFLAMMATORY RESPONSES TO MICROGEL CONFORMAL COATINGS	46
	Introduction	46
	Materials and Methods	48
	<i>Sample preparation</i>	48
	<i>Biomaterial surface characterization</i>	49
	<i>Fibrinogen adsorption</i>	49
	<i>Primary human monocyte isolation and culture</i>	50
	<i>In vitro murine and human macrophage adhesion</i>	52
	<i>Murine intraperitoneal implantation</i>	53
	<i>Immunofluorescence staining of adherent cells</i>	53
	<i>Intracellular cytokine staining and flow cytometric analysis</i>	54
	<i>Statistical analysis</i>	56
	Results	56
	<i>Deposition of microgel particles as conformal coatings</i>	56
	<i>Fibrinogen adsorption studies</i>	59

	<i>In vitro leukocyte adhesion</i>	60
	<i>Acute inflammatory cell responses to microgel coatings</i>	64
	Discussion	69
	Conclusion	74
6	CHRONIC INFLAMMATORY RESPONSES TO MICROGEL-BASED IMPLANT COATINGS	75
	Introduction	75
	Materials and Methods	77
	<i>Sample preparation</i>	77
	<i>Subcutaneous implantation</i>	79
	<i>Histological staining of explants</i>	79
	<i>Statistical analysis</i>	80
	Results	81
	<i>Fibrous capsule formation surrounding implants</i>	81
	<i>Inflammatory cell profile at the implant interface</i>	84
	Discussion	87
	Conclusion	96
7	FUTURE CONSIDERATIONS	97
	Base microgel coatings	97
	Bioactive microgel coatings	98
	APPENDIX A: COVALENT TETHERING OF FUNCTIONAL MICROGEL FILMS ONTO POLY(ETHYLENE TEREPHTHALATE) SURFACES	103
	Introduction	103
	Materials	106
	Methods	107

<i>Microgel synthesis</i>	107
<i>PET film functionalization</i>	108
<i>Carboxyl group determination</i>	109
<i>Particle deposition</i>	109
<i>Atomic force microscopy</i>	110
<i>In vitro cell adhesion</i>	110
Results and Discussion	111
Conclusion	117
REFERENCES	119

## LIST OF TABLES

	Page
Table 3.1: Examples of non-fouling ethylene glycol-based surface treatments	25
Table 3.2: Active surface treatments for biomaterial coatings	28

## LIST OF FIGURES

	Page
Figure 2.1: Events of host foreign body response to implanted materials	6
Figure 3.1: Passive anti-inflammatory surface coating for biomaterials	22
Figure 3.2: Bioactive implant coatings to deliver anti-inflammatory molecules	27
Figure 4.1: Levels of plasma fibronectin determined by Western blot analysis	37
Figure 4.2: Leukocyte adhesion to implanted biomaterials	38
Figure 4.3: Fibrous encapsulation of subcutaneously implanted biomaterials	39
Figure 4.4: Biomaterial-associated macrophages and FBGC determined by immunohistochemistry	41
Figure 4.5: Immunohistochemical staining for FN in fibrous capsules	42
Figure 5.1: Surface characterization of biomaterials	58
Figure 5.2: Topography of biomaterial surfaces	59
Figure 5.3: Protein adsorption profiles on biomaterial surfaces	60
Figure 5.4: Murine IC-21 macrophage adhesion to biomaterial surfaces	62
Figure 5.5: <i>In vitro</i> human primary macrophage adhesion to biomaterial surfaces	63
Figure 5.6: <i>In vivo</i> leukocyte adhesion to implanted biomaterials	65
Figure 5.7: Quantification of <i>in vivo</i> intracellular cytokine expression by flow cytometric analysis	68
Figure 6.1: Fibrous encapsulation of implanted biomaterials	83
Figure 6.2: Immunostaining of capsule-associated macrophages and foreign body giant cells	86
Figure 7.1: Bioactive microgel coating presenting tethered bioadhesive motifs of P2 or RGD to elucidate integrin-dependent macrophage behaviors	100
Figure 7.2: Stimuli-responsive microgel coatings to dynamically present biological molecules targeting inflammatory cells	102

Figure A.1: Strategy for covalent tethering of microgels onto a poly(ethylene terephthalate) surface	106
Figure A.2: Absorption spectra for desorbed Toluidine Blue O dye	112
Figure A.3: 3D rendering of AFM images	113
Figure A.4: Effects of benzophenone modification and photo-crosslinking on microgel functionalization process	115
Figure A.5: Macrophage adhesion to biomaterial surfaces	117



## LIST OF ABBREVIATIONS

$\alpha_M\beta_2$	leukocyte-specific integrin (CD11b/CD18, Mac-1)
$\alpha$ -MSH	$\alpha$ -melanocyte stimulating hormone
AFM	atomic force microscopy
ANOVA	analysis of variance
BSA	bovine serum albumin
C3	complement factor 3
cFN	cellular fibronectin
CSF	colony stimulating factor
DEX	dexamethasone
DNA	deoxyribonucleic acid
EG <sub>3</sub> SAM	tri(ethylene glycol)-terminated self-assembled monolayer
ELISA	enzyme-linked immunosorbent assay
ELP	elastin-like polypeptide
EU	endotoxin units
FBGC	foreign body giant cell
FBR	foreign body response
Fc	fragment crystallizable region of antibody
FDA	Food and Drug Administration
Fg	fibrinogen
FN	fibronectin
FSC	forward scatter
IACUC	institutional animal care and use committee
IFN	interferon

IgG	immunoglobulin G
IL	interleukin
IP	intraperitoneal
LAD-1	leukocyte adhesion deficiency type 1
LCST	lower critical solution temperature
LGC	Langhans-type giant cell
MAF	macrophage activating factor
MCP	monocyte chemotactic protein
MIF	migration inhibition factor
MMR	macrophage mannose receptor
P1	$\gamma$ 190-202 sequence of fibrinogen
P2	$\gamma$ 377-395 sequence of fibrinogen
pAAC	poly(acrylic acid)
PBS	phosphate buffered saline
PCR	polymerase chain reaction
PEG	poly(ethylene glycol)
PEO	poly(ethylene oxide)
PET	poly(ethylene terephthalate)
pFN	plasma fibronectin
PGE	prostaglandin E
pI-pC	polyinosinic-polycytidic acid
PMN	polymorphonuclear cell
pNIPAm	poly( <i>N</i> -isopropyl acrylamide)
SAM	self-assembled monolayer
SODm	superoxide dismutase mimetic

SSC	side scatter
TGF	transforming growth factor
TNF	tumor necrosis factor
UV	ultraviolet
XPS	x-ray photoelectron spectroscopy

## SUMMARY

Although medical devices and biomaterial implants are used clinically in a variety of applications, the process of implanting them damages local tissue and initiates a localized non-specific inflammatory response that is detrimental to device performance. Extensive research efforts have focused on developing material surface treatments and systems to deliver anti-inflammatory agents to prevent biofouling and abrogate biomaterial-mediated inflammation. Traditional surface modification strategies are capable of reducing protein adsorption and cell adhesion *in vitro*; however, their use as long-term implant coatings is limited due to reduced non-fouling behavior, continued inflammation and fibrous encapsulation. This work aims to address these limitations by developing a novel and versatile implant coating with non-fouling properties using a system based on hydrogel microparticles (i.e. microgels), which offers many material advantages over current methods. The **overall objective** of this project was to evaluate host responses to these microgel coatings. Using the **rationale** that macrophages are the key mediators of inflammatory and regenerative responses our **central hypothesis** was that macrophage adhesion and subsequent activities can be modulated, and the intensity of the foreign body response to biomaterials can be reduced using these novel coatings.

As a first step toward testing this hypothesis, we characterized the surface properties of the microgel coatings using multiple techniques. Microgel coatings were synthesized from poly(*N*-isopropyl acrylamide)-*co*-acrylic acid covalently crosslinked with poly(ethylene glycol)-diacrylate and deposited onto a clinically relevant substrate, poly(ethylene terephthalate). We found that microgel coatings can be successfully

deposited using a simple spin coating technique, and the incorporation of a photoaffinity label enables covalent attachment to the substrate and enhances long-term stability. We have confirmed the presence of nitrogen-rich pNIPAm microgel particles on the surface of PET and generated a homogeneous monolayer coating. Microgel particles effectively covered material defects commonly present on the surface of the underlying PET substrate. The ability to generate conformal and complete microgel coatings on heterogeneous/rough, biomedically relevant materials is a major advantage of this strategy over existing polymer chain grafting approaches. Importantly, using radiolabeled protein assays, we determined that microgel-coated samples also adsorbed significantly lower levels of human fibrinogen compared to unmodified PET controls.

Further characterization of these materials involved the evaluation of cellular responses using an *in vitro* culture system to model acute leukocyte interactions with biomaterial surfaces. Macrophages were cultured for 48 h on biomaterials, and adherent cells were imaged and scored for viability, adherent density, and spreading area. We demonstrated that microgel coatings significantly reduced the adhesion and spreading of macrophages compared to PET controls using a murine macrophage cell line, as well as primary human blood-derived monocytes. The low levels of *in vitro* cell adhesion and spreading combined with the protein adsorption-resistance characteristics on the microgels provide indirect evidence that these coatings impart non-fouling properties to biomaterial supports.

Implanted materials were then evaluated for early cellular responses in the intraperitoneal cavity of mice, a rigorous model of acute inflammation. Analyses of explanted biomaterials using immunofluorescence staining techniques revealed that

microgel-coated samples significantly reduced the density of surface-adherent cells; additionally, fewer CD68<sup>+</sup> macrophages were observed on these samples. Moreover, adherent cells were harvested and immunostained intracellularly for a panel of inflammatory cytokines (TNF- $\alpha$ , MCP-1, IL-1 $\beta$ , and IL-10), and were then analyzed by flow cytometry to quantify relative cytokine levels. We demonstrated that microgel-coated samples exhibited significantly lower levels of pro-inflammatory cytokines in adherent leukocytes compared to unmodified PET, indicating that these coatings modulate cellular pro-inflammatory activities. Microgel-coated samples did not elicit pro-inflammatory cytokine expression beyond levels associated with the surgical procedure (sham group); therefore, increased cytokine expression was associated with leukocyte adhesion to the implanted PET biomaterial. These reductions of *in vivo* leukocyte adhesion and pro-inflammatory cytokine expression associated with the microgel coating contrasts with results of other non-fouling surface treatments.

Finally, we used an established model of chronic inflammation to evaluate these coatings for their efficacy at longer implantation time points. Unmodified PET controls, microgel-coated samples, and EG<sub>3</sub> SAMs were implanted subcutaneously for 4 wk. Explants were processed histologically and stained for various markers. Collagen staining demonstrated that the microgel coatings significantly reduced fibrous capsule thickness, and those capsules appeared less compact and structurally ordered than PET controls. Microgel-coated samples also contained significantly fewer total cells within the capsule. Additional sections were stained for the macrophage marker CD68 using immunohistochemical methods to determine the inflammatory cellular profile at the cell-material interface. Unexpectedly, microgel-coated samples contained proportionately

more CD68+ cells (relative to total cell numbers) than PET controls. Sections were also scored for multinucleated FBGC, but no significant differences were found among treatment groups.

In summary, this research has established a simple and reproducible method of surface functionalization to create effective coatings that resist protein adsorption and leukocyte adhesion. Collectively, these results demonstrate that microgel particles can be applied as relatively stable implant coatings to modulate inflammation and achieve more desirable host responses *in vivo* with the potential to extend implant lifetime. This work is *innovative* because it applies hydrogel particles to the development of a novel micro-scale implant coating. Our strategy offers unique control over synthesis parameters with the possibility of generating complex coatings onto a variety of biomedically-relevant materials. Furthermore, this research provides the foundation for developing a hydrogel-based coating system incorporating various bioactive signaling agents within a low-fouling background. Such a system will support controlled interactions with inflammatory cells, which will enable unprecedented regulation of host responses to implanted biomaterials.

# CHAPTER 1

## INTRODUCTION

Medical devices and biomaterial implants are used clinically in a variety of applications, and their performance is critical to a patient's overall health and quality of life. During implantation, surgical procedures injure microvasculature and surrounding tissues, initiating a localized inflammatory response.<sup>1</sup> Although inflammation recruits native cells for remodeling and regenerating damaged tissue, persistent inflammatory stimuli significantly interfere with implant function and often result in device failure. Adverse host responses to implanted biomedical devices include thrombogenic responses on vascular grafts,<sup>2, 3</sup> degradation and stress cracking of pacemaker leads,<sup>4, 5</sup> tissue fibrosis surrounding mammary prostheses,<sup>6</sup> osteolysis and loosening of orthopaedic joint prostheses,<sup>7, 8</sup> reactive gliosis around neural probes,<sup>9</sup> and degradation in biosensor function.<sup>10</sup>

The host response to implanted biomaterials and tissue-engineered constructs is regulated largely by cell-material interactions. Immediately following implantation, proteins and other biomolecules present in the blood plasma and biological fluids rapidly adsorb onto the surface of biomaterials. This process occurs more rapidly than cell recruitment to the implantation site, and this complex protein milieu serves as an adhesive substrate supporting integrin receptor-mediated attachment of inflammatory leukocytes.<sup>11-13</sup>

Persistent inflammatory stimuli lead to insufficient healing of local tissue at the device interface. Macrophages fuse and form multinucleated FBGCs,<sup>14, 15</sup> which have



been implicated in biodegradation of polymeric implants.<sup>16, 17</sup> Additionally, fibroblasts recruited to the implant site generate a collagenous fibrous capsule around the implant. Long-term tissue fibrosis is particularly limiting for interactive implants such as biosensors, biomedical leads and electrodes, encapsulated cells, and drug delivery systems, because it impedes exchange of nutrients and cellular byproducts with the surrounding medium.<sup>10, 18-24</sup>

Extensive research efforts have focused on modifying material properties via surface treatments to generate more biocompatible implants, with the goal of appropriately integrating the device without eliciting undesirable effects.<sup>25</sup> Traditional strategies have aimed to develop non-fouling surface treatments to prevent protein adsorption and leukocyte adhesion (i.e. biofouling). Several passivation strategies have been explored to achieve this goal, including preadsorption of material surfaces with less inflammatory proteins or cells.<sup>26-28</sup>

Thin-layer polymeric coatings offer more substantial routes to reduce acute inflammatory responses, and these have been applied as molecularly thin SAMs, polymer brushes, and thin or bulk hydrogels. While these systems have indeed reduced biofouling and inflammation, significant limitations persist. SAMs are limited by lack of stability and mechanical properties, and their use is confined to a limited number of material substrates.<sup>29, 30</sup> Polymer brushes also have limitations, including uncontrolled/insufficient grafting density or the requirement of an initiator on the material surface when using “grafting to” and “grafting from” methods, respectively.<sup>31, 32</sup> Extensive research efforts have focused on hydrogel-based implant coatings, which offer many advantages over traditional surface modification strategies, including a viscoelastic network structure,

tunable material characteristics, incorporation of multiple chemical functionalities, nano-scale dimensions with complex architectures, and the ability to deposit onto a variety of material substrates.<sup>33-37</sup> Many of these techniques have effectively reduced protein adsorption and cell adhesion *in vitro*; however, they suffer from inadequate long-term stability and have only marginally reduced inflammation *in vivo*. Despite considerable research efforts, surface coatings that eliminate biofouling and fibrous encapsulation over the lifetime of a device have not been attained.

Microgels are colloiddally stable hydrogel particles that retain many of the same material properties as their macrogel counterparts, including phase transition behavior and a viscoelastic network structure that enables mass transport.<sup>38</sup> However, they offer many advantages over traditional hydrogel materials, such as colloidal stability, unique control over synthesis parameters, and the ability to incorporate co-monomers or biomolecules to achieve desirable properties.

In this work, microgel coatings were synthesized from poly(*N*-isopropyl acrylamide)-*co*-acrylic acid covalently crosslinked with PEG-diacrylate and deposited onto a clinically relevant substrate, PET. The ***overall objective*** of this project was to evaluate host responses to these microgel coatings. Using the ***rationale*** that macrophages are the key mediators of inflammatory and regenerative responses our ***central hypothesis*** was that macrophage adhesion and subsequent activities can be modulated, and the intensity of the foreign body response to biomaterials can be reduced using these novel coatings. The overall objective was accomplished by testing our central hypothesis according to the following ***specific aims***:

**Aim 1: Characterize the surface properties of microgel coatings and evaluate *in vitro* inflammatory cell responses to these materials.**

Our *working hypothesis* was that PEG-based microgel coatings will significantly reduce *in vitro* material biofouling. PNIPAm-*co*-PEG microgel particles were synthesized via free radical precipitation polymerization, deposited onto PET disks using a spin coating process, and covalently cross-linked onto the substrate. We characterized these coatings using the surface techniques XPS and AFM to identify chemical characteristics of the material and determine uniformity of the coating. Using radiolabeled human fibrinogen, we determined the extent of protein adsorption to our model surfaces. We also tested this hypothesis using *in vitro* culture systems, including an established murine macrophage cell line and isolated primary human monocytes, to determine the efficacy of microgel coatings in reducing cell adhesion.

**Aim 2: Evaluate *in vivo* acute and chronic host responses to microgel coatings.**

Our *working hypothesis* was that the addition of microgel-based coatings to the surface of PET would modulate *in vivo* host responses by reducing leukocyte adhesion and subsequent cellular activity and limiting long-term fibrosis. We first tested this hypothesis by implanting samples in the intraperitoneal cavity of mice to mimic acute inflammation. Explants were evaluated to determine the extent of leukocyte adhesion using immunofluorescence staining methods. In addition, we investigated the inflammatory activity of these cells by staining them for a panel of pro- and anti-inflammatory cytokines and then quantifying expression using flow cytometric analysis. An established model of chronic inflammation was used to evaluate long-term host

responses to microgel coatings implanted in subcutaneous pockets of rat dorsa. Explants were processed histologically and stained to determine the extent of fibrous encapsulation and to quantify levels of capsule-associated macrophages and foreign body giant cells implicated in ongoing foreign body reactions and long-term material degradation.

This work is *innovative* because it applies hydrogel particles to the development of a novel micro-scale implant coating. Furthermore, this research provides the foundation for developing a hydrogel-based coating system incorporating various bioactive signaling agents within a low-fouling background. Such a system will support controlled interactions with inflammatory cells, which will enable unprecedented regulation of host responses to implanted biomaterials. Our microgel-based coating strategy offers *significant* advantages over traditional surface treatments including (i) precise control of synthesis parameters in terms of particle composition and structure, (ii) the ability to generate complex architectures and/or functionalities, including controlled drug release, (iii) the ability to generate complex mosaic-like coatings containing variations in particle composition and/or spatial arrangement, and (iv) deposition onto a variety of material substrates, including biomedically-relevant materials.

## CHAPTER 2

### LITERATURE REVIEW: INFLAMMATORY RESPONSES TO BIOMATERIALS

#### Host Foreign Body Response

*Biocompatibility* is typically defined as the ability of a material or device to perform with an appropriate host response in a specific application;<sup>25</sup> the biocompatibility of a material with tissue has generally been described in terms of acute and chronic phase inflammatory responses.<sup>39</sup> Surgical procedures injure microvasculature and tissue surrounding the implanted device, initiating a localized non-specific inflammatory response (**Figure 2.1**).<sup>1</sup> The severity and extent of the response to an implanted material directly affects the probability for its successful integration.

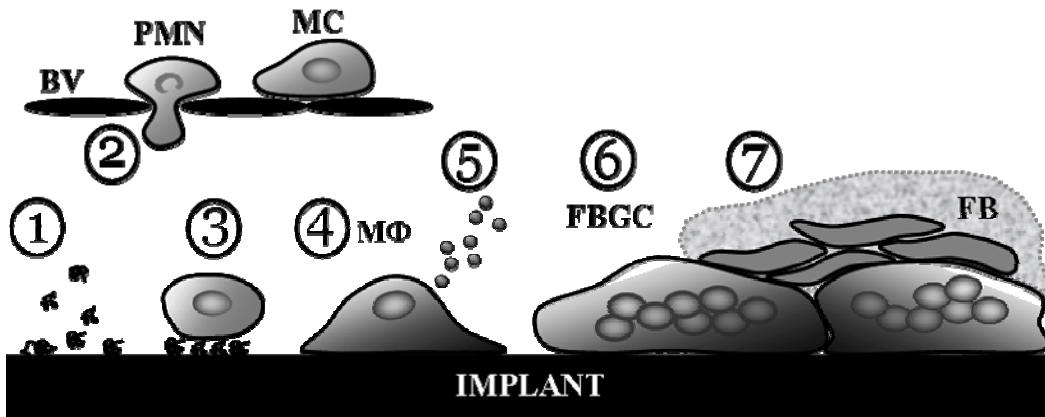


**Figure 2.1: Events of host foreign body response to implanted materials.** Neutrophils and monocytes recruited by stimulatory cues emigrate from the vasculature and adhere to the layer of adsorbed proteins on the implant surface (phases 1-3). Differentiated macrophages become activated, secreting a variety of inflammatory mediators, and often fuse into multinucleated foreign body giant cells (phases 4-6). Fibroblasts infiltrate the site and generate a collagenous fibrous capsule around the implant (phase 7). BV: blood vessel, PMN: polymorphonuclear leukocyte, MC: immature monocyte, MΦ: differentiated macrophage, FBGC: multinucleated foreign body giant cell, FB: fibroblast.

*Acute inflammation* comprises the primary sequence of events following implantation, and it typically characterizes the first 24 to 48 hours of this reaction (phases 1-5 in **Figure 2.1**). Immediately following implantation, proteins and other biomolecules present in the blood plasma and biological fluids rapidly adsorb onto the surface of biomaterials. This process occurs more rapidly than cell recruitment to the implantation site; therefore, the composition and configuration of this complex protein milieu dictates subsequent cellular responses.<sup>11-13</sup> During this phase of the inflammatory response, stimulatory signals at the site of implantation initiate integrin receptor-mediated leukocyte recruitment, adhesion to the implant surface, and activation.<sup>40-42</sup> Although injury initiates the inflammatory response, chemicals released from plasma, cells, and injured tissue continue to mediate the response proximal to the implant and determine the overall local tissue response.<sup>39, 43</sup>

Short-lived polymorphonuclear leukocytes (e.g. neutrophils) initially release damaging lysosomal proteases and oxygen-derived free radicals locally<sup>1, 44</sup> but are then replaced by inflammatory monocytes and macrophages.<sup>39</sup> The layer of surface-adsorbed proteins modulates macrophage phenotype and subsequent functions, including phagocytosis, cytokine expression, and fusion into foreign body giant cells (FBGCs).<sup>12, 13</sup> Professional phagocytes macrophages are considered the key mediators of implant-associated inflammation due to their distribution and motility, and their ability to generate a multitude of biologically active products.<sup>45-47</sup> They play central roles in directing both inflammatory and regenerative responses associated with implanted biomaterials.<sup>48-50</sup>

Persistent inflammatory stimuli lead to insufficient healing of local tissue at the device interface. The hallmark of a chronic response is fusion of monocyte-derived macrophages to form multinucleated FBGCs,<sup>1, 39</sup> a complex process involving numerous molecules (phase 6 in **Figure 2.1**).<sup>14, 15</sup> FBGCs have been implicated in biodegradation of polymeric implants through surface oxidation and enzymatic degradation.<sup>16, 17, 51</sup> Additionally, fibroblasts recruited to the implant site generate a thick fibrous capsule around the implant (phase 7 in **Figure 2.1**). This process is differentiated from the normal healing response, in which fibroblasts and vascular endothelial cells at the implant site proliferate and deposit a bed of collagen to create soft, pink granular tissue. The latter wound healing response is dependent on the level of tissue damage from surgical incision and the ability of cells to regenerate the local area, but this usually results in fibrosis and scar tissue formation. These cellular and tissue responses often impair *in vivo* device performance, and the extent of the host FBR to a biomaterial or implanted device depends largely on the form and topography of the material.<sup>1</sup>

### **Chemical Mediators of Inflammation**

The inflammatory response comprises a highly complex cascade of events orchestrated by a variety of stimulatory and inhibitory molecules mediating leukocyte chemotaxis, adhesion, activation, and aggregation, as well as phagocytosis. In response to vascular injury near the site of implantation, leukocytes emigrate through vessel walls into the biomaterial exudate. Increased leukocytic adhesion involves specific interactions between complementary adhesion molecules present on the leukocyte and endothelial surfaces.<sup>1</sup> Inflammatory agents, namely cytokines IL-1 and TNF- $\alpha$ , stimulate increased

surface expression of these adhesion molecules. This enables leukocytes to adhere to the endothelium of blood vessels and transmigrate through the wall into the tissue exudates. Their chemotaxis is mediated by stimuli including complement protein fragments, mediators of the kinin, clotting and fibrinolytic systems, and products created by leukocytes themselves.<sup>39</sup> In addition, soluble lymphokines released from activated T lymphocytes, such as monocyte chemotactic factor (MCF), attract macrophages while migration inhibition factor (MIF) immobilizes them at the site of injury. Other factors such as macrophage activating factor, macrophage fusion factor, and specific macrophage arming factors then activate the immobilized cells and promote their interaction with the implant. Leukotriene B<sub>4</sub>, an intermediate of arachidonic acid metabolism, also provokes inflammation by affecting leukocyte chemotaxis and lysosomal enzyme release.<sup>39</sup> In addition, protein degradation products such as fibrinopeptide B (from fibrin) and kallikrein (a clotting cascade enzyme) have chemotactic activity.

Soluble hormone-like factors called cytokines are produced by a wide variety of cell types including lymphocytes, monocytes, platelets, fibroblasts, and keratinocytes. These secreted proteins exert diverse biological effects on various target cells and regulate both immunological and inflammatory host responses by serving as intracellular messengers.<sup>39</sup> Specifically, TNF and IL-1 stimulate the production of a wide variety of cells and also initiate cell migration, differentiation, and tissue remodeling.<sup>1</sup>

The principle soluble mediator of macrophage activation is macrophage activating factor (MAF), also known as interleukin-2 (IL-2), another T cell-derived lymphokine. Once recruited and activated macrophages can, themselves, release a variety of chemicals to drive inflammation-associated activities. These include certain cytokines, interferons



(IFN), prostaglandins, lysosomal enzymes, leukocytic pyrogen, and other cytotoxic agents.<sup>39</sup> Macrophage-secreted interleukin-1 (IL-1) activates T cells to produce more IL-2 (activating more macrophages), stimulates fibroblast activity, and induces collagen and collagenase synthesis.<sup>39</sup> Colony stimulating factor (CSF), another cytokine produced by a variety of activated inflammatory cells, can also stimulate the production of phagocyte precursors or activate additional macrophages. Interferon Type 1 is synthesized by activated macrophages under the control of prostaglandins and CSF; prostaglandin E inhibits the synthesis of interferon, while CSF stimulates it. Interferon Type 1 can then feed back and further activate macrophages by enhancing their phagocytic capability.

In addition to downregulating IFN activity, prostaglandins play other important positive and negative regulatory roles. They have been shown to increase the numbers of both immunoglobulin Fc receptors and the lectin concanavalin A receptors on macrophage membranes. Macrophage-produced prostaglandin E<sub>2</sub> (PGE-2) inhibits proliferation of granulocyte-macrophage stem cells and will also inhibit macrophage spreading, adherence, and migration. Glucocorticoids, powerful anti-inflammatory and immunosuppressive drugs, also inhibit macrophage function by interacting with corresponding surface receptors to inhibit synthesis and secretion of neutral proteases (especially plasminogen activator) and IL-1.<sup>39</sup>

Macrophages also synthesize numerous complement components, including C3 and Factor B. C3b, a cleaved product of C3, further activates macrophages and also acts as an opsonin to enhance phagocytosis. In addition, macrophages also release plasminogen activator, which cleaves plasminogen to plasmin. Plasmin has multiple regulatory roles, including degrading fibrin into soluble products and cleaving C3 to the

active form C3b. Certain lymphokines have been described to enhance phagocytosis mediated by ligand binding to both C3b and Fc receptors. Leukocyte aggregation is another well characterized response to chemotactic factors, especially C5a and macrophage aggregating factor.<sup>39</sup>

### **Protein Adsorption and Cell Adhesion**

Implanted biomaterials trigger a wide variety of unwanted responses, including inflammation, thrombosis, infection, and fibrosis. In many cases, these adverse responses are associated with the rapid accumulation of large numbers of phagocytic cells, which is an important feature of the inflammatory reaction.<sup>52</sup> Overall, cell adhesion to a material is dependent on protein adsorption profiles, surface chemistry, and material morphology.<sup>12, 53, 54</sup> Chemical modifications to a surface induce changes in material compatibility that affect the overall biological response.<sup>13, 55-57</sup>

Adsorption of biomolecules from multi-component solutions, such as plasma and biological fluids, is a dynamic process involving competition, rearrangements, and displacement of adsorbed species (the Vroman effect).<sup>58, 59</sup> Material surface chemistry often drives hydrated biomolecules to partially release bound water molecules, leading to structural changes and reversible as well as irreversible physisorption of biomolecules onto the surface.<sup>60</sup> The composition and configuration of the adsorbed protein layer dictates which adhesive ligands will be exposed on these proteins, thus determining the adhesive nature of the surface.<sup>61</sup> In particular, macrophage phagocytic activity, migration, and fusion to form FBGCs are influenced by adhesion to different proteins; therefore, the adhesive substrate affects cellular phenotype and function.<sup>13, 62, 63</sup>

Albumin, fibrinogen, and immunoglobulin (IgG) are the most abundant proteins in plasma; they are involved in competitive binding events at the surface of biomaterials and subsequently mediate adherence of PMNs.<sup>64</sup> IgG and complement fragment C3b are natural opsonins and adsorb to biomaterials within seconds of implantation.<sup>46, 64</sup> There are conflicting arguments about the necessity for complement C3 and IgG binding leukocytes to initiate acute inflammation. McNally and Anderson<sup>63</sup> determined that interactions between the leukocyte Mac-1 integrin and adsorbed C3b are an important adhesion mechanism on all serum-adsorbed surfaces. A significant role for IgG has also been revealed; IgG depletion caused a significant decrease in initial adherent cell density,<sup>12</sup> and adsorbed IgG also effectively activates monocytes, causes cell spreading, and FBGC formation.<sup>13</sup> However, biomaterials implanted in mice with severe combined immunodeficiency or complement deficiency exhibit normal recruitment of phagocytic cells; therefore, neither surface-bound IgG nor complement activation are necessary in triggering acute inflammatory responses *in vivo*.<sup>64</sup> Opsonization of particles likely involves multiple protein species.<sup>53</sup> It is likely that combined adsorption of complement, IgG, and fibrinogen promotes strong interactions between leukocytes and biomaterial surfaces.<sup>52, 56, 63-66</sup>

### **Integrins in Inflammation**

The generally accepted model for inflammatory cell-biomaterial interactions is that leukocytes interact with the layer of spontaneously adsorbed proteins rather than with the material itself.<sup>52</sup> Moreover, when proteins bind hydrophobic surfaces they undergo conformational changes, causing them to unfold and develop strong bonds with the

surface.<sup>60, 65, 67</sup> In particular, material-induced conformational changes of adsorbed fibrinogen are critical in the early phases of the foreign body reaction to biomaterials.<sup>65</sup> Fibrinogen adsorption probably induces changes in its tertiary structure leading to the exposure of previously hidden epitopes that help initiate adverse reactions.<sup>52</sup> In addition, fibrinogen mediates platelet adhesion to surfaces and affects material blood compatibility.<sup>66</sup>

Integrins are heterodimeric transmembrane receptors composed of  $\alpha$  and  $\beta$  subunits.  $\beta_1$  integrins are expressed ubiquitously on many cell types and are used in binding to extracellular matrix ligands and biomaterial surfaces.<sup>68</sup> The  $\beta_2$  integrin (CD18) is expressed specifically on leukocytes.<sup>69</sup>  $\beta_2$  subunits can associate with three unique  $\alpha$  subunits (CD11a, b, or c) to form heterodimers, one of which is the Mac-1 integrin (CD11b/CD18,  $\alpha_M\beta_2$ ). These integrins are usually in resting state, but they can become rapidly activated by cytokines causing them to be adhesive to their counter-receptors on other cells, bacterial polysaccharides, or viral coat proteins. These adhesive interactions enhance leukocyte attachment to the endothelium and subsequent extravasation to areas of inflammation, and they also assist in phagocytosis.<sup>40</sup> Mutations in the  $\beta_2$  subunit can lead to life-threatening disorders such as leukocyte adhesion deficiency type 1 (LAD-1), which results in impaired endothelial cell adhesion and reduced extravasation.<sup>70</sup> In addition, research supports a requirement for monocyte  $\beta_2$  subunits during initial adhesion to a surface, and both  $\beta_1$  and  $\beta_2$  subunits are utilized during the process of macrophage fusion into multinucleated foreign body giant cells.<sup>41</sup> Leukocyte adhesion to a biomaterial surface stimulates transcription of genes for inflammatory mediators, such as cytokines, reactive oxygen intermediates, and tissue factor.<sup>63</sup>

On stimulated leukocytes, Mac-1 functions as a high affinity receptor for fibrinogen<sup>71, 72</sup> and promotes phagocyte accumulation on biomaterial surfaces.<sup>73</sup> In particular, a short sequence in the fibrinogen D domain was determined to be the minimal recognition sequence for this integrin.<sup>71, 74</sup> This domain,  $\gamma$ 190-202, is commonly known as P1 and represents less than one percent of the total fibrinogen molecule.<sup>73</sup> The P1 epitope is hidden in soluble fibrinogen, but adsorption onto the implant surface causes conformational changes, protein denaturation, and tight adherence of fibrinogen revealing its pro-inflammatory form.<sup>52, 72</sup> A second epitope ( $\gamma$ 377-395) in the D domain known as P2 interacts with Mac-1 only when adsorbed to a surface, as well.<sup>72, 74</sup>

Moreover, thrombin-mediated conversion of fibrinogen to fibrin also exposes both P1 and P2 epitopes. Phagocytes may recognize fibrinogen adherent to biomaterials or medical implants as fibrin and respond by initiating a series of inflammatory and wound-healing responses meant to ward off infection and initiate wound healing at sites of vascular injury.<sup>52</sup> As an important component of the provisional matrix formed during wound healing,<sup>75</sup> fibrin may be a universal cue triggering leukocytes and locally regulating their function.<sup>72</sup> The extent of biomaterial-mediated P1 and P2 exposure appears directly related to the severity of inflammatory responses to a test panel of biomaterials, given their ability to mediate phagocyte adhesion and activation.<sup>52, 73</sup> Although it is evident that macrophages utilize the  $\alpha_M\beta_2$  integrin to bind these motifs, it is unknown how these binding events affect subsequent macrophage activities.

## **Macrophage as a Central Regulator of Inflammation**

Different populations of macrophage exist including inflammatory, microbicidal, reparative, pro-angiogenic, pro-thrombotic, antigen presenting and immunosuppressive cells, resulting in diverse leukocyte functions.<sup>48</sup> Research has shown that macrophages become unresponsive to subsequent signals after being initially stimulated by a particular cytokine.<sup>76</sup> However, other results suggest that macrophage functions can adapt to changes in the environment and shift their phenotype rather than developing into discrete subsets.<sup>77, 78</sup> “Classically activated” macrophages are stimulated by microbes, opsonized particles, and interferon- $\gamma$  (IFN- $\gamma$ ). These macrophages have a destructive phenotype, inducing cellular apoptosis and degrading tissue via matrix metalloproteinases; they also phagocytose opsonized particles and immune complexes, degrade matrix, and generate pro-inflammatory cytokines and chemokines.<sup>79, 80</sup> By contrast IL-4, IL-10, IL-13, and TGF- $\beta$ 1 stimulate “alternatively activated” macrophages with an anti-inflammatory phenotype but an enhanced ability to present antigens and phagocytose particles or debris.<sup>48, 50, 81</sup> Instead of causing tissue destruction, alternatively activated macrophages are involved in healing processes such as matrix synthesis and stabilization, and induction of cell survival, proliferation, and angiogenesis.<sup>79, 82</sup> The balance of these macrophage phenotypes is necessary for proper healing and restitution of normal tissue.

Due to their abundance, distribution, motility, responsivity, and versatility, macrophages are considered key mediators of implant-associated inflammation and the foreign body response, and they generate myriad biologically active products.<sup>46, 47, 83</sup> More than 100 substances are secreted by macrophages including hormones, neutral proteases, lysosomal hydrolases, chemotactic factors, arachidonic acid metabolites,

reactive oxygen intermediates, complement components, coagulation factors, growth-promoting factors, and cytokines. Lysosomal hydrolases and neutral proteases, active at low and neutral pH respectively, degrade carbohydrates and connective tissue components and generate inflammatory mediators such as C3b and kinins.<sup>39, 47</sup>

Macrophages also have receptors on their surface for opsonins, namely the complement cleavage fragment C3b and the Fc portion of the immunoglobulin molecule. Membrane perturbation, through receptor-ligand binding and aggregation or internalization of receptor-ligand complexes, is believed to activate these cells.<sup>39</sup> These activated macrophages then exhibit increased phagocytic activity and upon attachment to a surface, spread more rapidly and extensively than do normal resting macrophages.<sup>1</sup> Upon contact of the cell plasma membrane with various surface-reactive materials or soluble substances that induce phagocytosis, macrophages undergo an associated “respiratory burst” and generate highly reactive oxygen metabolites (superoxide anions and hydroxyl radicals).<sup>83, 39</sup> These cellular byproducts can have disastrous effects on implanted materials, degrading their surface and leading to device failure.<sup>46</sup>

Due to the large size disparity between cells and implanted materials, it is hypothesized that monocytes and macrophages fuse to form large multinucleated foreign body giant cells (FBGCs).<sup>1, 83</sup> In addition to the  $\alpha_M\beta_2$  integrin, the macrophage mannose receptor (MMR) has been identified as critical to FBGC formation, which may itself occur by a phagocytic mechanism.<sup>84</sup> Macrophage fusion is accompanied by considerable cytoplasmic expansion, resulting in FBGCs exhibiting as many as 100 nuclei.<sup>85</sup> Multinucleated giant cells have been observed in chronically inflamed tissues, yet the physiological significance and precise role of FBGCs at the tissue-material interface is

poorly defined. Emerging research suggests two distinct possibilities: (i) macrophage fusion into FBGCs could be a mechanism for promoting inflammatory cell survival by escaping apoptosis,<sup>86</sup> or (ii) FBGCs could serve a more wound healing function by sequestering phagocytic cell activities at the cell-substrate interface to maintain the response at a local, less activated level.<sup>41</sup> Other cell populations, such as T lymphocytes, also play important roles in the attraction of macrophages, their formation into FBGCs, antigen presentation, and phagocytic abilities.<sup>87</sup> Therefore, it is likely that the FBR phenotype (inflammatory vs. reparative) and intensity depends on a composite response of macrophages and lymphocytes acting in concert.<sup>50, 88</sup>

### **Hydrogel materials for biomedical and biotechnological applications**

Extensive research efforts have focused on hydrogel-based implant coatings, which offer many advantages over traditional surface modification strategies including self-assembled monolayers and polymer brushes.<sup>29, 31, 32</sup> They are particularly useful in biomedical and biotechnological applications due to their high water content and soft consistency.<sup>89</sup> Structurally unique three-dimensional architectures can be formed by cross-linking hydrogel building blocks in the form of nanoparticles, microspheres, or dendrimers.<sup>90</sup> Responsive polymers lend themselves to a variety of applications. A number of polymeric systems, including chitosan, PEO-PPO-PEO triblock copolymers, and pAAc copolymers, possess thermoresponsive gelation properties.<sup>91</sup> Thermoresponsive pNIPAm is a generally biocompatible hydrogel<sup>92</sup> and has been studied extensively. At a lower critical solution temperature (LCST) pNIPAm undergoes a



reversible volume phase transition and hydrophobically collapses upon itself, expelling water in an entropically favored event.<sup>89</sup>

By controlling the gelation properties, bulk hydrogels (i.e. macrogels) can be formed *in situ* in the presence of cells or used to address *in vivo* tissue defects.<sup>93, 94</sup> These responsive hydrogels are also utilized as delivery vehicles for bioactive materials, offering controlled release of drugs or proteins.<sup>90, 91, 95-97</sup> Recently, these systems have been utilized in the development of vaccines, as well; examples include delivery of combination drugs, such as chemo- and immunotherapeutic drugs was used to treat cancer,<sup>98</sup> and delivery of improved non-viral vaccines to facilitate priming of the immune system.<sup>99, 100</sup> The release kinetics of macromolecular delivery systems are critical, and thermoresponsive polymers have been used to obtain on-off release profiles in response to stepwise temperature changes.<sup>92, 101</sup> Hydrogel synthesis parameters can be well controlled, enabling incorporation of biological features such as pendant peptides to create bioactive scaffolds. Spatial patterns and molecular gradients of biomolecules, such as adhesion motifs, can be used to investigate and direct cell-surface interactions.<sup>93, 102, 103</sup> Bioactive hydrogel networks with incorporated protease degradation sites encourage more advanced responses, as in the case of wound healing applications involving enzymes associated with cell migration.<sup>104</sup> Hydrogel polymers also continue to gain attention in the creation of more biocompatible materials. The development of such novel implantable materials offering efficacy *in vivo*, as well as long-term stability, is critical and highly desirable for many implant applications.

## CHAPTER 3

### LITERATURE REVIEW: ANTI-INFLAMMATORY POLYMERIC COATINGS FOR IN VIVO SENSORS \*

\* Modified from AW Bridges and AJ García. Anti-inflammatory polymeric coatings for *in vivo* sensors. *J Diabetes Sci Technol* (In press)

#### INFLAMMATION AND DEVICE PERFORMANCE

Medical devices and biomaterial implants are used clinically in a variety of applications, and their performance is critical to a patient's overall health and quality of life. Surgical procedures injure microvasculature and tissue surrounding the implanted device, initiating a localized non-specific inflammatory response.<sup>1</sup> Although inflammation recruits native cells for remodeling and regenerating the damaged tissue, persistent and inflammatory stimuli significantly interfere with implant function and often result in device failure. Adverse host responses to implanted biomedical devices include thrombogenic responses on vascular grafts,<sup>2, 3</sup> degradation and stress cracking of pacemaker leads,<sup>4, 5</sup> tissue fibrosis surrounding mammary prostheses,<sup>6</sup> osteolysis and loosening of orthopaedic joint prostheses,<sup>7, 8</sup> reactive gliosis around neural probes,<sup>9</sup> and degradation in biosensor function.<sup>10</sup>

In the case of indwelling biosensors, including continuous glucose sensors, cell-mediated inflammatory responses and fibrous scarring adversely impact sensor performance, including fluctuations in biosensor sensitivity, decreased response time, and material degradation.<sup>105-107</sup> Accurate performance of glucose biosensors is critical to monitoring patient health, because diabetes is among the leading causes of death in the

United States.<sup>108</sup> Currently, many glucose sensors only function reliably for a few days *in vivo* before failing.<sup>18</sup> It has been suggested that these implants may require a stabilization period during fibrous capsule development, resulting in erroneous analyte measurements for weeks after implantation.<sup>109, 110</sup> Novel, probably multi-pronged, approaches are needed to abrogate long-term inflammatory responses and extend the *in vivo* lifetime of medical implants in order to avoid the need for multiple surgical procedures.

## **ANTI-INFLAMMATORY COATING STRATEGIES**

The severity and extent of the biological response to an implanted biomaterial or device influences the probability for its successful integration with surrounding tissue, as well as overall device performance. Initial stages of the FBR are dictated largely by the extent of injury and surgical technique, implantation site, implant shape and size, material chemical and physical properties, and local and systemic health of the recipient.<sup>1, 111-113</sup> Significant research efforts have focused on modifying material properties using various anti-inflammatory surface coatings to generate more biocompatible implants.

### ***I. Passive Strategies: Non-fouling Surface Treatments***

The initial stages of the FBR involve non-specific protein and biomolecule adsorption and subsequent leukocyte adhesion onto the biomaterial surface, events termed “biofouling.” It is generally believed that reducing biofouling can ameliorate subsequent adverse inflammatory responses such as leukocyte activation and tissue fibrosis. Several passive strategies have been explored to achieve this goal, including

preadsorption of material surfaces with less inflammatory proteins or cells. Such passivation strategies are attractive, because they are relatively straightforward and simple.<sup>26, 27</sup> However, these coatings suffer from a lack of stability as other proteins, such as fibrinogen, can passively displace preadsorbed proteins, such as albumin. Even covalently-tethered non-adhesive proteins can be degraded by leukocytes, resulting in deposition of pro-inflammatory, adhesive components. Approaches involving cell deposition onto surfaces prior to implantation offer a possible strategy to promote wound healing by encouraging mass transport and reducing fibrotic responses at the tissue-implant interface.<sup>28</sup> However, issues related to cell sourcing, host responses to the donor cells, and long-term stability limit these strategies.

Non-fouling (protein adsorption-resistant) thin-layer polymeric coatings offer more substantial routes to reduce acute inflammatory responses. The design requirements for implanted materials and devices vary considerably depending on the *in vivo* application and site of implantation. In particular, non-fouling polymeric surface coatings for implantable biosensors must ideally conform to the following considerations:

- Use of non-toxic materials
- Effectively prevent *in vivo* biofouling
- Appropriate thickness and permeability to allow analyte detection
- Techniques to deposit coating onto a variety of materials and architectures
- Mechanical, chemical, and electrical stability to withstand surface deposition, sterilization methods, implantation procedures, and *in vivo* environment.

Despite considerable research efforts, surface coatings that completely eliminate protein adsorption over the lifetime of a device have not been attained. Nevertheless, significant progress has been made in understanding the mechanisms driving protein adsorption, and several chemical groups that resist protein adsorption have been identified. Polyethylene glycol (PEG,  $-\text{[CH}_2\text{CH}_2\text{O]}_n$ ) has proven to be the most protein-resistant functionality and remains the standard for comparison (**Figure 3.1**).<sup>114</sup> PEG chain density, length, and conformation strongly influence resistance to protein adsorption.<sup>115, 116, 117</sup> The mechanism of resistance to protein adsorption by PEG surfaces probably involves a combination of the ability of the polymer chain to retain interfacial water and the resistance of the polymer chain to compression, due to its tendency to remain an extended coil conformation.<sup>118-120</sup> Other hydrophilic polymers, such as poly(2-hydroxyethyl methacrylate),<sup>121</sup> poly(*N*-isopropyl acrylamide),<sup>89, 122</sup> poly(acrylamide), and phosphoryl choline-based polymers,<sup>123-126</sup> also resist protein adsorption. In addition, mannitol, oligomaltose, and taurine groups have emerged as promising moieties to prevent protein adsorption.<sup>127-129</sup>

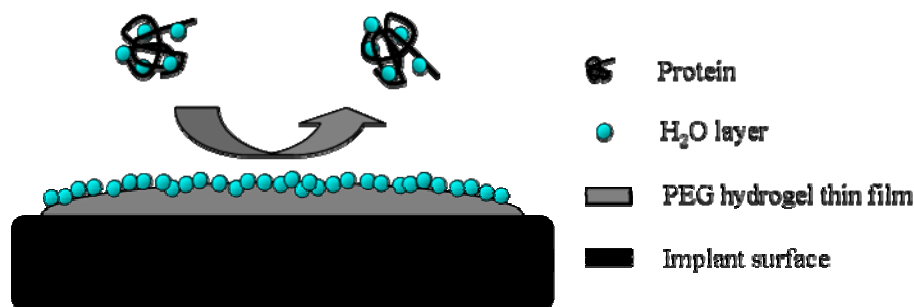


**Figure 3.1: Passive anti-inflammatory surface coating for biomaterials.** Hydrophilic polymeric coatings, such as PEG-based hydrogels, retain interfacial water molecules rendering them highly resistant to protein adsorption.

These coatings have been applied as molecularly thin self-assembled monolayers (SAMs), polymer brushes, and thin or bulk hydrogels (**Table 3.1**) capable of reducing protein adsorption and leukocyte adhesion. SAMs are confined to inorganic, planar surfaces and are only stable short-term in aqueous environments, limiting their use as coatings for *in vivo* biosensors.<sup>30</sup> Polymer brushes are more mechanically robust than SAMs and can be generated on non-planar surfaces, including colloidal suspensions and polymeric substrates. Moreover, surface-initiated polymerizations allow control over functionality, grafting density, and thickness of the brushes.<sup>31, 32</sup> Extensive research efforts have focused on hydrogel-based implant coatings, which are particularly useful in biomedical and biotechnological applications due to their high water content and soft consistency.<sup>89</sup> Hydrogels offer many advantages over traditional surface modification strategies, including a viscoelastic network structure, tunable material characteristics, incorporation of multiple chemical functionalities, nano-scale dimensions with complex architectures, and the ability to deposit onto a variety of material substrates.<sup>33-37, 92, 93</sup>

## ***II. Microgel-Based Implant Coatings***

While bulk hydrogels have already realized potential in many biotechnological applications, micro- and nano-scale hydrogels have recently emerged to create the next generation of “smart” biomaterials. Microgels are colloidally stable hydrogel particles that retain many of the same material properties as their macrogel counterparts, including phase transition behavior and a viscoelastic network structure that enables mass transport.<sup>38</sup> However, they offer many advantages over traditional hydrogel materials, such as colloidal stability, unique control over synthesis parameters, and the ability to

incorporate co-monomers with desirable properties. Microgels are commonly prepared via precipitation polymerization reactions, which can generate particles of desired size by optimizing synthesis parameters.<sup>130</sup>

Thermoresponsive pNIPAm is commonly used in the development of microgels due to its predictable phase transition behavior. By incorporating various co-monomers during synthesis, these so-called “smart” pNIPAm-based materials can respond to temperature, pH, light, and ionic strength.<sup>37</sup> The introduction of functional groups, such as acrylic acid co-monomers, yields microgel particles with pendant acid groups serving as reactive sites for conjugation of biomolecules and expands the utility of these pNIPAm-based materials.<sup>131</sup> Additionally, more structurally complex microgel-based systems have been developed with an inner core and outer shell.<sup>37</sup> Such strategies lend themselves to the development of hydrogel-based materials for controlled drug delivery or applications targeting specific cells.<sup>131</sup> Microgel systems also have great potential in the development of novel surface treatments for a variety of applications, including non-fouling implant coatings.

**Table 3.1: Examples of non-fouling ethylene glycol-based surface treatments.**  
A • denotes materials that were only tested *in vitro*.

Coating Structure	Selected References
Self-assembled monolayer	Prime & Whitesides (1993) <sup>30</sup> • Chapman <i>et al.</i> (2001) <sup>132</sup> • Zhang <i>et al.</i> (2001) <sup>133</sup> •
Polymer brush or surface graft	Espadas-Torre & Meyerhoff (1995) <sup>134</sup> • Lee <i>et al.</i> (1997) <sup>135</sup> • Du <i>et al.</i> (1997) <sup>136</sup> • Zhang <i>et al.</i> (1998) <sup>137</sup> • Jenney & Anderson (1999) <sup>138</sup> • Shen <i>et al.</i> (2001) <sup>139</sup> • Otsuka <i>et al.</i> (2001) <sup>140</sup> • Boulmedais <i>et al.</i> (2004) <sup>141</sup> • Ma <i>et al.</i> (2004) <sup>142</sup> • Ma <i>et al.</i> (2006) <sup>143</sup> • Zhou <i>et al.</i> (2007) <sup>144</sup> • Waku <i>et al.</i> (2007) <sup>145</sup> • Cao <i>et al.</i> (2007) <sup>146</sup> •
Hydrogel	West & Hubbell (1995) <sup>94</sup> Quinn <i>et al.</i> (1995) <sup>147</sup> Quinn <i>et al.</i> (1997) <sup>148</sup> Collier <i>et al.</i> (2004) <sup>149</sup> • Nolan <i>et al.</i> (2005) <sup>89</sup> • Singh <i>et al.</i> (2007) <sup>122</sup> • Yu <i>et al.</i> (2008) <sup>150</sup>



### ***III. Active Strategies: Delivery of Anti-inflammatory Agents***

In contrast to passive non-fouling surface treatments, coatings presenting anti-inflammatory agents offer a more interactive and directed approach to modulate cell behavior. Broad-spectrum drugs have typically been used to control chronic tissue inflammation. However, orally administered drugs may not achieve adequate local concentrations, and their long-term systemic use can cause major side effects. Therefore, it is desirable to deliver therapeutics locally in a controlled, site-specific manner to improve the tissue-material response.

Various immunomodulatory agents can be immobilized onto non-fouling polymeric coatings or delivered in soluble form from the coating (**Figure 3.2**). Possible strategies for controlled release of agents include passive diffusion from coatings or polyelectrolyte layers,<sup>151, 152</sup> bioerodible/degradable coatings to release drugs by passive dissolution,<sup>153</sup> swelling coatings that release drug by passive mechanisms, and hydrolysable or enzyme-degradable linkages to release the agent.<sup>154-157</sup> These “smart” delivery systems offer several advantages over passive methods, including highly controlled presentation of immunomodulatory agents, control over reaction kinetics, and versatility through hybrid designs. In addition to the basic requirements for passive coatings, designs for these bioactive coatings must consider the following properties:

- Retain bioactivity of anti-inflammatory molecules for the intended lifetime
- Optimal tethering distance for recognition of immobilized agents
- Appropriate release profiles in terms of amounts, rates, total dosage, and release time (acute vs. chronic release)
- Drug character (e.g. hydrophobicity), residence times, and stability

- Safety issues related to drug release (designed or accidental)
- Agent-matrix (coating) interactions
- Effects of material sterilization.

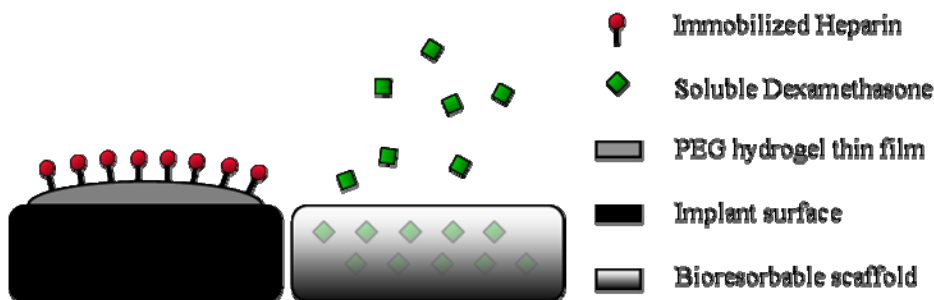


**Figure 3.2: Bioactive implant coatings to deliver anti-inflammatory molecules.** Representative schemes depict mechanisms for active delivery of various immunomodulatory agents to reduce leukocyte adhesion and activation.

Examples of anti-inflammatory factors delivered from surface coatings are summarized in **Table 3.2**. Dexamethasone (DEX) is a synthetic glucocorticoid hormone with many applications in biomedical research, including treatment of inflammatory responses.<sup>158</sup> DEX modulates macrophage behavior and reduces the levels of numerous pro-inflammatory cytokines, including TNF- $\alpha$ , IL-1 $\beta$ , IL-6, and IFN- $\gamma$ .<sup>159, 160</sup> DEX-releasing coatings have reduced tissue inflammation and cell activation surrounding implanted glucose biosensors and neural implants.<sup>161-164</sup> In addition, polypyrrole-based electrode coatings designed to electrically control delivery of DEX lowered the amount of reactive astrocytes *in vitro*.<sup>165</sup>

**Table 3.2: Active surface treatments for biomaterial coatings.** A • denotes materials that were only tested *in vitro*.

Agent	Delivery Mechanism	Selected References
<b>DEX</b>	electrochemical release	Wadhwa <i>et al.</i> (2006) <sup>165</sup> •
	passive release	Kim & Martin (2006) <sup>163</sup>
	passive release	Norton <i>et al.</i> (2007) <sup>161</sup>
	passive release	Zhong & Bellamkonda (2007) <sup>162</sup>
	passive release	Patil <i>et al.</i> (2007) <sup>164</sup>
<b>α-MSH</b>	passive release	Benkirane-Jessel <i>et al.</i> (2004) <sup>151</sup> •
	passive release	Schultz <i>et al.</i> (2005) <sup>152</sup>
	passive release	Zhong & Bellamkonda (2005) <sup>166</sup> •
	surface immobilization	He <i>et al.</i> (2007) <sup>167</sup>
<b>Heparin</b>	surface immobilization	Gerritsen <i>et al.</i> (2000) <sup>168</sup>
	surface immobilization	Wang <i>et al.</i> (2003) <sup>169</sup> •
	surface immobilization	van Bilsen <i>et al.</i> (2004) <sup>170</sup>
	surface immobilization	Sung <i>et al.</i> (2004) <sup>171</sup> •
	surface immobilization	Fu <i>et al.</i> (2005) <sup>172</sup> •
	surface immobilization	Rele <i>et al.</i> (2005) <sup>173</sup>
	surface immobilization	Tseng <i>et al.</i> (2006) <sup>174</sup> •
	surface immobilization	Du <i>et al.</i> (2007) <sup>175</sup> •
<b>IL-1Ra</b>	immobilized or soluble	Kim <i>et al.</i> (2007) <sup>176</sup> •
<b>SODm</b>	surface immobilization	Udipi <i>et al.</i> (2000) <sup>177</sup>
<b>Curcumin</b>	passive release	Nguyen <i>et al.</i> (2004) <sup>178</sup> •
	passive release	Su <i>et al.</i> (2005) <sup>179</sup> •
	passive release	Pan <i>et al.</i> (2006) <sup>180</sup> •
<b>Vitamin E</b>	passive release	Hahn <i>et al.</i> (2004) <sup>181</sup> •

Heparin is a highly sulfated glycosaminoglycan with strong anti-coagulant activity, and it also exhibits anti-inflammatory properties. It is synthesized and secreted by mast cells at sites of infection and inhibits endotoxin-induced monocyte activation.<sup>182</sup> Heparin pretreatment significantly attenuates leukocyte transmigration through its actions on P- and L-selectin<sup>42, 183</sup> and the leukocyte-specific  $\alpha_M\beta_2$  integrin, and it also binds cytokines and suppresses superoxide generation by neutrophils.<sup>182, 184</sup> Heparin-based coatings have reduced protein adsorption, leukocyte extravasation from the vasculature, and recruitment to implant surfaces.<sup>170, 173-175</sup>

Alpha melanocyte-stimulating hormone ( $\alpha$ -MSH) is an endogenous linear peptide with potent anti-inflammatory properties. *In vitro*,  $\alpha$ -MSH reduced levels of pro-inflammatory TNF- $\alpha$  while increasing levels of anti-inflammatory IL-10 in stimulated human monocytes.<sup>151</sup> It stimulated production of the anti-inflammatory cytokine IL-10 and revealed a less obstructive cell layer on coatings for tracheal prostheses.<sup>152</sup> In addition,  $\alpha$ -MSH inhibited nitric oxide production by stimulated microglia, and reduced the magnitude of electrical impedance of implanted neural implants.<sup>166</sup>

Receptor antagonists, antibodies, and soluble receptors are endogenous molecules that competitively inhibit binding to the corresponding agonist, effectively acting as a molecular trap. Decoy antagonists have been developed against pro-inflammatory cytokines, such as IL-1, as a strategy to regulate inflammation.<sup>185, 186</sup> In one interesting study, a fusion protein of recombinant human IL-1 receptor antagonist and elastin-like polypeptide (IL-1ra-ELP) was formed and covalently immobilized onto SAMs.<sup>176</sup> This fusion protein was able to prevent endotoxin-stimulated human monocytes from

differentiating, and reduced expression of pro-inflammatory cytokines while increasing the production of anti-inflammatory and pro-wound healing cytokines.

Superoxide anions are potent cytotoxic oxidants secreted during macrophage phagocytosis. Superoxide dismutase is an endogenous scavenger enzyme that catalyzes its breakdown into less reactive hydrogen peroxide and oxygen. Superoxide dismutase mimetics (SODm) were developed as an anti-inflammatory mechanism. When covalently attached to ultra high molecular weight polyethylene, neutrophil recruitment was significantly reduced.<sup>177</sup>

## **EXISTING CONSIDERATIONS AND FUTURE PROSPECTS**

Biomaterial-mediated inflammation poses a complex problem, limiting the function of implanted devices and overall patient health. Significant efforts have focused on developing passive non-fouling surface treatments to prevent protein adsorption and leukocyte adhesion, as well as active mechanistic approaches for the delivery of anti-inflammatory agents. While these coating technologies have reduced protein adsorption and cell adhesion *in vitro*, considerable fibrous encapsulation and adverse inflammatory responses are still evident following implantation.<sup>161, 170, 187</sup> These marginal reductions in adverse inflammation can be attributed to persistent leukocyte adhesion and activation *in vivo* and sub-optimal pharmacodelivery.<sup>161, 188</sup>

Although current polymeric coatings successfully modulate acute inflammatory events, new strategies will be critical to extend the *in vivo* lifetime and performance of implanted devices. Coating designs will probably need to be material and application-specific in order to achieve the desired *in vivo* response. Biologically interactive implants are gaining considerable interest. Tunable, stimuli-responsive materials and biomimetic

molecules may be able to actively direct cell behavior and activity surrounding the implant, encouraging more desirable interactions.<sup>33, 34</sup> In addition, these “smart” materials will lend a higher degree of sensitivity and specificity to polymeric coatings, enabling tighter control over pharmacokinetics and complex dosing schemes using multiple biomolecules or drugs. For instance, delivery of oligonucleotides have proved to be an effective strategy to down-regulate specific endogenous inflammatory factors.<sup>189</sup> These approaches may create less inflammatory macrophages and attract wound healing cells. It will also be important to focus on successful integration of the device with surrounding tissue and regenerating damaged microvasculature. Tissue integration is particularly important in neural and orthopedic applications.<sup>9, 11</sup> In addition, the delivery of angiogenic factors may help facilitate *in vivo* performance of implanted biosensors by offsetting tissue fibrosis.<sup>161, 164, 190</sup> Clearly, progress in the development of effective and long-term *in vivo* sensors will require the integration of multiple strategies and disciplines, as well as rigorous testing in relevant *in vivo* models.

## CHAPTER 4

### ROLE OF PLASMA FIBRONECTIN IN THE FOREIGN BODY RESPONSE TO BIOMATERIALS \*

\* Modified from BG Keselowsky, AW Bridges, KL Burns, CC Tate, JE Babensee, MC LaPlaca, AJ García. Role of plasma fibronectin in the foreign body response to biomaterials. *Biomaterials* 28 (2007): 3626-3631.

AW Bridges contributed scientifically to a significant portion of this work, including quantification of Verhoeff-van Geisson staining (Figure 4.3) and all histological processing, staining, imaging, and quantification of immunohistochemistry (Figures 4.4 and 4.5).

#### INTRODUCTION

Host responses to biomaterials control the biological performance of implanted medical devices, tissue-engineered constructs, and delivery vehicles for therapeutics.<sup>1, 191</sup>

Upon implantation, synthetic materials dynamically adsorb proteins and other biomolecules which trigger an inflammatory cascade comprising blood coagulation, leukocyte recruitment and adhesion, foreign body reaction, and fibrous encapsulation.<sup>1, 191</sup>

<sup>191</sup> The foreign body reaction and ensuing fibrous encapsulation result in a physicochemical barrier that severely limits device integration and the *in vivo* performance of numerous devices, including chemical biosensors, electrical leads/electrodes, therapeutic delivery systems, and orthopaedic and cardiovascular prostheses.<sup>2, 192-194</sup> Extensive research has identified mechanisms governing acute inflammatory responses to implanted synthetic materials. Adsorption of fibrinogen and complement fragments from plasma onto biomaterial surfaces results in integrin receptor-mediated leukocyte recruitment and adhesion.<sup>52, 63, 65</sup> Adherent monocytes/macrophages secrete cytokines and growth factors and mature into foreign body giant cells that

coordinate the recruitment and activities of other cell types,<sup>41, 85</sup> leading to neovascularization and connective tissue formation.<sup>1</sup> Despite our understanding of acute inflammation to implanted synthetic materials, mediators of chronic inflammation and fibrous encapsulation of implanted biomaterials remain poorly understood.

Fibronectins (FNs) are widely expressed, cell-adhesive glycoproteins present as soluble forms in body fluids (e.g., plasma FN, pFN) and insoluble fibrils in extracellular matrices (cellular FN, cFN).<sup>195</sup> FNs are generated from a single gene, but alternative splicing gives rise to different isoforms.<sup>195</sup> Deletion of the *FN* gene is embryonically lethal due to defects in mesoderm, neural tube and vascular development.<sup>196</sup> FN is also required for cleft formation during epithelial branching morphogenesis.<sup>197</sup> Extensive *in vitro* analyses have demonstrated that FNs promote cell adhesion and regulate the survival, cell cycle progression, and expression of differentiated phenotypes in various cell types. Despite the vast amounts of studies on the role of FN in cellular functions, the role of the pFN isoform in adult physiology and pathology has been difficult to analyze because of the embryonic lethality of the *FN* gene deletion. Recent studies with FN conditional knock-out mice have shown that pFN promotes thrombus growth and stability in injured arterioles and supports neuronal survival following cerebral ischemia, but is not essential to skin-wound healing, likely due to contributions from cFN.<sup>198, 199</sup> In the present analysis, we used pFN conditional knock-out mice to examine the contributions of pFN to host responses to implanted biomaterials.



## MATERIALS AND METHODS

### *pFN conditional knockout mice*

pFN conditional knock-out mice based on the *Cre-loxP* system were previously developed by Erickson and Fässler<sup>198</sup> and rederived by Hynes.<sup>199</sup> The *Cre-loxP* system provides a genetic tool to control site-specific recombination events in genomic DNA, thereby affording a mechanism for deleting a specific gene in response to a stimulus that results in Cre recombinase expression. These mice have the *FN* gene flanked by loxP sites and express Cre recombinase under control of the interferon- and polyinosinic-polycytidic acid (pI-pC)-inducible *Mx* promoter. Deletion of the *FN* gene is induced by intraperitoneal injections of pI-pC and results in complete and stable deletion of *FN* in the liver (hepatocytes produce pFN) for at least eight months.<sup>198</sup> Breeding pairs of mice containing a floxed (fl; loxP-site containing) fibronectin allele and *Mx-Cre* were kindly provided by H.P. Erickson and R.O. Hynes. Floxed mice were crossed with *Mx-Cre* mice to generate *FN* (fl/fl) animals carrying the *Mx-Cre* transgene. The presence of the transgene was verified by PCR of DNA extracted from tail tissue with *Cre*-specific primers. Deletion of the *FN* gene was induced in 8-12 week-old female mice by 3 intraperitoneal injections of pI-pC (250 µg) at 2 day intervals. Blood samples were drawn from the saphenous vein from intraperitoneal space at least 3 days following the last pI-pC injection to assess pFN levels by Western blotting using a rabbit polyclonal antibody against human fibronectin (Sigma; this antibody cross-reacts with mouse fibronectin). Lavage from intraperitoneal space was obtained from animals at the time of disk explant. All experiments were conducted under IACUC-approved protocols.

### ***Biomaterial implantation and analysis***

Discs (9.5 mm diameter, 0.5 mm thick) were cut from PET sheets, washed, and sterilized in ethanol. Samples had endotoxin levels below the recommended maximum FDA level (0.5 EU/ml) as determined by the LAL chromogenic assay. Discs were implanted either intraperitoneally (n = 8 samples/group) or subcutaneously (n = 4-5 samples/group) following IACUC-approved procedures. For intraperitoneal implants, discs were explanted at 16 hours. Adherent cells were trypsinized and either analyzed in a Coulter counter (for total leukocyte cell counts) or fixed and stained with May-Grunwald-Geimsa for differential cell counts in cytopins. For subcutaneous implants, PET discs were explanted at 14 days, formalin-fixed and paraffin-embedded. Histological sections (5 µm thick) were stained with Verhoeff-van Geisson stain for nuclei (dark blue) and collagen (pink). For immunohistochemical staining, sections were incubated in rabbit polyclonal antibody against fibronectin (Sigma, St. Louis, MO) or rat monoclonal antibody against the F4/80 antigen of resident murine tissue macrophages (clone BM8, Accurate Chemical & Scientific), biotinylated secondary antibodies, and an avidin-linked alkaline phosphatase-based reagent (Vector Labs, Burlingame, CA), and counterstained with hematoxylin. For cell macrophage/FBGC counting, high magnification (60X oil objective) images were blindly scored for total nuclei, F4/80+ cells with one nucleus, and F4/80+ multinucleated cells.

### ***Statistical Analysis***

Results were analyzed by ANOVA using SYSTAT 8.0 (SPSS Inc., Chicago, IL). For macrophage/FBGC, a nested one-way ANOVA design (animal nested within

treatment) was used to account for the variance across subjects.<sup>200</sup> Pair-wise comparisons were performed using Tukey post-hoc test with a 95% confidence level considered significant.

## RESULTS

We used pFN conditional knock-out mice based on the *Cre-loxP* system<sup>198, 199</sup> to examine the role of pFN in host responses to implanted biomaterials. Deletion of the *FN* gene in these mice is induced by intraperitoneal injections of pI-pC and results in complete and stable deletion of *FN* in the liver (hepatocytes produce pFN) for at least eight months.<sup>198</sup> The extent of FN deletion in other tissues is variable, and some cell types retain the ability to produce cFN. Importantly, these mice express normal levels of other extracellular matrix components such as collagen I, laminin-1, and tenascin. Following pI-pC induction, these mice exhibit less than 2% of pFN in normal mouse plasma (**Figure 4.1a**) and display no overt phenotype under standard laboratory conditions. As expected, deletion of pFN also eliminated FN in the intraperitoneal fluid (**Figure 4.1b**). We refer to these mice as pFN-null mice throughout this paper. No differences between untreated (no pI-pC treatment) mice carrying the *Mx-Cre* transgene and pI-pC-treated wild-type littermates were observed in any assay, and we refer to these mice as control throughout this manuscript.

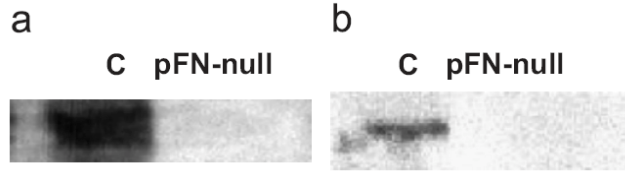


**Figure 4.1: Levels of plasma fibronectin determined by Western blot analysis.** pI-pc induction effectively deletes FN from (a) plasma and (b) intraperitoneal fluid in mice carrying the *Mx-Cre* transgene (pFN-null) but not control (C) animals. Western blot analysis with polyclonal antibody against fibronectin demonstrated approximately 98% reduction of FN levels.

To investigate the role of pFN on leukocyte recruitment during the acute inflammatory response to biomaterials, polyethylene terephthalate (PET) discs were implanted in the intraperitoneal space for 16 hours and then explanted for analysis of leukocyte recruitment and adhesion. This model has been extensively used to analyze leukocyte recruitment to biomaterials.<sup>64, 65, 201</sup> PET is a widely used biomaterial which elicits a moderately strong inflammatory response.<sup>65</sup> The knitted form of this material, Dacron<sup>®</sup>, is widely used in vascular grafts. No differences were observed in total leukocyte counts of cells attached to implanted discs between pFN-null and control mice ( $p = 0.79$ ) (**Figure 4.2a**). Furthermore, differential cell counts revealed no differences in lymphocyte, neutrophil, and monocyte adhesion to PET discs between pFN-null and control mice ( $p = 0.19$ ) (**Figure 4.2b**). These results indicate that pFN does not play a major role in the recruitment and adhesion of leukocytes to implanted materials during the acute inflammatory response.

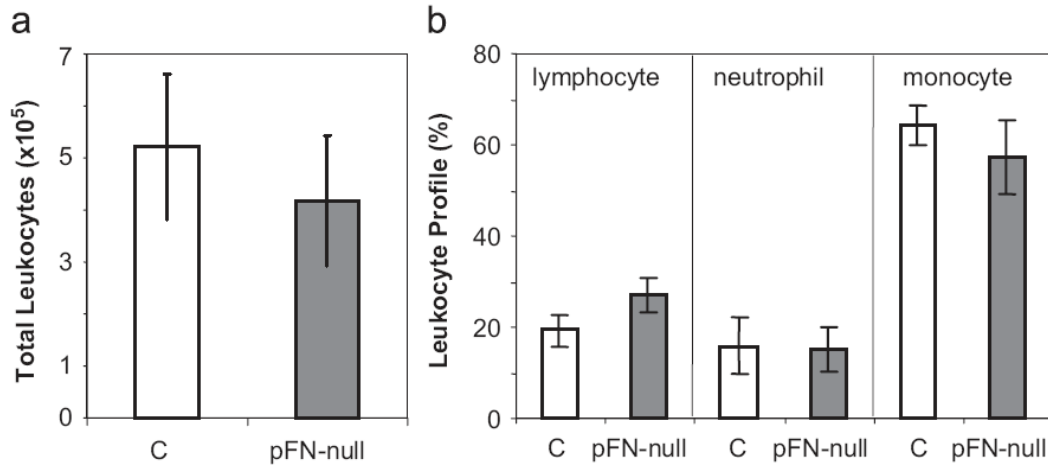


**Figure 4.2: Leukocyte adhesion to implanted biomaterials.** pFN does not influence acute leukocyte recruitment and adhesion to implanted biomaterials. PET disks were implanted in the intraperitoneal cavity in mice with pFN deleted (pFN-null) and control (C) animals. No differences were observed in adherent (a) total or (b) differential leukocyte cell counts ( $n = 8$  animals/group).

PET discs were also implanted subcutaneously for 14 days to assess the contributions of pFN to the foreign body reaction and fibrous encapsulation of implanted materials. Measurement of fibrous capsule thickness following subcutaneous implantation is a standard measure of chronic inflammation to synthetic materials.<sup>1</sup> PET discs implanted in pFN-null mice were encapsulated by thick, dense fibrous membranes (Figure 4.3a), while discs implanted in control animals exhibited considerably thinner capsules (Figure 4.3b). Fibrous capsules were thicker on the implant side facing the dermis compared to the implant side facing the body wall as is often seen in this model, but the relative difference in capsule thickness between pFN-null and control animals was equivalent. Measurements of capsule thickness indicated a 2-fold increase in fibrous capsule thickness for pFN-null mice compared to controls (dermis,  $p < 0.04$ ; body wall,  $p < 0.02$ ) (Figure 4.3c,d). These results indicate that pFN modulates the foreign body reaction and fibrotic response to implanted materials.

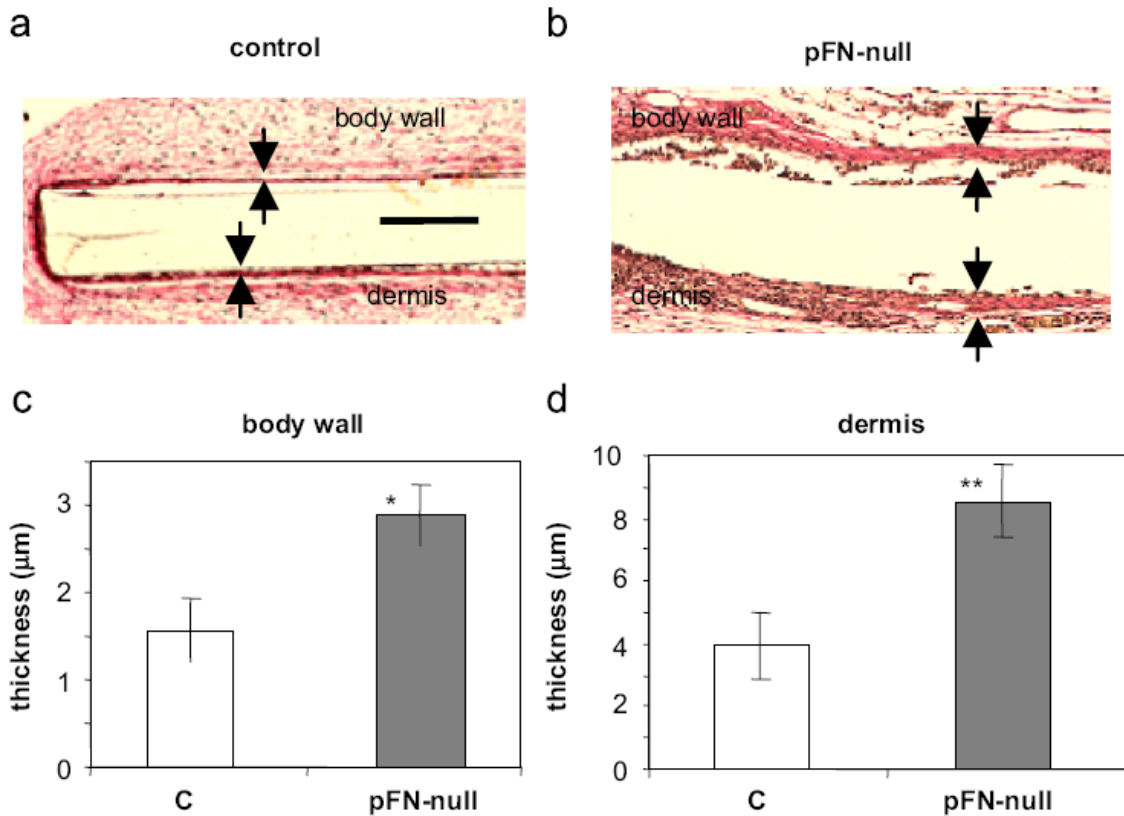


**Figure 4.3: Fibrous encapsulation of subcutaneously implanted biomaterials.** pFN modulates the foreign body reaction and fibrotic response to PET disks implanted subcutaneously for 14 days. Verhoeff-van Geisson stained sections (collagen: pink; cell nuclei: dark blue) of tissue response to implanted biomaterials showing fibrous capsules (arrows) in (a) control (C) and (b) mice with deleted pFN (pFN-null). Measurement of capsule thickness revealed thicker capsules around PET implants in pFN-null mice compared to controls (C) for both (c) body wall ( $p < 0.02$ ) and (d) dermis ( $p < 0.04$ ) faces of the implants (scale bar  $50 \mu\text{m}$ ;  $n = 5$  animals/group).

To evaluate whether pFN is involved in macrophage recruitment and fusion into foreign body giant cells (FBGC), sections were stained for the F4/80 antigen (a marker of resident tissue macrophages) and scored for total nuclei, F4/80+ cells with one nucleus (macrophages), and F4/80+ cells containing multiple nuclei (FBGC). More intense staining for the macrophage marker F4/80 antigen was observed for mice lacking pFN than control animals (**Figure 4.4a,b**). A three-fold increase in the number of FBGC associated with the implant was detected in pFN-null mice compared to controls ( $p < 0.04$ ) (**Figure 4.4c**). No differences were observed in the number of total cells ( $p = 0.40$ ) or macrophages ( $p = 0.45$ ). This result suggests that pFN regulates the formation of biomaterial-associated FBGC.

Immunohistochemical staining for FN showed intense staining localized to the fibrous capsule for both pFN-null and control animals (**Figure 4.5**). FN was distributed throughout the dense fibrous capsule associated with the biomaterial. Since the polyclonal antibody used recognizes both pFN and cFN, the staining most likely indicates the presence of cFN within the fibrous capsule. As discussed above, for this conditional knock-out model, some tissues retain expression of cFN even though pFN is effectively deleted.<sup>198</sup> Monocytes/macrophages and fibroblasts associated with the fibrous capsule are the likely source of this cFN.

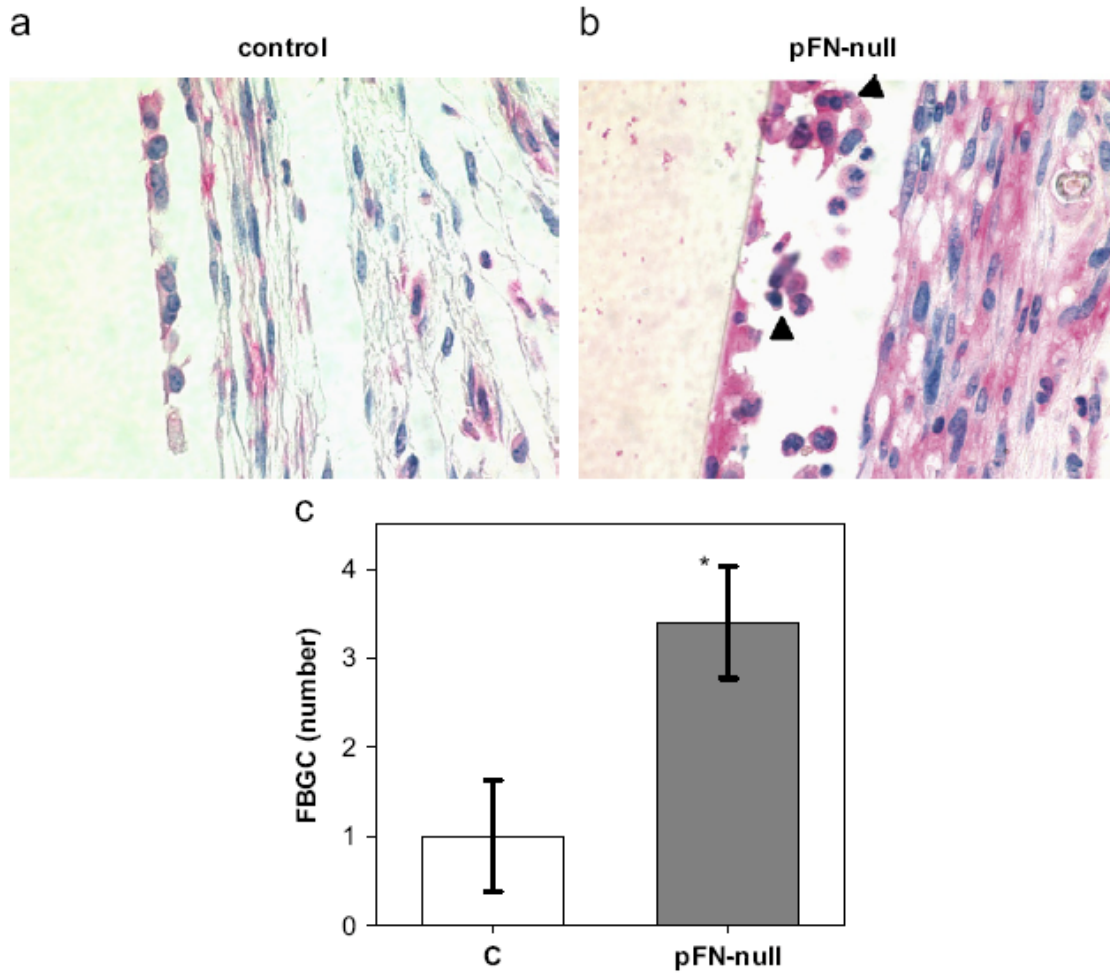


**Figure 4.4: Biomaterial-associated macrophages and FBGC determined by immunohistochemistry.** Staining for macrophage marker F4/80 (pink) is more intense in pFN-null animals (b) compared to control mice (a). Multinucleated F4/80+ cells are indicated by black arrowhead. (c) Cell counts showing elevated biomaterial-associated FBGC in pFN-null mice ( $p < 0.04$ ) ( $n = 4$  animals/group).



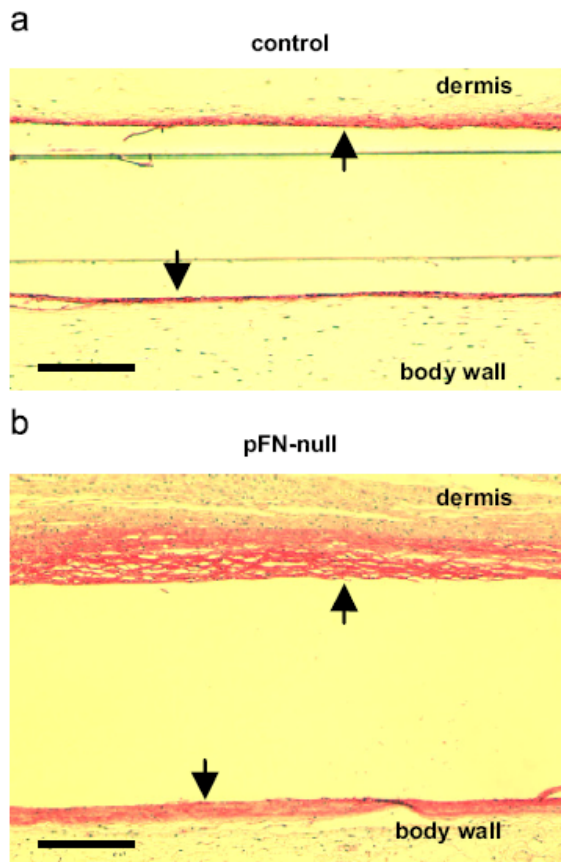


**Figure 4.5: Immunohistochemical staining for FN in fibrous capsules.** FN (arrows, dark pink) is localized at the tissue-material interface of encapsulated PET disks implanted subcutaneously in control (**a**) and pFN-null mice (**b**) (scale bar 50  $\mu$ m).

## DISCUSSION

Our results demonstrate that pFN modulates the foreign body response and fibrous encapsulation of implanted materials. This is the first report directly linking pFN to host inflammatory responses to implanted synthetic materials. Deletion of pFN, however, did not influence leukocyte recruitment and adhesion to the implanted biomaterial, indicating that pFN regulates chronic, but not acute, inflammatory responses to biomaterials. The lack of involvement of pFN in acute leukocyte adhesion to synthetic materials *in vivo* is consistent with other *in vitro* and *in vivo* analyses showing that fibrinogen is the major plasma component mediating leukocyte recruitment to biomaterials.<sup>65, 202</sup> Unexpectedly, collagenous capsules surrounding implanted PET discs were twice as thick in pFN-null mice compared to wild-type mice. This finding that collagen capsules are thicker in the absence of pFN is surprising given the requirement of FN on collagen assembly.<sup>203, 204</sup> This result indicates that pFN is involved in the deposition and/or remodeling of the fibrous capsule surrounding implanted materials. The mechanism(s) by which pFN regulates fibrous capsule thickness remains unclear, but pFN may modulate host responses by adsorbing directly onto the material or by interacting with other proteins associated with the biomaterial, such as fibrinogen and collagen. pFN associated with the biomaterial may influence the adhesion and/or function of cells involved in the foreign body reaction, including the ability to assemble and remodel the collagenous capsule or secrete cytokines regulating fibrosis. Indeed, we observed a significant increase in the number of FBGC associated with the implant in pFN-null compared to control mice. This result suggests that pFN regulates the formation or maturation of FBGC. This model is consistent with *in vitro* findings

implicating fibronectin-binding  $\beta_1$  integrins and fibronectin-derived binding motifs in FBGC fusion and maturation.<sup>41, 205</sup> Moreover, Horbett and colleagues demonstrated that monocyte adhesion to adsorbed fibronectin reduced FBGC formation.<sup>13</sup>

Interestingly, considerable levels of FN, corresponding to cFN, were present on the capsules of both pFN-null and control mice. This observation suggests that the differences in fibrous capsule thickness are specific to pFN, and cFN cannot compensate for the loss of pFN. There is evidence that different isoforms of FN support cell adhesion and migration to different extents.<sup>206-209</sup> Finally, host responses to implanted materials are often interpreted in the context of classical wound healing. However, the important role of pFN in the inflammatory response and foreign body reaction observed in our study contrasts with the ability of skin wounds to heal normally in the absence of pFN in the same animal model.<sup>198</sup> These results highlight inherent differences between classical wound healing and host responses to implanted materials.

The use of a conditional knock-out model provides a robust system to evaluate the role of specific proteins in host responses to implanted materials in adult animals without complicating compensatory effects associated with conventional knock-out models. For example, Bornstein and colleagues demonstrated that mice lacking the angiogenesis inhibitor thrombospondin 2 mount an altered foreign body reaction to implanted materials characterized by increased capsule thickness and vascularity.<sup>210</sup> However, interpretation of the results is complicated by the fact that these mice exhibit connective tissue abnormalities, including disordered collagen fibrillogenesis and vascular density.<sup>211</sup>

Our results identify a potential target for therapeutic intervention to enhance the biological performance of biomedical devices. Control of pFN activity via drug-,

protein-, or gene-based manipulations of plasma concentration, availability, or presentation on the material could be exploited to manipulate host responses. For instance, we have shown that biomaterial surface chemistry-dependent changes in the activity of adsorbed FN modulate integrin receptor binding and cell differentiation responses.<sup>212</sup> Moreover, biomaterial-based strategies focusing on presenting FN or FN-derived adhesion motifs enhance host integration and function in model systems, including bone and cartilage.<sup>213-215</sup> These enhancements are attributed to improved interactions with the host target tissue (e.g. bone) rather than altered inflammatory responses. Our results support pFN-mediated regulation of the foreign body reaction and chronic inflammatory responses as a new mechanism for controlling host responses to synthetic biomedical materials.

## CONCLUSION

Using plasma fibronectin conditional knock-out mice, we demonstrate that plasma fibronectin modulates the foreign body response to biomaterial discs implanted subcutaneously. Fibrous collagenous capsules were two-fold thicker and three-fold higher numbers of foreign body giant cells were observed in mice depleted of plasma fibronectin compared to controls. In contrast, deletion of plasma fibronectin did not alter acute leukocyte recruitment to the biomaterial, indicating that plasma fibronectin modulates chronic fibrotic responses. These results implicate plasma fibronectin in the host response to implanted materials and identify a potential target for therapeutic intervention to enhance the biological performance of biomedical devices.

## CHAPTER 5

### REDUCED ACUTE INFLAMMATORY RESPONSES TO MICROGEL CONFORMAL COATINGS \*

\* Modified from AW Bridges, N Singh, KL Burns, JE Babensee, LA Lyon, and AJ García. Reduced acute inflammatory responses to microgel conformal coatings. *Biomaterials* (In press)

#### INTRODUCTION

Host inflammatory responses to implanted biomaterials limit device integration and biological performance for most classes of medical devices, including chemical biosensors, leads and electrodes for monitoring and/or stimulation, drug delivery systems, and orthopaedic implants.<sup>15</sup> These inflammatory responses to synthetic materials involve dynamic, multi-component and inter-dependent reactions comprising biomolecule (e.g., protein) adsorption, leukocyte recruitment, adhesion and activation, cytokine expression/release, macrophage fusion into multi-nucleated foreign body giant cells, tissue remodeling and fibrous encapsulation.<sup>15, 191</sup> The duration and intensity of these stages is dependent upon the extent of injury created at the implantation site and the biomaterial physicochemical properties.<sup>15</sup>

Significant biomaterial-based efforts have focused on engineering implant surface coatings to attenuate host inflammatory responses to implanted devices. Strategies focusing on the presentation/delivery of anti-inflammatory and/or pro-wound healing agents, such as heparin, dexamethasone, and superoxide dismutase mimetics, have demonstrated promising reductions in inflammatory responses and fibrous encapsulation.<sup>161, 177, 216</sup> These approaches, however, are limited by complex delivery

pharmacokinetics. For example, Reichert and colleagues demonstrated that combined release of dexamethasone and vascular endothelial growth factor reduced fibrous capsule thickness without changes in vascularization around implanted devices.<sup>161</sup> However, these benefits were lost at longer implantation times, possibly due to reductions in the release of bioactive agents. In addition to these bioactive approaches, non-fouling (i.e. protein adsorption-resistant) coatings, including dense polymeric films and brushes as well as hydrogels have been pursued to modulate inflammatory responses to implanted materials.<sup>147, 149, 188, 217-219, 220, 221, 222, 223</sup> The rationale for these passive approaches is that reduction in protein adsorption will lead to reduced leukocyte adhesion and activation, thereby attenuating the extent of the foreign body reaction. Although many of these coatings exhibit reduced protein adsorption and leukocyte adhesion/activation *in vitro*, inconsistent results have been obtained regarding the ability of these materials to reduce *in vivo* acute and chronic inflammatory responses.<sup>147, 188, 221, 224</sup> Possible explanations for the mixed *in vivo* results with these coatings include insufficient non-fouling behavior, coating degradation, and inflammatory mechanism(s) independent from protein adsorption.

Micro- and nano-structured hydrogels offer distinct advantages over traditional surface modifications, including high water content, high diffusivity for solute transport within polymer network, and the ability to incorporate multiple chemical functionalities to generate complex architectures.<sup>38, 225</sup> We recently developed a biomaterial coating strategy based on films of microgel particles of poly(*N*-isopropylacrylamide) (pNIPAm) cross-linked with short chains of non-fouling poly(ethylene glycol) (PEG) that render glass and polymeric substrates resistant to fibroblast adhesion *in vitro*.<sup>89</sup> The objective of

the present study was to evaluate *in vitro* and *in vivo* inflammatory cell responses to these microgel films tethered onto poly(ethylene terephthalate) (PET). PET was chosen as the base material because this polymer is used in many biomedical devices, including sutures, vascular grafts, sewing cuffs for heart valves, and components for percutaneous access devices. PET elicits acute and chronic inflammatory responses characterized by leukocyte adhesion and fibrous encapsulation.<sup>65, 226</sup> Furthermore, PET has been used a model biomaterial for numerous basic biomaterial-host interactions. We demonstrate that these microgel conformal coatings reduce *in vitro* monocyte/macrophage adhesion and spreading as well as leukocyte recruitment, adhesion, and pro-inflammatory cytokine expression to implanted PET in an *in vivo* acute inflammation model.

## **MATERIALS AND METHODS**

### ***Sample preparation***

Thin sheets of PET (AIN Plastics/ThyssenKrupp Materials NA, Madison Heights, MI) were cut into disks (8 mm diameter) using a sterile biopsy punch (Miltex Inc., York, PA) and rinsed briefly in 70% ethanol to remove contaminants introduced during the manufacturing process. pNIPAm microgel particles (100 mM total monomer concentration) were synthesized with 2 mol% PEG diacrylate (MW 575) by free radical precipitation polymerization.<sup>89</sup> Particles were synthesized with 10 mol% acrylic acid as a co-monomer to incorporate functional groups for future modification. Particle composition was confirmed by NMR. Particle size (hydrodynamic radius) and polydispersity were  $334 \pm 30$  nm and  $1.11 + 0.03$ , respectively. Microgels were deposited on the surface of PET disks using a spin coating process as previously

described.<sup>122</sup> All samples were rinsed in 70% ethanol on a rocker plate for 4 days, changing the solution daily to clean the samples and remove endotoxin contaminants. Prior to use, samples were rinsed three times in sterile phosphate buffered saline (PBS) and allowed to rehydrate for at least 1 h. Samples contained 10-fold lower levels of endotoxin than the United States Food and Drug Administration's recommended 0.5 EU/mL, as determined by the LAL chromogenic assay (Cambrex, East Rutherford, NJ).

### ***Biomaterial surface characterization***

X-ray photoelectron spectroscopy (XPS) analysis was performed on a Surface Science SSX-100 small spot ESCA Spectrometer using monochromatic Al K alpha X-rays, 800  $\mu\text{m}$  spot size, 150 eV pass energy, and take-off angle of 55°. Atomic force microscopy (AFM) images were obtained in AC mode on an Asylum Research MFP-3D atomic force microscope. Spring constants were calculated using the thermal method. Imaging and analysis was performed using the Asylum Research MFP-3D software (written in the IgorPro environment, WaveMetrics, Inc., Lake Oswego, OR). An Olympus AC160 cantilever with  $k = 42 \text{ N/m}$ ,  $f_0 = 300 \text{ kHz}$  was used for imaging.

### ***Fibrinogen adsorption***

Fibrinogen was selected as a model plasma protein to quantify protein adsorption onto biomaterial surfaces. The amount of surface-adsorbed protein was determined using a purified solution of radiolabeled fibrinogen diluted with unlabeled fibrinogen. Samples were incubated for 1 h in a mixture of <sup>125</sup>I-labeled human fibrinogen (65% purity, 95% clottable, specific activity of 0.86  $\mu\text{Ci}/\mu\text{g}$ , MP Biomedicals, Irvine, CA) and unlabeled



human fibrinogen (65% purity, 95% clottable, Sigma-Aldrich, St. Louis, MO) to generate a range (2-200  $\mu\text{g/mL}$ ) of coating concentrations. Tri(ethylene glycol)-terminated self-assembled monolayers on gold-coated glass coverslips and unmodified glass coverslips were used as controls. Following incubation in fibrinogen solutions, samples were rinsed in PBS, incubated for 30 min in a 1% solution of heat-denatured bovine serum albumin (BSA), and rinsed in PBS to remove loosely adsorbed proteins. A Packard Cobra II gamma counter was used to measure the level of radiolabeled fibrinogen adsorbed onto the samples. After correcting for background and label dilution, the amount of protein adsorbed on each sample was calculated as the radioactive counts divided by the surface area and specific activity. Pilot experiments demonstrated that the albumin incubation and buffer rinses only displace a small amount ( $< 10\%$ ) of adsorbed fibrinogen from these surfaces.

### ***Primary human monocyte isolation and culture***

Peripheral human whole blood was obtained from healthy volunteer donors at the Georgia Institute of Technology Student Health Center in accordance with an approved Institute Review Board protocol (H05012). To prepare autologous human serum, blood (120 mL) was centrifuged (3000 rpm, 10 min, room temperature) to pellet red blood cells. The supernatant was collected, pushing down clots manually using a sterile pipette tip, and allowing further clotting (90 min, room temperature) with clearance by another centrifugation (3000 rpm, 15 minutes, room temperature).

Human monocytes were isolated from whole blood immediately after collection using an established method developed by Anderson's group<sup>63, 85</sup> with slight

modifications. Cell isolations were performed on blood from three separate donors for three independent experiments (unpooled samples) with equivalent results. Blood (120 mL) was collected in heparin-coated syringes (333 U/mL blood, Baxter Healthcare, Deerfield, IL). The heparinized blood was transferred to polystyrene bottles (Corning, Corning, NY), diluted 1:1 with sterile PBS without calcium/magnesium, and gently swirled to mix. Peripheral blood mononuclear cells were separated using lymphocyte separation medium (Cellgro MediaTech, Herndon, VA) by differential gradient centrifugation (400g, 30 min at room temperature in a Thermo Fisher centrifuge, model # 5682, rotor IEC 216). The mononuclear cell layer was collected and erythrocytes lysed (155 mM ammonium chloride, 10 mM potassium bicarbonate and 0.1 mM EDTA) and washed twice with sterile PBS to remove the lysis buffer. This isolation procedure yielded > 95% viable cells as determined by Trypan blue exclusion. Flow cytometric analyses indicated  $50 \pm 5\%$  monocytes (CD14+) and  $46 \pm 3\%$  lymphocytes (CD14-). These yields for cell viability and monocyte fractions are consistent with previous reports.<sup>63, 202</sup>

Cells were resuspended at a concentration of  $5 \times 10^6$  cells/mL in culture media (RPMI-1640 containing 25 mM HEPES, 2 mM L-glutamine (Invitrogen), 100 U/mL penicillin/streptomycin (Cellgro) and 25% filter-sterilized autologous human serum), plated in a volume of 10 mL onto 100-mm Primaria™ culture plates, and incubated at 37 °C and 5% CO<sub>2</sub>. After 2 h, non-adherent cells were removed by rinsing three times with warm media. Cells were cultured for 10 days prior to plating onto experimental/control surfaces based on previous results showing that this time period provides for sufficient macrophage maturation.<sup>85</sup> Media changes occurred on days 3 and 6 of culture with

media containing heat-inactivated autologous serum (56 °C, 1 h) used on day 6. By day 10 in culture, this procedure yielded  $61 \pm 18\%$  macrophages (CD64+) and  $29 \pm 18\%$  lymphocytes. The purity of macrophages increases with time in culture as non-adherent lymphocytes are washed away. We note that there is evidence that lymphocytes modulate and support monocyte differentiation as well as monocyte activities on biomaterials,<sup>88</sup> suggesting that it is relevant to include this lymphocyte population in culture.

### ***In vitro murine and human macrophage adhesion***

Murine IC-21 macrophages (TIB-186, ATCC, Manassas, VA) were plated at a density of 67,000 cells/cm<sup>2</sup> on unmodified PET controls and microgel-coated samples. IC-21 cells were maintained in RPMI-1640 containing 25 mM HEPES, 2 mM L-glutamine, 100 U/mL penicillin/streptomycin and 10% fetal bovine serum at 37 °C and 5% CO<sub>2</sub>. Human monocytes were plated at 50,000 cells/cm<sup>2</sup> on microgel-coated PET or unmodified PET controls and maintained in culture media supplemented with 25% autologous human serum at 37 °C and 5% CO<sub>2</sub>. Following 48 h of culture, biomaterial samples were rinsed three times with sterile PBS to remove loosely adherent cells. Remaining adherent cells were stained with calcein-AM (live cells) and ethidium homodimer-1 (dead cells) (Invitrogen) and imaged using a Nikon E-400 microscope equipped with epifluorescence optics and image analysis. Five representative fields per sample (4-5 independent samples per condition) were acquired (10X Plan Fluor Nikon objective, 0.30 NA), and image analysis software (ImagePro, Media Cybernetics, Silver

Spring, MD) with in-house macros was used to count adherent cells and quantify cell spreading.

### ***Murine intraperitoneal implantation***

An established intraperitoneal implantation model was used to assess acute inflammatory responses.<sup>52, 65</sup> Animal procedures were conducted in accordance with an IACUC-approved protocol. Male 10-14 wk old C57BL/6 mice (Charles River Laboratories, Wilmington, MA) were anesthetized by isoflurane. Following a midline incision into the peritoneal cavity, sterile samples (two disks per mouse) were implanted for 48 h. Sham surgeries were performed on additional mice to be used as controls. Prior to explantation, the IP cavity was injected with 3 mL of sterile PBS containing sodium heparin (50 U/mL, Baxter Healthcare, Deerfield, IL) as an anticoagulant. The abdomen was then massaged briefly, the IP lavage fluid was collected using a syringe, and disks were retrieved for analysis. One disk was used for immunofluorescence staining of adherent cells, and the second disk was used to harvest adherent cells for flow cytometric analysis of intracellular cytokine levels. Animals were sacrificed using a CO<sub>2</sub> chamber.

### ***Immunofluorescence staining of adherent cells***

Following careful explantation from the intraperitoneal cavity, biomaterial disks were stored briefly in PBS until completion of the retrieval surgery. Samples were then rinsed three times in PBS and fixed with 10% neutral buffered formalin. Adherent cells were permeabilized using 0.1% Triton-X 100 in PBS. Fetal bovine serum (5%) in PBS was used to block non-specific protein binding. Explants were then incubated at room

temperature with a primary monoclonal antibody against the macrophage marker CD68 at a 1:200 dilution (clone KP1, Abcam, Cambridge, MA). After rinsing to remove excess antibody, explants were incubated in AlexaFluor 488-conjugated goat anti-mouse IgG antibody (1:200 dilution) and counterstained with rhodamine-phalloidin (1:100 dilution) and Hoechst (1:10,000 dilution) to stain actin filaments and nuclei, respectively. Isotype control antibodies and additional staining controls demonstrated specific staining of target epitopes with minimal background. Antibodies were diluted in a solution of 1% heat-denatured BSA in PBS, and all reagents were used at 4 °C. Samples were then rinsed five times in PBS and once in deionized H<sub>2</sub>O, mounted on glass slides with coverslips, and stored in the dark at 4 °C until imaged. Eight fields per sample were acquired (20X Plan Fluor Nikon objective, 0.45 NA), and ImagePro software (Media Cybernetics, Silver Spring, MD) with custom-designed macros was used to count the adherent cells. Results shown represent 5 or more animals per treatment group from a single implantation experiment.

#### ***Intracellular cytokine staining and flow cytometric analysis***

The second disk explanted from the intraperitoneal cavity was used for measurements of cytokine expression in implant-associated cells via flow cytometry. Explanted samples were rinsed briefly in PBS and quickly transferred to a 24-well plate, and lavage samples were centrifuged to pellet cells. Cytokine staining was performed using fluorophore-labeled antibodies according to the manufacturer's protocol (eBioscience, San Diego, CA). Briefly, 1.0 mL of warm brefeldin A solution (3 µg/mL) in serum-containing media was added to each sample (disk or lavage fluid) to inhibit

protein secretion into the media, and cells were incubated for 4 h at 37 °C to allow for cytokine accumulation within the cells.

Pilot experiments with different dissociation conditions were performed to identify protocols to efficiently isolate implant-associated cells with minimal cellular debris and appropriate staining and instrument settings for flow cytometry analysis. For cell harvest, samples were rinsed three times in cold PBS without calcium/magnesium. Disk-adherent cells were removed using warm trypsin (0.05% containing 0.53 mM EDTA), transferred to microcentrifuge tubes, and centrifuged at 300g. The resultant cell pellet was resuspended in 1.0 mL of 10% neutral buffered formalin, and tubes were shaken at low speed on a vortexer for 10 min. A series of rinse-and-centrifuge cycles were used to remove excess fixative, and cell pellets were resuspended in a combined permeabilization/blocking buffer and replaced on the vortexer for 20 min. Fluorophore-conjugated antibodies (APC-conjugated anti-mouse TNF- $\alpha$  (clone MP6-XT22), FITC-labeled anti-mouse IL-1 $\beta$  polyclonal antibody, PE anti-mouse MCP-1 (clone 2H5), FITC-labeled anti-mouse IL-10 polyclonal antibody, eBioscience) were added to the microcentrifuge tubes at the manufacturer's recommended dilutions and shaken in the dark for 1 h. A subset of samples were stained using macrophage- and neutrophil-specific markers (PE-conjugated anti-mouse F4/80 (clone BM8) and APC-labeled anti-mouse Gr1 (clone RB6-8C5) from eBioscience and Miltenyi Biotec, Auburn, CA) to label and identify the cell populations of interest. Cells were then subjected to another series of rinse-and-centrifuge cycles to remove excess antibody and resuspended in PBS. A Becton Dickinson BD LSR digital flow cytometer was used to measure the fluorescently-labeled intracellular cytokines (counting 10,000 events per sample), and

FlowJo software v7.2 (Tree Star Inc., Ashland, OR) was used to analyze the data. Results shown represent 4-8 animals per treatment group from a single implantation experiment.

### *Statistical analysis*

Data are presented as mean  $\pm$  standard error. Statistical analysis was performed by ANOVA using Systat 11.0 (Systat Software Inc., San Jose, CA). Flow cytometry histograms were compared using the Kruskal-Wallis non-parametric test. Pair-wise comparisons were performed using Tukey post-hoc tests with a 95% confidence level considered significant.

## **RESULTS**

### *Deposition of microgel particles as conformal coatings*

PET substrates (**Figure 5.1a**) were functionalized with p(NIPAM-co-AAc-co-PEGDA) microgel particles (**Figure 5.1b and c**), which were covalently attached to the surface via the incorporation of an aminobenzophenone photoaffinity label followed by UV excitation to form a covalently cross-linked coating<sup>122</sup> (**Figure 5.1**). Biomaterial surfaces were analyzed for both chemical composition and the uniformity of microgel deposition using XPS and AFM, respectively. XPS survey scans revealed the presence of carbon and oxygen groups on unmodified PET controls and microgel-coated surfaces (**Figure 5.1d and e**, respectively). Nitrogen groups (400 eV binding energy) were present only on microgel-coated surfaces (**Figure 5.1e**). With respect to elemental composition, PET substrates contained approximately 72% carbon and 25% oxygen,

whereas microgel coatings contained 77% carbon, 15% oxygen, and 9% nitrogen (all 1s orbitals). Additional high resolution scans confirmed multiple carbon bonds corresponding to the chemical structures of the PET substrate and microgel coatings (**Figure 5.1f and g**, respectively). In particular, there was an abundance of amide bonds characteristic of pNIPAm in the microgel coating. This chemical composition is consistent with the theoretical values.

AFM images were obtained and rendered in three dimensions (**Figure 5.2**) to visualize surface topography of the biomaterials. PET displayed a generally smooth surface (< 200 nm) exhibiting scratches and surface defects (**Figure 5.2a**), most likely arising from the manufacturing process. Spin coating-based deposition of the microgel particles resulted in a conformal coating on the surface with microgel particles effectively filling in scratches and covering ridges commonly present on the surface of the underlying PET substrate (**Figure 5.2b**). The thickness of these microgel coatings is on average 160 nm (dry) and 300 nm (swollen), as determined by AFM. Comparisons between AFM analyses of substrates with incomplete and full microgel coverage indicated monolayer particle deposition, with no evidence of multilayer formation. More expansive 50 x 50  $\mu\text{m}^2$  scans also confirmed uniform microgel coverage (results not shown). The presence of these pNIPAm-specific nitrogen groups, along with AFM image analysis, confirms that the microgel particles were successfully deposited on the surface of PET disks.



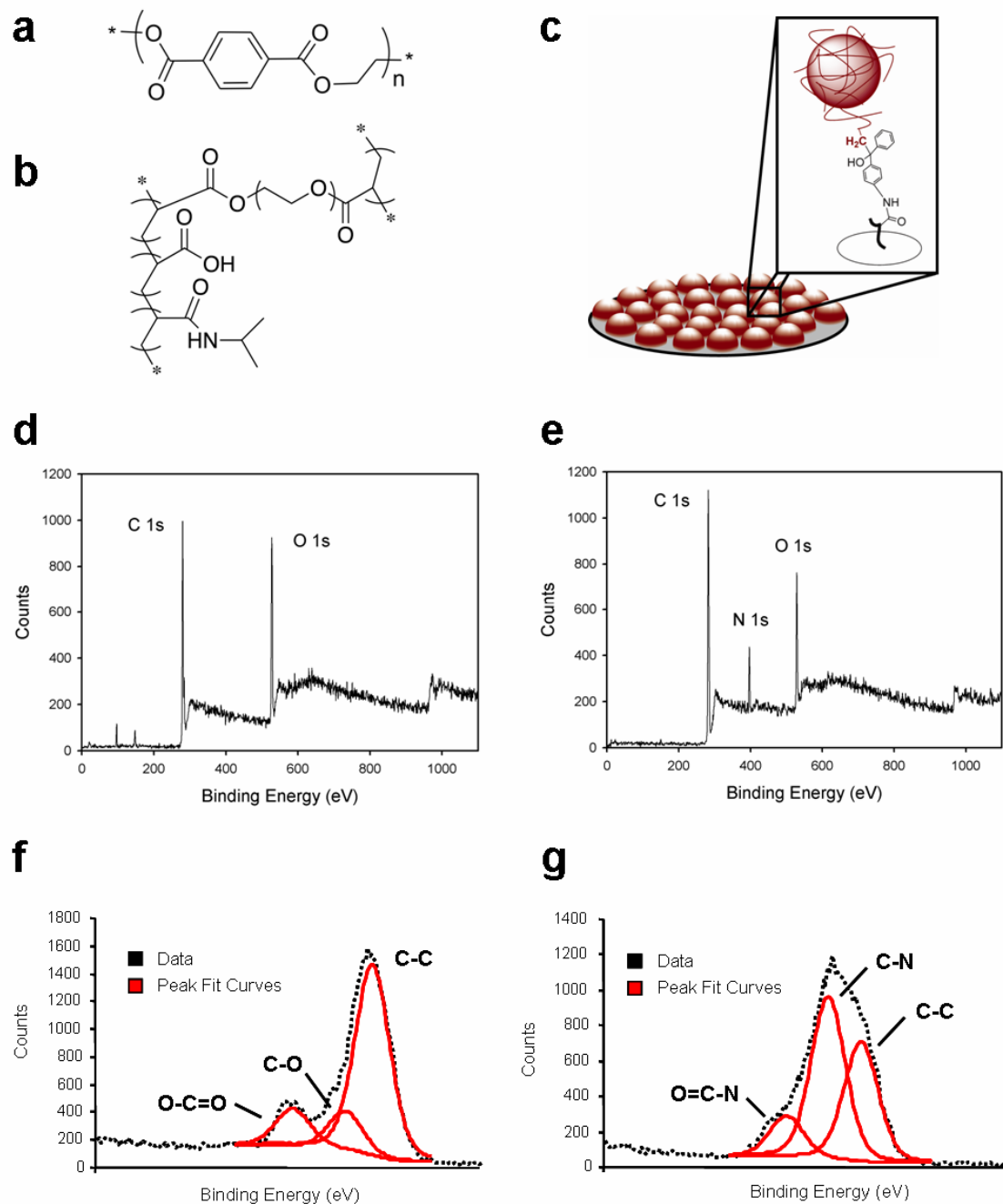


**Figure 5.1: Surface characterization of biomaterials.** Chemical structures of the unmodified PET (a) and p(NIPAM-co-AAc-co-PEGDA) microgel particles (b) are shown for reference. (c) Microgel particles (red spheres) are covalently attached to the surface of the underlying PET substrate (gray disk) by photo-crosslinking to create a polymeric coating. XPS analysis reveals the presence of nitrogen groups characteristic of C-N bonds on the surface of microgel-coated PET (e) that are absent in unmodified PET controls (d). High resolution carbon 1s data was deconvoluted, and software was used to assign peak values and determine individual carbon bonds. Results are shown for unmodified PET (f) and microgel-coated PET (g). Importantly, microgel coatings contain C-N bonds, characteristic of the amide groups in the pNIPAm particles.

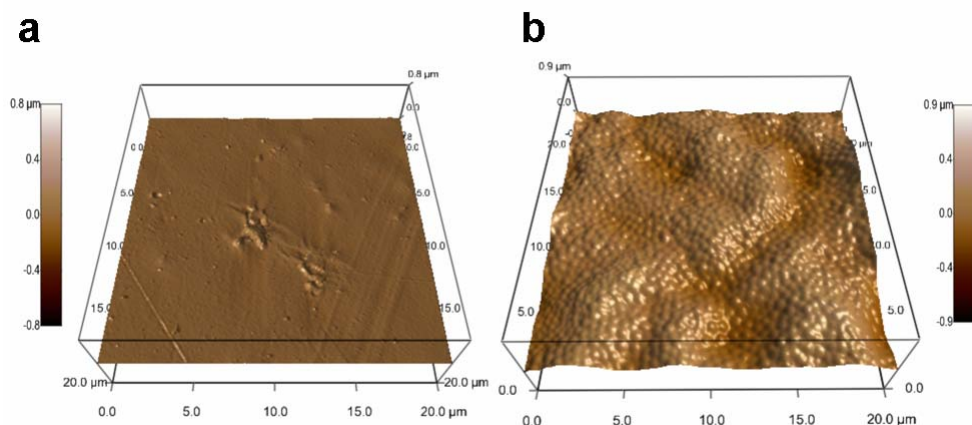


**Figure 5.2: Topography of biomaterial surfaces.** Representative 3D renderings of atomic force microscopy images demonstrate that the functionalization strategy yields a conformal coating of microgel particles (b) compared to unmodified PET controls (a).

### *Fibrinogen adsorption studies*

We next examined the ability of these microgel coatings to attenuate protein adsorption. Fibrinogen was selected as the model protein for adsorption studies as this plasma component has been extensively studied in the context of host responses to synthetic materials. In addition to playing a central role in platelet adhesion to blood-contacting materials, fibrinogen adsorption promotes *in vitro* and *in vivo* leukocyte recruitment and adhesion to biomedical materials.<sup>52, 65, 202</sup> Protein adsorption onto the surfaces was measured using <sup>125</sup>I-labeled human fibrinogen from a purified solution (Figure 5.3). Microgel-coated samples adsorbed 7-fold lower levels of fibrinogen compared to unmodified PET disks. Additionally, the PEG-based microgel coatings performed comparably to tri(ethylene glycol)-terminated self-assembled monolayers (EG<sub>3</sub> SAMs) on gold-coated glass substrates, which have been extensively examined as model non-fouling surfaces.<sup>30</sup> Moreover, we previously demonstrated that microgel coatings reduce albumin adsorption to background levels.<sup>89</sup> Taken together, these results

demonstrate that microgel-based coatings significantly reduce protein adsorption onto the underlying biomaterial substrate.

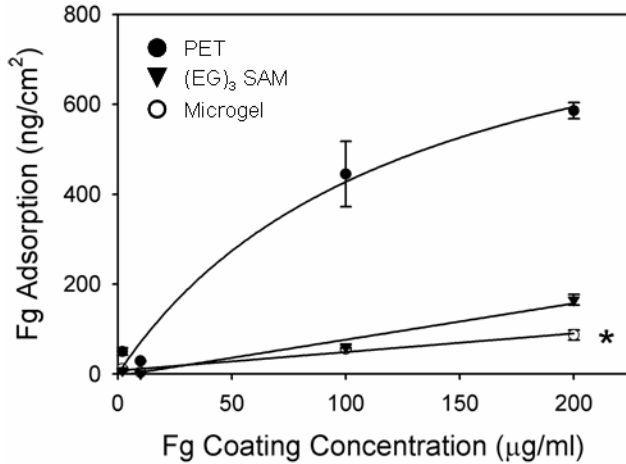


**Figure 5.3: Protein adsorption profiles on biomaterial surfaces.** Microgel-coated surfaces adsorb 7-fold lower levels of purified human fibrinogen than unmodified PET controls and also display comparable biofouling resistance to tri(ethylene glycol)-terminated self-assembled monolayers on gold, \*  $p < 0.001$ .

### *In vitro leukocyte adhesion*

We evaluated *in vitro* monocyte/macrophage adhesion to microgel-coated and unmodified PET as a model of the leukocyte recruitment/adhesion events in the acute phase of biomaterial-induced inflammation. Murine IC-21 macrophages were plated and cultured for 48 h on biomaterials, and adherent cells were imaged and scored for viability, adherent cell density, and spread area. Unmodified PET control samples supported significant levels of cell adhesion, whereas microgel coatings exhibited 40-fold lower levels of IC-21 macrophage adhesion (**Figures 5.4a and b**, respectively), as

quantified in **Figure 5.4c** ( $p < 1.2 \times 10^{-5}$ ). Furthermore, cells adherent to unmodified PET samples had almost double the cytoplasmic spread area of those associated with microgel-coated samples (**Figure 5.4d**,  $p < 1.2 \times 10^{-5}$ ). Calcein-AM/ethidium homodimer (Live/Dead™) staining showed  $> 98\%$  viability for both surfaces.

We performed similar studies with primary human monocytes/macrophages isolated from whole blood, as these primary cells represent a more clinically relevant model.<sup>15</sup> After 48 h in culture with biomaterial surfaces, adherent cells were imaged and scored for viability, adherent cell density, and spreading area. In good agreement with the murine macrophage line results, unmodified PET supported high numbers of adherent primary monocytes (**Figure 5.5a**), whereas microgel coatings (**Figure 5.5b**) reduced primary human monocyte/macrophage adherent cell numbers by 3-fold compared to control substrates. These results are shown graphically in **Figure 5.5c** ( $p < 1.1 \times 10^{-4}$ ). In addition, cells adherent to unmodified PET control surfaces exhibited more cell extensions and had double the cytoplasmic spread area of those associated with microgel-coated samples (**Figure 5.5d**,  $p < 1.2 \times 10^{-5}$ ). Calcein-AM/ethidium homodimer staining showed  $> 95\%$  viability for both substrates. These results demonstrate that microgel coatings significantly reduce monocyte/macrophage adhesion and spreading compared to control PET supports.

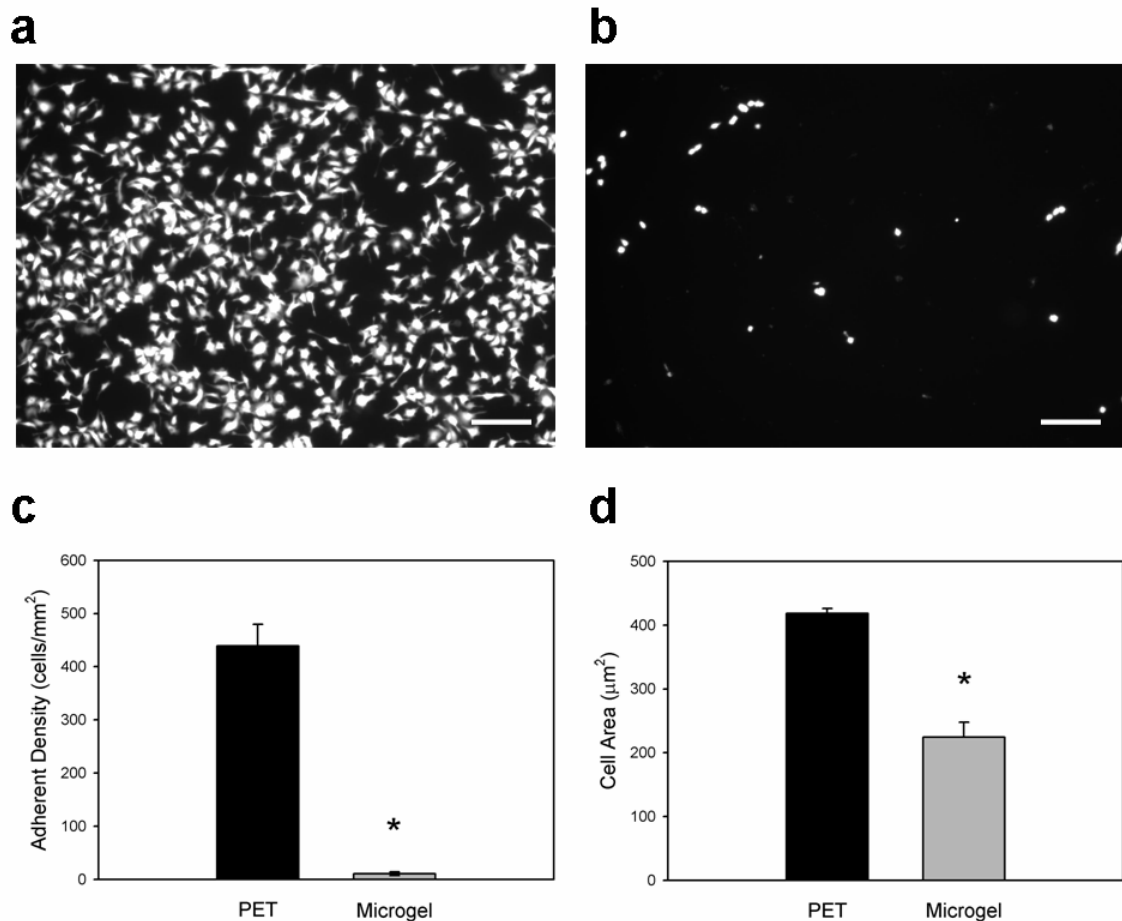


**Figure 5.4: Murine IC-21 macrophage adhesion to biomaterial surfaces.** Adherent cells were scored for viability, and cell density and area were quantified. Compared to unmodified PET substrates (a), microgel coatings (b) reduce macrophage adhesion to biomaterial surfaces. (c) Unmodified PET supported 40-fold higher levels of adherent macrophages compared to microgel-coated samples, which virtually eliminated cell adhesion, \*  $p < 1.2 \times 10^{-5}$ . (d) Adherent macrophages also exhibited more cell extensions and significantly larger surface areas on unmodified PET controls than on microgel-coated surfaces, \*  $p < 1.2 \times 10^{-5}$ . Data is presented as the average value  $\pm$  standard error of the mean using  $n = 5$  samples per treatment group. Scale bar is 100  $\mu\text{m}$ .

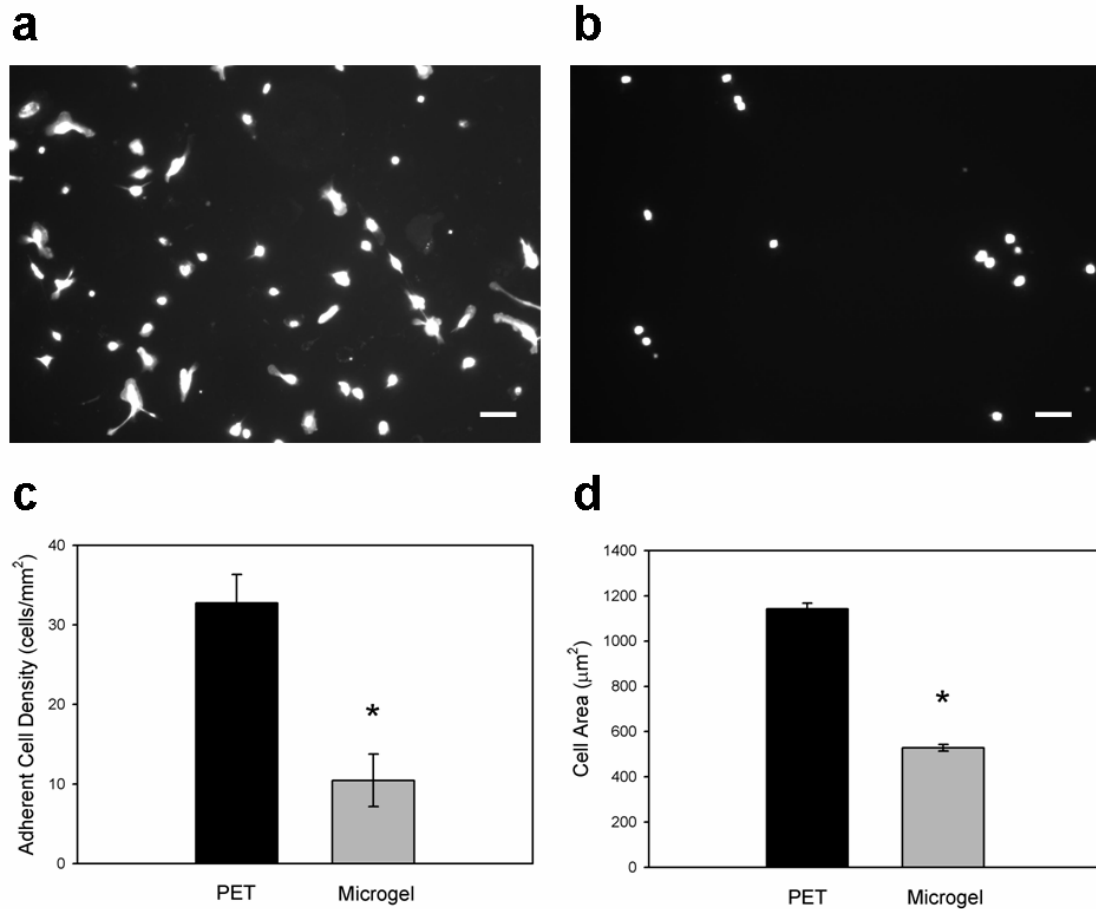


**Figure 5.5: *In vitro* human primary macrophage adhesion to biomaterial surfaces.** Adherent cells were scored for viability, and cell density and spread area were quantified. Compared to unmodified PET substrates (a), microgel coatings (b) reduce macrophage adhesion to biomaterial surfaces. (c) Microgel coatings elicit a 3-fold reduction in cell adhesion compared to unmodified PET surfaces, \*  $p < 1.1 \times 10^{-4}$ . (d) Adherent macrophages also exhibit more cell extensions and 2-fold larger surface areas on unmodified PET controls than on microgel-coated surfaces, \*  $p < 9.5 \times 10^{-7}$ . Data is presented as the average value  $\pm$  standard error of the mean using  $n = 5$  samples per treatment group. Scale bar is 100  $\mu\text{m}$ .

### *Acute inflammatory cell responses to microgel coatings*

We next evaluated early cellular responses to biomaterials implanted in the intraperitoneal cavity of mice. Tang and colleagues have established this model to examine leukocyte recruitment to implanted biomaterials during the acute inflammatory process.<sup>52, 65</sup> Unmodified and microgel-coated PET disks (2 samples per mouse) were implanted for 48 h and then explanted and analyzed to determine leukocyte recruitment and adhesion as well as pro-inflammatory cytokine expression. Mice surgically treated but not receiving any biomaterial disks were used as sham controls.

One disk explanted from each mouse was used to examine leukocyte recruitment and adhesion by cell staining and fluorescence microscopy. Following fixation and permeabilization, adherent cells were stained using an antibody against CD68 (macrophage marker), rhodamine phalloidin (actin filaments), and Hoechst (nuclei). Unmodified PET control samples displayed a dense monolayer of adherent cells (**Figure 5.6a**). In contrast, significantly fewer cells were attached to the microgel-coated samples (**Figure 5.6b**). Quantification of adherent cells demonstrated a 4.6-fold reduction in cell density for microgel-coated samples compared to unmodified PET ( $p < 1.1 \times 10^{-5}$ , **Figure 5.6c**). Furthermore, higher magnification images demonstrated fewer CD68+ macrophages on microgel-coated samples (**Figure 5.6d**) compared to unmodified PET controls (**Figure 5.6e**). Similar results in terms of differences in adherent cell numbers between microgel-coated and unmodified PET surfaces were observed for in a small number of samples implanted in the murine intraperitoneal space for 16 h.

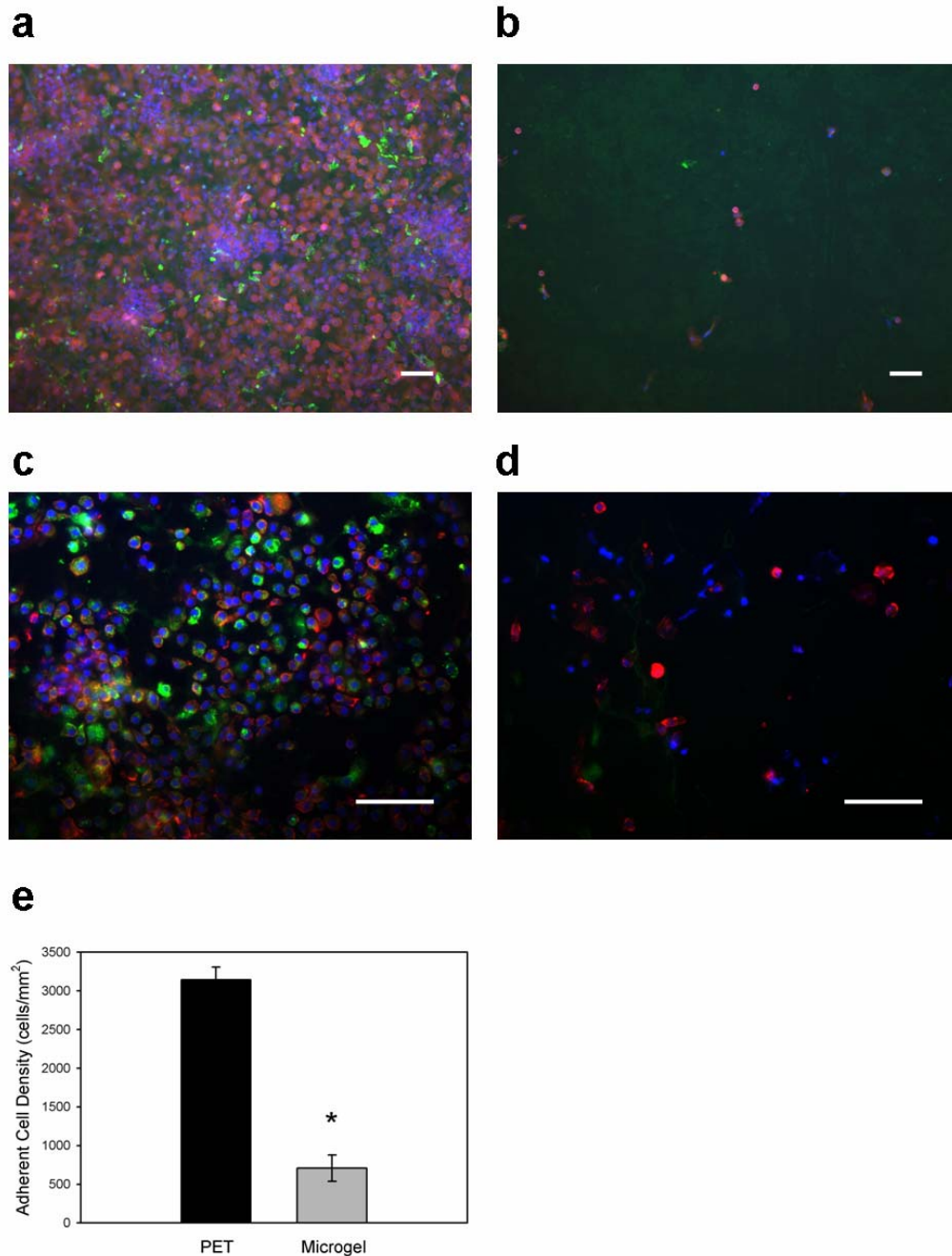


**Figure 5.6: *In vivo* leukocyte adhesion to implanted biomaterials.** Biomaterial disks were implanted in the murine peritoneal cavity for 48 h. Explants were immunostained for macrophage marker CD68 (green), actin (red), and DNA (blue). Representative images taken with 20X (**a, b**) and 40X (**c, d**) objectives are presented. In contrast to unmodified PET controls (**a**), microgel-coated disks (**b**) effectively reduced leukocyte adhesion on these implants by a factor greater than 4-fold as quantified in (**e**), \*  $p < 1.1 \times 10^{-5}$ . In addition, fewer macrophages were observed on microgel-coated (**d**) surfaces than on unmodified PET controls (**c**). Data is represented as the average value  $\pm$  standard error of the mean using  $n = 5$  or more samples per treatment group. Scale bar is 50  $\mu\text{m}$ .



We also examined the expression of inflammatory cytokines (TNF- $\alpha$ , IL-1 $\beta$ , MCP-1, and IL-10) in implant-associated cells at 48 h of implantation by flow cytometry as a measure of leukocyte activation. This cytokine profile was selected based on previous reports of acute cytokine expression around biomaterial implants.<sup>111, 227, 228, 229</sup> To ensure that the flow cytometry analysis was performed on whole cells and not debris for the harvest procedure, we first stained a subset of the harvested samples for markers characteristic of the cell populations, mainly macrophages and neutrophils. **Figure 5.7a** shows a contour profile for forward scatter (FSC, proportional to particle size) vs. side scatter (SSC, proportional to antibody staining). The profile was gated for two major areas (P1, P2). The cell population in P1, which corresponds to 85-90% of the total number of events recorded, contains particles that (i) are large enough to represent whole cells (based on FSC values) and (ii) stain positive for macrophages and neutrophils. We therefore performed analyses for cytokine expression on this P1 cell population. This type of analysis is consistent with standard immunology flow cytometric analysis.<sup>230</sup>

**Figures 5.7b-d** present histograms showing cell counts (y-axis) as a function of cytokine staining intensity (x-axis). For TNF- $\alpha$ , IL-1 $\beta$ , and MCP-1, the histograms for microgel-coated PET show a left-ward shift compared to the histograms for untreated PET. Kruskal-Wallis non-parametric tests indicated that the histograms for microgel-coated PET were statistically different from histograms for control PET ( $p < 0.02$ ). In addition, ANOVA of the geometric means for histograms from independent samples showed that microgel-coated samples contained significantly lower levels of pro-inflammatory TNF- $\alpha$ , IL-1 $\beta$ , and MCP-1 than unmodified PET controls (**Figure 5.7e-g**, respectively;  $p < 0.003$ ). No significant differences were detected between groups for

levels of anti-inflammatory IL-10 (results not shown). Additionally, a peritoneal lavage was performed to collect fluid in the tissue exudates proximal to the implant. No differences were detected between surface treatments for pro-inflammatory cytokine expression of cells in the exudate, and these levels of cytokine expression were similar to the sham controls. These results demonstrate that leukocyte activation was dependent on adhesion to the biomaterial implant. Furthermore, microgel coatings attenuate leukocyte activation and significantly reduce expression of pro-inflammatory cytokines compared to PET substrates.

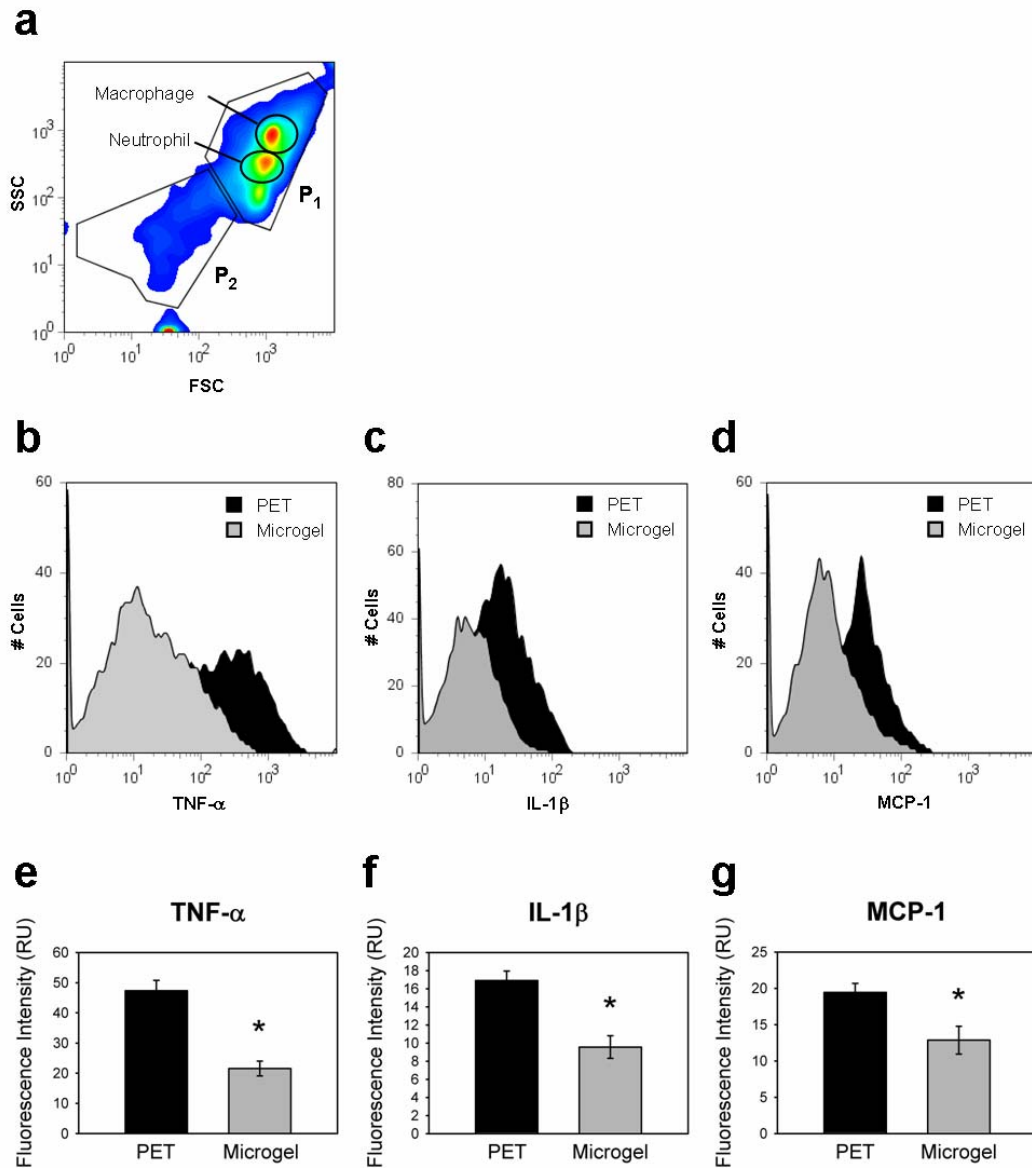


**Figure 5.7: Quantification of *in vivo* intracellular cytokine expression by flow cytometric analysis.** Disk-associated cells were harvested from implants and stained intracellularly for various cytokines, and several samples were stained for macrophage- or neutrophil-specific extracellular markers. (a) Two main populations of cells (P<sub>1</sub> and P<sub>2</sub>) were observed on FSC vs. SSC plots. Macrophage and neutrophil populations of interest were both contained within P<sub>1</sub>, so cytometry profiles were gated using P<sub>1</sub> for all subsequent data analysis. (b, c, d) Representative histograms show a significant population shift between unmodified PET controls and microgel-coated PET for the three cytokines examined. (e, f, g) Cells adherent to unmodified PET samples contained significantly higher levels of intracellular TNF-α (e), IL-1β (f), and MCP-1 (g) than microgel-coated samples, \*  $p < 0.003$ . Data is presented as the unbiased geometric means of the populations  $\pm$  standard error of the mean using  $n = 4$  or more samples per treatment group.

## DISCUSSION

We present a coating strategy based on thin films of poly(*N*-isopropylacrylamide-*co*-acrylic acid) hydrogel microparticles cross-linked with PEG diacrylate. These microgel particles were spin-coated and covalently grafted onto PET substrates. XPS and AFM analyses demonstrated that these particles were deposited as dense conformal coatings. Attractive features of this coating technology include (i) precise control over particle synthesis in terms of composition and structure, (ii) ability to generate complex architectures and/or functionalities, including controlled drug release, and (iii) ability to generate “mosaic” complex coatings containing variations in particle composition and/or spatial arrangement via modular assembly and soft lithography.<sup>38</sup> In addition, these particles can be deposited onto different substrates by various means, including spin coating, centrifugation, and dip-coating. We note that the amount of mass attached with just a few chemical reactions at the surface is potentially extraordinarily high, which should be beneficial for obtaining high densities of PEG and good surface coverage. Compared to many “grafting-to” and surface polymerization reactions, this approach provides a more controllable route. Nevertheless, generation of dense, conformal microgel coatings requires optimization of particle deposition parameters, including covalent tethering, and may not be easily applicable to surfaces with complex geometries/topographies.

We examined *in vitro* protein adsorption onto microgel-coated and uncoated PET using radiolabeled fibrinogen as a model plasma protein. Microgel coatings significantly reduced fibrinogen adsorption compared to unmodified PET. Additionally, the PEG-based microgel coatings performed equivalently to self-assembled monolayers presenting

tri(ethylene glycol). The significant reductions in adsorbed fibrinogen for microgel coatings are in good agreement with previous results for low adsorption of serum albumin to these films.<sup>89</sup> We attribute the reductions in protein adsorption to microgel coatings to the presentation of PEG ‘loops’ at the microgel surface resulting from temperature-induced deswelling of pNIPAm at physiological temperatures.<sup>89, 231</sup> The levels of fibrinogen adsorbed onto microgel coatings (60 ng/cm<sup>2</sup> at 30 µg/mL coating concentration) are comparable to protein densities (40-60 ng/cm<sup>2</sup>) adsorbed onto PEG/PEO polymers grafted onto surfaces.<sup>232, 233</sup> However, the density of fibrinogen adsorbed onto the microgel coatings is considerably higher than protein densities (< 10 ng/cm<sup>2</sup>) adsorbed onto dense brushes of oligo(ethylene glycol)methacrylate and poly(2-methacryloyloxyethyl phosphorylcholine) generated by surface-initiated polymerization reactions.<sup>217, 234, 235</sup> Furthermore, the fibrinogen adsorption levels for the microgel coating are also higher than fibrinogen adsorption values (< 10 ng/cm<sup>2</sup>) reported for glow discharge plasma-deposited tetraethylene glycol dimethyl ether densely cross-linked coatings (“tetraglyme”).<sup>146, 202</sup> The differences in protein adsorption resistance among these coating technologies probably arise from differences in the architecture/structure of the PEG chains as the chain length and grafting density strongly influence “non-fouling” behavior.<sup>116, 217</sup> An alternative explanation for the higher values of adsorbed fibrinogen to the microgel coatings is that there are spaces between microgel particles below the resolution of the AFM rendering that provide sites for protein adsorption. This potential limitation could be addressed by using a different deposition technique or multi-layers of microgel particles. Finally, it is important to note that additional experiments with more

complex protein solutions, such as plasma, are required to fully characterize the protein-adsorption resistant properties of these coatings.

Microgel-coated PET exhibited significant reductions in *in vitro* cell adhesion and spreading compared to untreated PET for both an established murine macrophage cell line and primary human monocytes/macrophages. The reduced levels of cell adhesion and spreading on microgel-coated surfaces provide indirect evidence for the lack of adsorption of cell-adhesion promoting proteins. We observed high levels of viability between surface conditions, so we do not attribute the differences in adherent cell numbers and spreading to differences in cell viability between the surfaces. These cell adhesion results are consistent with previous reports of very low *in vitro* monocyte/macrophage adhesion to PEG-functionalized materials such as tetraglyme and PEG-star coatings.<sup>188, 220</sup> In contrast, other studies showed high monocyte/macrophage adhesion to surfaces grafted with PEO polymers or PEG-containing interpenetrating networks;<sup>138, 149</sup> however, *in vitro* macrophage fusion into foreign body giant cells was significantly decreased on these coatings. The reason(s) for these discrepancies in monocyte/macrophage adhesion among PEG-based coatings remains poorly understood. These PEG-based coatings significantly reduce protein adsorption, albeit to different extents, and prevent adhesion of other cell types such as osteoblasts and endothelial cells. Possible explanations include (i) differences in adhesion receptor repertoire or numbers between primary monocytes/macrophages and other cell types and (ii) increased cell type-dependent degradation/modification of the underlying PEG coating.

We evaluated acute inflammatory cellular responses to microgel coatings in a murine intraperitoneal implant model. Microgel coatings significantly reduced the

number of adherent leukocytes compared to uncoated PET at 48 h of implantation. Similar differences were observed in a small number of samples implanted for 16 h. These reductions in *in vivo* leukocyte adhesion for the microgel coatings are in good agreement with our *in vitro* cell adhesion findings. Furthermore, analysis of cytokine expression in adherent leukocytes demonstrated that microgel coatings reduced expression of the pro-inflammatory cytokines TNF- $\alpha$ , IL-1 $\beta$ , and MCP-1 compared to untreated microgel coatings following 48 h implantation. This analysis is based on comparing equal numbers of cells; because microgel-coated implants contained 4.6-fold fewer cells than untreated PET implants, we expect that the total cytokine load will be significantly reduced for the microgel-coated implants. Differences in cytokine expression were only detected for adherent cells and were not evident in cells isolated from lavage fluid, suggesting that adhesion to the implant was necessary for increased cytokine expression. Taken together, these results indicate that microgel coatings reduce acute inflammatory cell adhesion and cytokine expression *in vivo*. Finally, we note that the use of flow cytometry for analysis of cytokine expression provides a sensitive and powerful “per cell” assay that allows direct comparisons between cell populations, especially when compared to population-averaged assays such as ELISA. However, the flow cytometry-based assay is limited to measuring intracellular, but not secreted, cytokines and provides relative (not absolute) measurements.

The significant reductions in leukocyte adhesion and activation (cytokine expression) for microgel-coated PET contrast with reports for *in vivo* leukocyte adhesion to PEG/PEO-coated materials.<sup>188, 224, 236</sup> For instance, Horbett and colleagues demonstrated high levels of leukocyte adhesion to tetraglyme coatings after 1-day

subcutaneous implantation,<sup>188</sup> even though they reported reduced *in vitro* adhesion of monocytes/macrophages.<sup>139</sup> These investigators attributed the increased levels of *in vivo* leukocyte adhesion to degradation of the tetraglyme coating and inadequate non-fouling behavior. Interestingly, *in vitro* cell adhesion studies in the presence of whole blood or 10% autologous plasma revealed increased levels of leukocyte adhesion and spreading, consistent with the *in vivo* observations. The differences in adhesive activities between various media conditions (whole blood, 10% plasma, and 10% serum) suggest that differences in protein adsorption, possibly fibrinogen, account for the observed responses. This possibility warrants further examination. Nonetheless, it is evident from the preceding discussion that there is no simple correlation among protein adsorption, *in vitro* monocyte/macrophage adhesion, and *in vivo* leukocyte adhesion for PEG-based coatings.

Several mechanisms could explain the ability of microgel coatings to significantly reduce *in vivo* leukocyte adhesion and cytokine expression, especially when considering that these coatings exhibited higher levels of protein adsorption compared to tetraglyme and other PEO-based films. First, the higher levels of adsorbed proteins may be due to adsorption in spaces between microgel particles that are inaccessible to cells, resulting in dense conformal coatings with respect to the cells. Alternatively, because our assembly process deposits a high volume polymer film (swollen microgel coatings are ~ 300 nm thick, tetraglyme coatings are 100 nm<sup>146</sup>) it is possible that the microgel coatings undergo slower overall degradation than other coatings. Finally, an intriguing possibility is that the topography, in combination with the surface chemistry, of the microgel coating reduces leukocyte adhesion. Siedlecki *et al.* recently demonstrated that sub-micron



surface features (pillars) reduce platelet adhesion and activation.<sup>237</sup> Regardless of the underlying mechanism(s) responsible for the observed acute cellular responses, additional analyses with longer implantation times to examine chronic inflammatory responses and fibrous encapsulation are required to establish the potential of this microgel technology as a coating strategy for biomedical devices.

## CONCLUSION

We present a coating strategy based on thin films of poly(*N*-isopropylacrylamide-*co*-acrylic acid) hydrogel microparticles cross-linked with poly(ethylene glycol) diacrylate. Simple spin coating and cross-linking of these particles to substrates generated conformal coatings that significantly reduced fibrinogen adsorption and *in vitro* adhesion and spreading of an established macrophage cell line and primary human monocytes. More importantly, these coatings reduced leukocyte adhesion to polymer implants and attenuated the expression of pro-inflammatory cytokines *in vivo*. These microgel coatings can be applied to biomedical implants as a protective coating to attenuate biofouling as well as leukocyte adhesion and activation in biomedical and biotechnological applications.

## CHAPTER 6

### CHRONIC INFLAMMATORY RESPONSES TO MICROGEL-BASED IMPLANT COATINGS

#### INTRODUCTION

Although biomaterials and implantable devices are widely used to treat a variety of medical conditions, they elicit a host foreign body response (FBR) that often impairs wound healing and tissue remodeling.<sup>1</sup> The severity and extent of the response to an implanted material directly affects the probability for its successful integration. Inflammatory responses significantly interfere with the biological performance of these devices, often resulting in failure that may require secondary surgeries and ultimately puts a patient's health at risk. Short-term or temporary implants, such as degradable scaffolds, may not cause extensive issues. However, inflammatory events cause a range of adverse responses on long-term or permanent implants including thrombogenic responses on vascular grafts,<sup>2, 3</sup> degradation and stress cracking of pacemaker leads,<sup>4, 5</sup> tissue fibrosis surrounding mammary prostheses,<sup>6</sup> reactive gliosis around neural probes,<sup>9</sup> degradation in glucose biosensor function,<sup>10</sup> and generation of wear debris around orthopedic joint prostheses.<sup>7, 8</sup>

Chemicals released from cells and injured tissue continue to mediate the response proximal to the implant,<sup>39</sup> and these persistent inflammatory stimuli lead to insufficient healing of tissue at the device interface. Fibrous capsule formation around the implant and the presence of foreign body giant cells (FBGCs) at the tissue-material interface are the hallmarks of a chronic phase inflammatory response. The  $\alpha_M\beta_2$  integrin and macrophage mannose receptor (MMR) have been identified as critical components for

FBGC formation.<sup>84</sup> Although the molecular mechanisms leading to macrophage fusion have not been fully elucidated, soluble molecules, signal transducers, and numerous receptors are likely involved.<sup>15</sup> FBGCs have been implicated in biodegradation of polymeric implants through surface oxidation and enzymatic degradation.<sup>16, 17, 51</sup> Multi-nucleated giant cells have been observed in chronically inflamed tissues, yet the physiological significance and precise role of FBGCs at the tissue-material interface is poorly defined. The cell-cell interactions of the FBR are quite complex, and the overall biological response to implanted materials is likely a composite of macrophages, fibroblasts, lymphocytes, and FBGCs. Further elucidation of the molecular events governing inflammation will aid in the development of implantable materials with more appropriate host responses.

Significant research efforts have focused on modifying material properties to generate implants that appropriately integrate with the host tissue while eliciting minimal undesirable effects. A common approach to reduce inflammatory responses is the use of non-fouling (protein adsorption-resistant) thin-layer polymeric coatings, which have been developed in various forms including polymer brushes and thin or bulk hydrogels. Although many of these methods have been effective when tested *in vitro*, these coatings usually exhibit high levels of adherent leukocytes, persistent inflammation, and fibrous encapsulation of the implant.<sup>161, 170, 188</sup> Long-term tissue fibrosis is particularly limiting for interactive implants such as biosensors, biomedical leads and electrodes, encapsulated cells, and drug delivery systems, because it impedes exchange of nutrients and cellular byproducts with the surrounding medium.<sup>10, 18-24</sup> By controlling capsule thickness,

implant coatings may have the ability to maintain an open exchange of key biomolecules and extend the *in vivo* lifetime of these constructs.

Previously, we engineered and characterized a hydrogel-based coating composed of pNIPAm-*co*-AA microgel particles cross-linked with PEG diacrylate tethered onto a poly(ethylene terephthalate) (PET) substrate.<sup>238</sup> PET was chosen as the base material because this polymer is used in many biomedical devices, including sutures, vascular grafts, sewing cuffs for heart valves, and components for percutaneous access devices. PET elicits acute and chronic inflammatory responses characterized by leukocyte adhesion and fibrous encapsulation.<sup>65, 226</sup> Our previous results showed that these microgel coatings reduced events associated with acute inflammation (i.e. protein adsorption and cell adhesion) and significantly reduced leukocyte recruitment and cytokine expression *in vivo* at early time points.<sup>238</sup> In the present study, we evaluated chronic host responses to these microgel coatings. We demonstrate that these conformal microgel coatings reduce fibrous capsule thickness and alter the cellular composition at the implant interface.

## **MATERIALS AND METHODS**

### ***Sample preparation***

Thin sheets of poly(ethylene terephthalate) (AIN Plastics/ThyssenKrupp Materials NA, Madison Heights, MI) were cut into disks (8 mm diameter) using a sterile biopsy punch (Miltex Inc., York, PA) and rinsed briefly in 70% ethanol to remove contaminants introduced during the manufacturing process. Microgel particles were synthesized with 10 mol% acrylic acid as a co-monomer to incorporate functional groups

for future modification. pNIPAm-*co*-AA microgel particles (100 mM total monomer concentration) were synthesized with 2 mol% PEG diacrylate (M.W. 575) by a free radical precipitation polymerization method and deposited on the surface of PET disks using a spin coating process as previously described.<sup>122</sup> Unmodified PET disks were used as controls.

Self-assembled monolayers (SAMs) of alkanethiols on gold were used as a reference material, since they have been extensively characterized as non-fouling substrates.<sup>30</sup> Gold-coated substrates were prepared by sequential deposition of titanium (100 Å) and gold (200 Å) films via an electron beam evaporator (Thermionics Laboratories, Hayward, CA,  $2 \times 10^{-6}$  Torr, 1 Å/s) onto clean PET disks (8mm diameter). Self-assembled monolayers were prepared by immersing gold-coated slides in a 1.0 mM solution of tri(ethylene glycol)-terminated alkanethiols (HS-(CH<sub>2</sub>)<sub>11</sub>-(OCH<sub>2</sub>CH<sub>2</sub>)<sub>3</sub>-OH; EG<sub>3</sub>) in ethanol for 4 h. Self-assembled monolayers were then rinsed in ethanol and deionized H<sub>2</sub>O.<sup>239</sup>

After surface functionalization, all samples were rinsed in 70% ethanol on a rocker plate for 4 days, changing the solution daily to remove endotoxin contaminants, and were stored in 70% ethanol until use. Samples contained 10-fold lower levels of endotoxin than the United States Food and Drug Administration's recommended 0.5 EU/mL,<sup>240</sup> as determined by the LAL chromogenic assay (Cambrex, East Rutherford, NJ). Prior to use, samples were rinsed three times in sterile phosphate buffered saline (PBS) and allowed to rehydrate in PBS for at least 1 hour.

### ***Subcutaneous implantation***

Samples (unmodified PET, microgel-coated PET, or EG<sub>3</sub>-coated PET;  $n = 8$  samples/group) were implanted subcutaneously following IACUC-approved procedures to evaluate the chronic phase foreign body response. Male 5-6 wk old Wistar rats (Charles River Laboratories, Wilmington, MA) were anesthetized by isofluorane. A single 1-cm incision was made on the dorsum proximal to the spine, and a subcutaneous pocket laterally spanning the dorsum was created. Sterile samples (two per subject on either side of the spine) were implanted, and the incision was closed using sterile wound clips. After four weeks, rats were sacrificed using a CO<sub>2</sub> chamber and samples were explanted, rinsed in sterile PBS, and fixed in formalin. Samples were carefully explanted with the surrounding tissue intact to avoid disrupting the cell-material interface. Explants were bisected in order to avoid edge effects and standardize the sectioning location for analysis, and they were paraffin-embedded for histological processing.

### ***Histological staining of explants***

Histological sections (5  $\mu\text{m}$  thick) were stained for various markers. A Verhoeff-van Gieson kit (Accustain® Elastic Stain kit from Sigma-Aldrich, St. Louis, MO) was used to stain collagen (pink), elastin fibers (black), and nuclei (dark blue). Sixteen total fields per sample (eight fields on both the muscle and skin sides of the implant) were acquired using a high magnification 60X Plan Apo Nikon objective (1.40 NA). ImagePro software (Media Cybernetics, Silver Spring, MD) was used to quantify fibrous capsule thickness. Results shown represent 4-7 animals per treatment group from a single implantation experiment.

Sections were also stained using immunohistochemical methods to determine the inflammatory cellular profile at the cell-material interface. Following proteolytic antigen retrieval with pronase (1 mg/mL solution for 10 min), sections were incubated in a mouse monoclonal antibody against the CD68 antigen of macrophages (clone ED1, AbD Serotec, Raleigh, NC), a biotinylated secondary antibody, and an avidin-linked alkaline phosphatase-based developing reagent (Vectastain® ABC-AP Kit, Vector Labs, Burlingame, CA), and counterstained with hematoxylin. Control sections (secondary antibody-only controls and tissue-specific controls) confirmed specificity of the primary antibody for this marker. Sixteen total fields per sample (eight fields on both the muscle and skin sides of the implant) were acquired using a high magnification 60X Plan Apo Nikon objective (1.40 NA). Images were blindly scored for total nuclei, CD68+ cells with one nucleus (macrophages), and CD68+ multi-nucleated cells (foreign body giant cells).

### ***Statistical analysis***

Data are presented as mean  $\pm$  standard error. Statistical analysis was performed by ANOVA using Systat 11.0 (Systat Software Inc., San Jose, CA). Pair-wise comparisons were performed using Tukey post-hoc tests with a 95% confidence level considered significant.

## RESULTS

### *Fibrous capsule formation surrounding implants*

Implanted materials were evaluated using an established subcutaneous rat model to determine the extent of chronic inflammation.<sup>1</sup> Unmodified PET, EG<sub>3</sub>-terminated SAMs coated on PET, and microgel-coated PET disks were randomized and implanted for 4 wk. Explants were processed histologically, and sections were analyzed for fibrous capsule development using a Verhoeff van Gieson kit to stain collagen and elastin fibers; all nuclei were counterstained for reference (**Figure 6.1**). The capsule was defined as the dense tissue adjacent to the implant, and image analysis of high magnification images was used to measure capsule thickness as the perpendicular distance starting at the capsule-implant interface and moving outward. Measurement of fibrous capsule thickness following subcutaneous implantation is a standard measure of chronic inflammation to synthetic materials.<sup>1</sup>

Unmodified PET controls promoted formation of a thick and dense collagenous fibrous capsule (**Figure 6.1a**). Importantly, microgel-coated samples (**Figure 6.1c**) significantly reduced fibrous capsule thickness by 22% compared to unmodified PET controls, as quantified in **Figure 6.1d** ( $p < 0.04$ ). No significant differences were detected between microgel-coated PET and EG<sub>3</sub> SAM or PET and EG<sub>3</sub> SAM (**Figure 6.1b**). The average capsule thickness was  $112.3 \pm 5.1$ ,  $98.7 \pm 2.4$ , and  $87.3 \pm 2.9$   $\mu\text{m}$  for PET controls, EG<sub>3</sub> SAMs, and microgel-coated samples, respectively. In addition, the thinner fibrous capsules surrounding microgel samples also appear less compact and structurally ordered than PET controls, which tended to have highly organized collagen fibers deposited along the entire implant length.



The density of total cells present in the fibrous capsule was scored using counterstained nuclei, and sections were quantified in 100  $\mu\text{m}$  increments along the implant interface (**Figure 6.1e**). Both EG<sub>3</sub> SAM- and microgel-coated samples contained significantly fewer (33% and 39%, respectively) capsule-associated cells than their unmodified PET control counterparts ( $p < 5.6 \times 10^{-3}$  and 0.01, respectively). The average cell density was  $51.2 \pm 2.2$ ,  $34.5 \pm 1.0$ , and  $31.1 \pm 1.2$  cells per 100  $\mu\text{m}$  length of implant for PET controls, EG<sub>3</sub> SAMs, and microgel-coated samples, respectively. These results demonstrate that microgel coatings modulate both thickness and cell density of fibrous capsules surrounding implanted biomaterials. Additionally, these coatings may alter collagen deposition and organization by infiltrating fibroblasts.

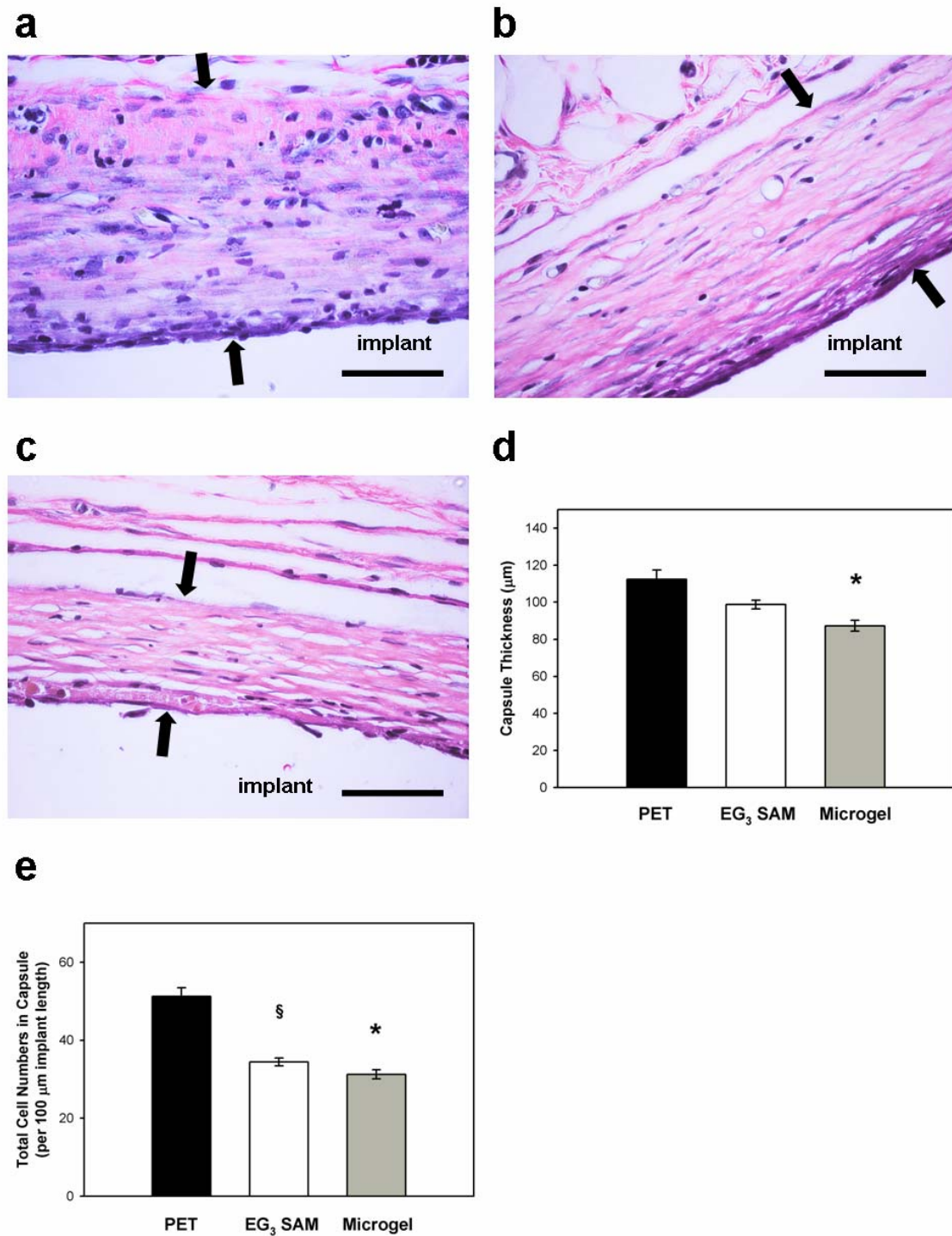


**Figure 6.1: Fibrous encapsulation of implanted biomaterials.** Biomaterials were implanted subcutaneously in the rat dorsum for 4 wk. Explants were evaluated by staining collagen (pink), elastin (black), and nuclei (black). Representative images taken with a 60X objective are presented for unmodified PET (a), EG<sub>3</sub> SAMs coated on PET (b), and microgel-coated PET (c) disks, and the original implant location is designated. Black arrows indicate capsule measurements. Microgel coatings effectively reduced

fibrous capsule thickness by 22% compared to unmodified PET controls as quantified in **(d)**, \*  $p < 0.04$ . The density of capsule-associated cells was also significantly reduced in microgel-coated samples (\*  $p < 5.6 \times 10^{-3}$ ) and EG<sub>3</sub> SAMs (§  $p < 0.01$ ) compared to unmodified PET controls as quantified in **(e)**. Data is represented as the average value  $\pm$  standard error of the mean using  $n = 4-7$  samples per treatment group. Scale bar is 50  $\mu\text{m}$ .

### ***Inflammatory cell profile at the implant interface***

Explant sections were processed to evaluate the composition of cells at the implant-tissue interface (**Figure 6.2**). Immunohistochemistry was used stain for the CD68 antigen, a classical marker of monocytes and tissue macrophages, and all nuclei were counterstained for reference. Images were scored for total CD68+ cells containing one nucleus (macrophages) and CD68+ cells fused to form multi-nucleated foreign body giant cells.

High magnification images of unmodified PET controls (**Figure 6.2a**), EG<sub>3</sub> SAM coatings (**Figure 6.2b**), and microgel-coated disks (**Figure 6.2c**) revealed that CD68 staining was localized to the capsule, primarily along the capsule-implant interface. All implanted samples, regardless of coating, contained similar levels of CD68+ cells as quantified in **Figure 6.2d** (no differences among treatment groups). The average number was  $19.5 \pm 1.8$ ,  $14.9 \pm 0.9$ , and  $20.4 \pm 1.1$  CD68+ cells per 100  $\mu\text{m}$  of implant length for PET controls, EG<sub>3</sub> SAM, and microgel-coated samples, respectively. CD68+ cell counts were then normalized to total cells in the fibrous capsule (as quantified in **Figure 6.1e**) to determine the relative numbers of macrophages in the capsule. Microgel-coated samples contained significantly higher relative levels of macrophages than either unmodified PET controls or EG<sub>3</sub> SAM (**Figure 6.2e**,  $p < 0.02$  for both). The average values were  $37.8 \pm 10.4$ ,  $41.0 \pm 6.5$ , and  $68.1 \pm 5.8$  % CD68+ cells for PET controls, EG<sub>3</sub> SAMs, and

microgel-coated samples, respectively. It should be noted that this marker can potentially stain CD68 antigens in both adipose tissue<sup>241</sup> and fibroblasts,<sup>242</sup> the latter of which are also localized in the fibrous capsule and participate in collagen deposition. Although F4/80 is the classical macrophage marker and may be the most specific to the macrophage lineage, antibodies were not available in the species-specific clone necessary for our experiments.

Sections were also scored for multi-nucleated FBGC, designated by black arrows (**Figure 6.2f**). Few samples contained extensive development of multi-nucleated FBGC. The average values were  $4.1 \pm 1.3$ ,  $1.4 \pm 0.4$ , and  $5.9 \pm 0.8$  FBGCs per mm of implant length for PET controls, EG<sub>3</sub> SAM, and microgel-coated samples, respectively. Numbers of FBGC per sample ranged from 1.4-11.1 and 3.0-11.8 cells/mm implant length for PET controls and microgel-coated disks, respectively. However, no statistical differences were found among treatment groups.

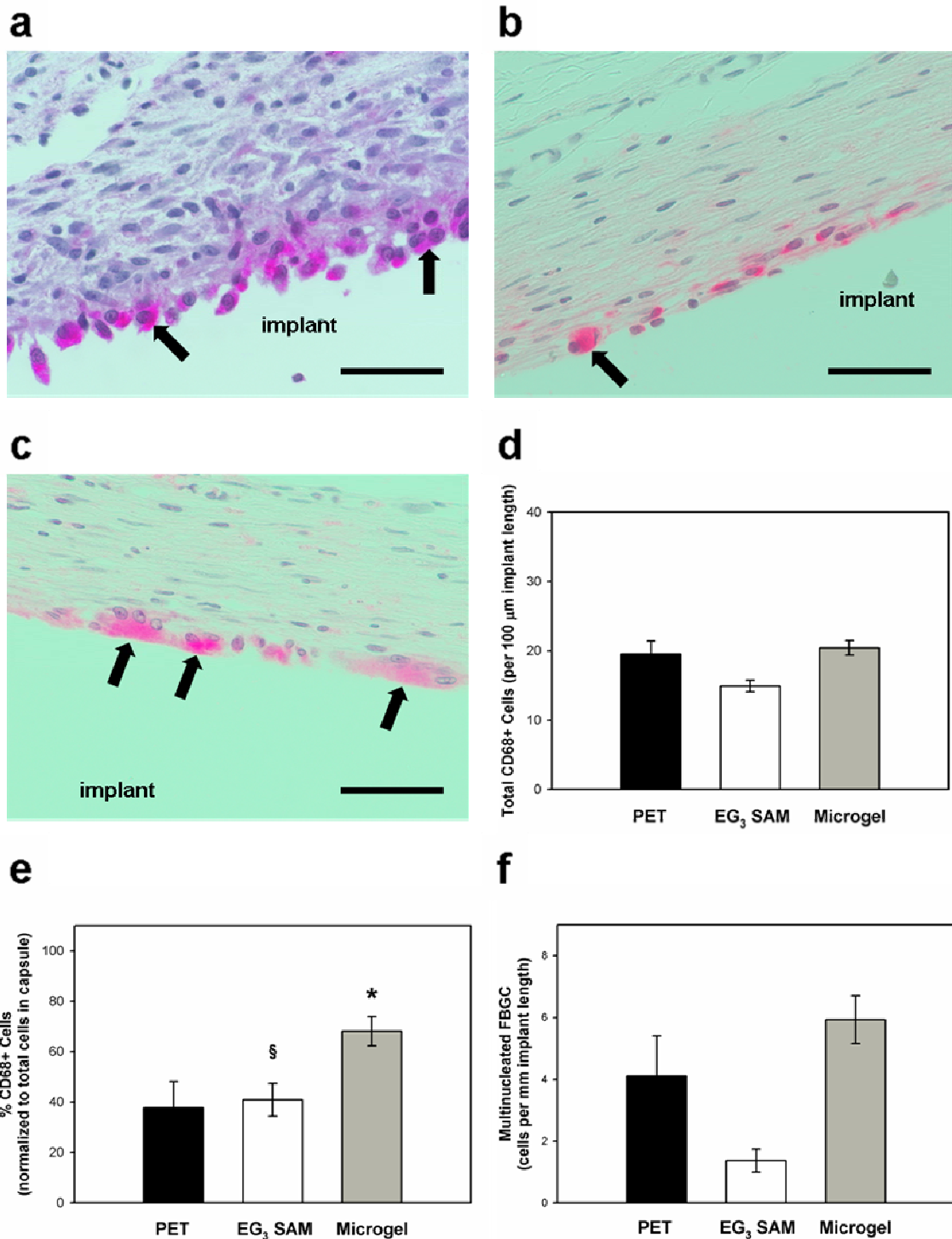


**Figure 6.2: Immunostaining of capsule-associated macrophages and foreign body giant cells.** Biomaterials were implanted subcutaneously in the rat dorsum for 4 wk. Explant sections were stained via immunohistochemical methods for macrophage marker CD68 (pink) and counter-stained with hematoxylin to label nuclei (blue). Representative images taken with a 60X objective are presented for unmodified PET (a), EG<sub>3</sub> SAMs coated on PET (b), and microgel-coated PET (c) disks, and the original implant location

is designated. Total CD68+ cells were quantified in (d), but no statistical differences were found between treatment groups. (e) When normalized to total capsule-associated cells (from Fig. 6.1e), unmodified PET and EG<sub>3</sub> SAM controls both contained proportionately less CD68+ cells than microgel-coated PET (§ and \* p < 0.02). Multinucleated CD68+ cells (FBGCs) at the cell-implant interface were also quantified (f), but no statistical differences were found between treatment groups. FBGCs are designated by black arrows. Data is represented as the average value ± standard error of the mean using n = 4-7 samples per treatment group. Scale bar is 50 μm.

## DISCUSSION

We have engineered a hydrogel-based polymeric coating composed of PEG-crosslinked pNIPAm-co-AA microparticles, which are applied to PET substrates using a spin coating method with high reproducibility to generate a conformal monolayer.<sup>122</sup> This coating strategy offers many advantages over traditional surface modification methods, including precise control over particle synthesis, the ability to generate complex architectures including “mosaic” coatings containing variations in particle composition or spatial arrangement, and deposition onto biomedically-relevant materials. We have demonstrated these coatings reduce protein adsorption and leukocyte adhesion.<sup>89, 122</sup> Importantly, these microgel coatings have effectively reduced leukocyte adhesion and activation, as well as expression of pro-inflammatory cytokines, to biomedical polymer implants *in vivo* at acute time points.<sup>238</sup> The results of the current study demonstrate that our microgel coatings also modulate chronic inflammatory events, including fibrous capsule thickness and cell density within the capsule.

Research efforts have focused on modifying material properties using various anti-inflammatory surface coatings, including both passive and active strategies, to modulate biomaterial-mediated inflammation.<sup>151, 153, 161, 162, 177, 243</sup> Since polyethylene glycol has proven to be the most protein-resistant functionality,<sup>114</sup> passive PEG-based

coatings have been used extensively in the development of implantable materials. In contrast to passive non-fouling surface treatments, coatings presenting or delivering anti-inflammatory agents offer a more directed approach to modulate cell behavior. However, these types of drug delivery systems are limited by the amount of therapeutic molecule incorporated and the drug half-life and activity. Although these materials have reduced biofouling *in vitro*, many of these coating strategies still exhibit high levels of adherent leukocytes and continued inflammation *in vivo* with fibrous encapsulation of the implant.<sup>161, 170, 188, 244</sup> Measurement of fibrous capsule thickness following subcutaneous implantation represents a standard measure of chronic inflammation to synthetic materials.<sup>1</sup>

Compared to uncoated PET controls, microgel-coated samples were surrounded by thinner, loosely organized fibrous capsules. Microgel coatings reduced capsule thickness to approximately 85  $\mu\text{m}$ , a similar thickness to that of dihydroxypropyl methacrylate (DHPMA) hydrogels ( $\sim 60 \mu\text{m}$  thick capsule).<sup>121</sup> Moussy and colleagues developed these DHPMA hydrogels as coatings for glucose biosensors, and they demonstrated a functional increase in sensor responsivity compared to controls when tested *in vitro*.<sup>121</sup> These authors attributed the enhanced *in vivo* sensor performance to a reduced capsule thickness and improved analyte transport. Other types of non-fouling or non-inflammatory materials have achieved varied levels of *in vivo* success in modulating fibrous encapsulation of implants. Polyethylene glycol-based copolymers effectively reduced tissue fibrosis surrounding implanted glucose sensors, although these materials were evaluated after only 3 d implantation.<sup>147</sup> Phosphorylcholine (PC)-based materials contained fibrous capsules of relatively similar thickness to those surrounding our

microgel-coated samples after 4 wk implantation, but this capsule thickness was not significantly reduced compared to their controls.<sup>126</sup> Fluorinated diamond-like carbon has recently gained considerable interest in biosensor and blood-contacting applications due to its favorable coagulation responses; however, it yields much thicker fibrous capsules (~ 300  $\mu\text{m}$  after 28 d implantation) than our microgel-coated samples.<sup>245</sup> *In vitro* protein adsorption was suppressed by photochemically immobilized polymer coatings on silicone rubber substrates and by polyethylene oxide-like tetraglyme coatings, yet neither treatment significantly reduced fibrous capsule thickness when implanted subcutaneously.<sup>187, 188</sup> In addition to reducing capsule thickness, capsules surrounding microgel-coated samples were populated by significantly fewer cells (39% less) than PET controls. After 4 wk implantation, PC-based coatings also reduced cellular density by 39% (~ 160 cell/ $\text{mm}^2$  compared to control value of ~ 270 cells/ $\text{mm}^2$ ).<sup>126</sup> Our results are also consistent with another report of an implanted polyethylene oxide-based material, in which increased PEO content in these triblock copolymers decreased the cellular density during implantation.<sup>224</sup> Although microgel coatings significantly reduce tissue fibrosis, our current study is limited in that only one time point (4 wk) was examined for chronic responses. It will be important to conduct more extensive studies in order to determine inflammatory responses at longer clinically-relevant implantation times.

It is likely that the dynamics and extent of fibrous capsule formation are affected by the underlying material, as well as implantation site. Recent work suggests that material surface properties may influence both acute and chronic inflammatory events.<sup>112, 113, 246-248</sup> Using microspheres presenting  $-\text{OH}$  and  $-\text{COOH}$  groups, Tang and colleagues demonstrated that surface functionality modulates fibrous capsule formation,



inflammatory cell recruitment, and cell infiltration into microspheres; they found that the –OH group prompted the strongest capsule formation.<sup>113</sup> However, variations in surface density of those groups had only a minor effect on the extent of fibrotic tissue reactions; the authors suggest that further increases in the density may be relatively ineffective ones as a threshold density value has been reached on the surface. In another study, SAMs presenting various functionalities revealed that CH<sub>3</sub>-terminated samples recruited higher levels of inflammatory cells and caused significantly thicker fibrous capsule formation than either OH- or COOH-terminated surfaces.<sup>248</sup> By systematically adjusting the length of alkyl side chains on poly(alkyl methacrylates), Andersson *et al.* showed that surface molecular mobility influences cell recruitment and cytokine activity, as well as the extent of fibrous encapsulation.<sup>112</sup> Results also suggest that material surface properties are associated with angiogenesis during tissue repair.<sup>247</sup> Moreover, using well-defined features, surface topography was also shown to mediate early cellular responses, such as adhesion and proliferation.<sup>237, 249</sup>, as well as angiogenesis during the FBR.<sup>250</sup> In addition, the site of implantation significantly affects leukocyte recruitment and expression of matrix metalloproteinases *in vivo*,<sup>111</sup> as well as biosensor function.<sup>251</sup> Regardless of the mechanism of *in vitro* biofouling resistance, there appears to be no clear trend among surface treatments for their ability to modulate tissue fibrosis *in vivo*. In addition to surface chemistry and topography, it is likely that implantation site and host species also play a role in fibrotic responses. Other possible explanations for these differences include presentation (surface density and orientation) of the non-fouling component (e.g. PEG), kinetics and activity of incorporated drugs (for active coatings), and material stability.

In this study, microgel coatings reduced fibrous capsule thickness by 22% compared to unmodified control samples. Such a reduction may translate into increased device longevity and support proper *in vivo* performance, which would directly benefit patients by requiring fewer follow-up surgeries and causing less pain throughout a patient's lifetime. Nevertheless, functional testing in specific applications (e.g., glucose sensors, pacing leads, neural electrodes) is required to evaluate the potential of these microgel coatings to ameliorate chronic inflammatory responses to implanted devices. Fibrous capsules on the order of 85  $\mu\text{m}$  thick (as in our current study) may still pose a significant barrier to certain implanted devices or therapeutics by blocking the key exchange of nutrients or impeding signal transduction to an external medium. For example, Moussy and colleagues recently demonstrated a correlation between increased collagen deposition surrounding implanted glucose sensors and decreased sensor sensitivity; natural angiogenesis failed to overcome the barrier to glucose diffusion caused by the associated fibrous capsule.<sup>252</sup> Bioprotective membranes have demonstrated enhancements in glucose sensitivity following implantation, possibly by protecting the inner analyte sensing layers from inflammatory macrophage activity.<sup>110</sup> In another study using poly(L-lactic acid) (PLLA) sensor coatings, Reichert and colleagues recently demonstrated that surface texturing through porosity increases vascularization and decreases collagen deposition around implants.<sup>251</sup> Despite increased vessel density, sensors with porous coatings experienced an initial rapid signal reduction before stabilization. Other studies have suggested the requirement for an initial "break in" period during fibrous capsule formation, after which glucose sensitivity increases.<sup>18, 109</sup> These porous PLLA coatings displayed less variability in signal transduction throughout

the implantation period, probably because of better integration with the surrounding tissue.<sup>251</sup> Although our current results are promising, it will be important to functionally evaluate these microgel coatings in the context of such devices to determine their efficacy and to evaluate effects of the microgel coating itself (~ 300 nm thick in swollen state) on baseline device performance.

Although there were no differences among groups when comparing total CD68+ cell numbers, the microgel-coated samples contained proportionately more macrophages than unmodified PET controls. Additional studies are needed to determine the inflammatory phenotype of these CD68+ cells, because macrophages regulate both inflammatory and regenerative responses to biomaterial implants. Emerging data suggests that macrophage phenotype is dictated by initial stimuli, causing them to become pro- or anti-inflammatory.<sup>81</sup> T lymphocytes generate distinct immune responses based on the cytokine profile they secrete, where IFN- $\gamma$  stimulates pro-inflammatory (Th1) responses and IL-4 and IL-10 (among others) stimulate anti-inflammatory (Th2) responses resulting in very different metabolic programs.<sup>81</sup> Macrophages and lymphocytes likely act in concert during inflammatory or regenerative responses, and research indicates that distinct M1- or M2-subtypes of macrophages also exist.<sup>50, 88</sup> “Alternatively activated” cells, such as alveolar and placental macrophages, functionally down-regulate inflammation and immunity and secrete anti-inflammatory mediators such as IL-10 and PGE<sub>2</sub> to suppress Th1 responses.<sup>79</sup> Further studies are necessary to identify the macrophage phenotype and determine their overall involvement in fibroblast recruitment and collagen deposition around these microgel-coated implants.

In the current study, there were no significant differences among treatment groups in levels of FBGC at the implant interface. Recent work suggests that polyethylene oxide polymers may alter the foreign body reaction by affecting the density of FBGC surrounding implanted hydrogels.<sup>221</sup> Other types of polymeric coatings, such as phosphorylcholine, have also effectively reduced FBGC formation after 28 d implantation.<sup>177</sup> FBGC have been observed in chronically inflamed tissues and have traditionally been associated with a pro-inflammatory phenotype because of their capacity to degrade implanted biomaterials. However, the precise role of FBGCs at the tissue-material interface is poorly defined. Emerging research suggests two distinct possibilities: (i) macrophage fusion into FBGCs could be a mechanism for promoting inflammatory cell survival by escaping apoptosis,<sup>86</sup> or (ii) FBGCs could serve a more wound healing function by maintaining the inflammatory response at a local, less activated level.<sup>41</sup> Longer-term implantations of our microgel-based coatings are needed to determine any negative effects of associated FBGC on the implant or surrounding tissue. Possible explanations for why we observed no significant differences among treatment groups in FBGC numbers include (i) effects of soluble factors on tissue fibrosis, and (ii) influence of surface-bound receptors on activity of inflammatory cells. A number of soluble mediators including extracellular matrix proteins (such as osteopontin) and inflammatory cytokines been shown to play a role in macrophage fusion and formation of FBGC.<sup>15, 189</sup> Anderson and colleagues have demonstrated a requirement for the  $\beta_1$  integrin in macrophage fusion.<sup>41</sup> In addition, other receptors including dendritic cell-specific transmembrane protein (DC-STAMP), for which inflammatory MCP-1 may be a ligand, and the macrophage mannose receptor is necessary for cell

fusion.<sup>84, 253, 254</sup> It is possible that activity levels of these integrins are similar on cells participating in the FBR, regardless of the differences between implant surfaces that affects acute responses.

Previously, we demonstrated that microgel coatings significantly reduce protein adsorption, leukocyte adhesion, and activation at acute times *in vivo*.<sup>122</sup> One possible explanation for these observations is that temperature-induced deswelling of pNIPAm at physiological temperatures results in phase segregation of non-fouling PEG “loops” and subsequent presentation on the surface.<sup>89, 231</sup> While the structure and presentation of PEG, including chain length and grafting density, may strongly influence protein resistance,<sup>116, 217</sup> additional parameters likely affect chronic responses to implanted materials. For example, our microgel coatings are covalently cross-linked onto the substrate, which likely imparts bio-stability *in vivo*. Tang and colleagues recently demonstrated a correlation between the rate of material degradation and the degree of resultant inflammatory responses; they suggest that degradation products are potent triggers of phagocyte activation, including superoxide production.<sup>255</sup> Other groups have reported material degradation following implantation, possibly due to oxidative effects of chemicals released by phagocytes, for both tetraglyme coatings and polyethylene oxide copolymer hydrogels.<sup>188, 221</sup> The method of cross-linking PEG has also been shown to affect *in vivo* efficacy.<sup>94</sup> Moreover, our assembly process deposits a high volume polymer film (swollen microgel coatings are ~ 300 nm thick), which may result in slower overall degradation than thinner coatings such as tetraglyme (100 nm thick).<sup>146</sup> Therefore, surface degradation may result in loss of non-fouling PEG activity and likely

plays a role in extensive capsule development. Studies examining the degradation and stability of these coatings are still needed.

In addition to influencing protein adsorption and cell adhesion, surface chemistry may also influence complement activation,<sup>56, 256, 257</sup> providing an alternative route to chronic events. In particular, surface hydroxyl (-OH) groups have been linked to leukocyte adhesion and contact activation of the complement system, possibly involving a direct covalent thioester linkage of complement fragment C3.<sup>257</sup> Moreover, there is a proposed role for the C1q receptor (CD93) on monocytes/macrophages in activation and enhanced phagocytic capacity of targets opsonized with complement.<sup>258</sup> It is evident that there is no simple correlation among protein adsorption, *in vitro* monocyte/macrophage adhesion, and *in vivo* leukocyte activities for PEG-based coatings. Extensive research efforts should be focused on elucidating the molecular mechanisms governing material biocompatibility during the transition from acute to chronic events, including the dynamics of fibrous capsule development.

This work provides the foundation for developing a microgel-based coating system incorporating various signaling agents and bioactive therapeutics within a low-fouling background. These “smart” delivery systems offer several advantages over passive methods, including highly controlled presentation of immunomodulatory agents, control over reaction kinetics, and versatility through hybrid designs. Fibrous capsule thickness could potentially be reduced further using such complex coatings with tunable active release mechanisms to deliver anti-inflammatory agents, such as IL-1Ra, angiostatin, or dexamethasone, which have improved biological responses to implanted materials.<sup>161, 162, 176, 185, 259</sup>

## CONCLUSION

Using a model of chronic biomaterial-mediated inflammation, we demonstrate that surface coatings comprised of pNIPAm-*co*-PEG hydrogel microparticles reduce long-term fibrous encapsulation and alter the cellular composition at the implant interface. Microgel coatings effectively reduced collagen capsule thickness by 22%, and those capsules appeared less compact and structurally ordered than PET controls. These coatings also contained significantly fewer total cells within the capsule. Our current results demonstrate that microgel particles can be applied as implant coatings to modulate inflammation and achieve more desirable chronic host responses *in vivo*, with the potential to extend implant lifetime.

## CHAPTER 7

### FUTURE CONSIDERATIONS

#### BASE MICROGEL COATINGS

Biomaterial-mediated inflammation poses a complex problem, limiting the function of implanted devices. Over the last few decades significant progress has been made toward the development of material surface treatments and coating strategies to prevent non-specific protein adsorption and leukocyte adhesion, the critical events of acute inflammation; it is generally believed that reducing such biofouling can ameliorate subsequent adverse responses. However, many technologies that have modulated early events to some degree of success are still plagued by chronic phase host responses such as fibrous capsule formation. By contrast, we have demonstrated that our novel pNIPAm-co-PEG microgel coatings significantly reduce adhesion and inflammatory activity at early time points of implantation. More importantly, we have shown that these coatings also modulate chronic inflammatory events by reducing development and organization of the fibrous capsule and maintaining cell density at low levels around the implant interface.

Further evaluation of these coatings is critical in order to determine the extent of vascularization within the capsules, as this could indicate the propensity for wound healing and regeneration of the surrounding tissue. Additionally, it would be interesting to determine the contributions of other proteins to capsule development. For example, fibronectin is required for collagen assembly,<sup>203, 204</sup> and it also modulates chronic inflammatory responses.<sup>212</sup> Recent evidence has also revealed important roles for



osteopontin expressed by inflammatory cells, including macrophage recruitment and contribution to wound fibrosis,<sup>189</sup> and other findings suggest it inhibits FBGC formation.<sup>260</sup> The precise role of FBGCs at the tissue-material interface is poorly understood; therefore, further investigation is critical in understanding the role of these proteins and the inflammatory nature of multinucleated FBGC.

## BIOACTIVE MICROGEL COATINGS

Future coating designs will probably need to be material and application-specific in order to achieve the desired *in vivo* response. Biologically interactive implants are gaining considerable interest. Tunable, stimuli-responsive materials and biomimetic molecules may be able to actively direct cell behavior and activity surrounding the implant, encouraging more desirable interactions.<sup>33, 34</sup> These delivery systems offer several advantages over passive methods, including highly controlled presentation of immunomodulatory agents, control over reaction kinetics, and versatile designs.

Although significant progress has been made in understanding the mechanisms of initial protein adsorption onto surfaces, the molecular events driving macrophage and FBGC phenotype and activities at the implant interface are poorly understood. Monocytes and macrophages express the leukocyte-specific  $\alpha_M\beta_2$  integrin, which is capable of interacting with a variety of ligands and mediating cell-cell and cell-substrate interactions.<sup>41, 71-73</sup> Importantly, integrins are key mediators of signal transduction between the extracellular and intracellular environments, and they also play a role in focal adhesions and cellular migration.<sup>40, 70</sup> Studying the interactions of protein and surface chemistry effects has been difficult due to the complexity of macrophage receptor

expression, protein adsorption and conformation on the biomaterial surface, and maturation and fusion into FBGCs. Moreover, little is known about integrin-dependent behavior in macrophages. Macrophage adhesion to two particular motifs, P2 (from fibrinogen) and RGD (from fibronectin), via the leukocyte-specific  $\alpha_M\beta_2$  integrin has been implicated in inflammation.<sup>41, 71-73</sup> However, we do not know how integrin binding numbers and specificity regulate macrophage function. It is possible that different densities or combinations of ligands differentially regulate macrophage activities.

This thesis work provides the foundation for developing a hydrogel-based coating system incorporating various signaling agents and bioactive therapeutics within a low-fouling background. By creating a tunable system to interact with macrophages, the key mediators of inflammation, our long-term goal is to systematically control macrophage adhesion and subsequent activities. We will take advantage of our ability to engineer well-defined interfaces to direct integrin binding and evaluate macrophage responses to these interfaces. Therefore, bioadhesive ligand motifs P2 and RGD have been selected for tethering to microgel particles to address the above issues. Using these coatings with embedded signals to control integrin binding, we will address the current knowledge gap by providing vital information about various integrin-dependent macrophage behaviors. We will determine the effects of ligand density and presentation on macrophage adhesion to biomaterial surfaces, subsequent activation, signaling, cytokine release, and their fusion into FBGCs. Using blocking antibodies, we will also determine the contributions of  $\beta_1$  and  $\beta_2$  integrins to these activities. These proposed studies represent a systematic evaluation of macrophage functions to well-defined biomaterial interfaces.

Microgel coatings separately presenting tethered (static) bioadhesive motifs of P2 or RGD have been developed (**Figure 7.1**). Using standard peptide chemistry, these biomolecules have been conjugated to microgel particles using 2% of the available acrylic acid co-monomer groups. Early results were promising and indicated the system was successful; however, the project has encountered numerous problems with reproducibility using the current methods. Although it is currently unclear, possible explanations for these problems include reduced bioactivity after tethering or improper peptide exposure. To determine appropriate bioactivity of these ligands, we conducted cell adhesion studies at early time points (48 h). We created model mixed SAM surfaces (EG<sub>3</sub>/EG<sub>6</sub>-COOH alkanethiols) on gold substrates using previously characterized techniques,<sup>239</sup> and standard peptide chemistry was used to conjugate peptides to 2% of the SAMs.<sup>261</sup> Murine macrophages and NIH 3T3 fibroblasts (for their known adhesive behavior on RGD-tethered surfaces) were then cultured on samples, and results from multiple experiments indicated that both RGD and P2 retained their bioactivity on model SAMs.

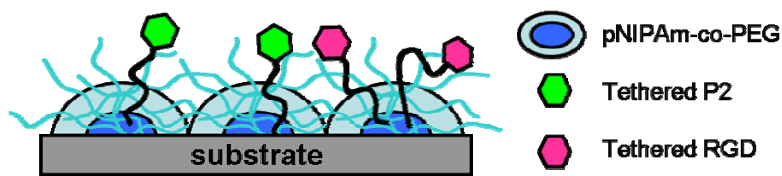


**Figure 7.1: Bioactive microgel coating presenting tethered bioadhesive motifs of P2 or RGD to elucidate integrin-dependent macrophage behaviors.**

To determine whether cells have proper access to these peptides, additional studies may be necessary to alter the microgel dimensions and determine an optimal

tethering distance. For example, short PEG spacer arms could be incorporated into the microgel particles to extend the tethered ligands further from the non-fouling background, providing cells more access to elicit binding and signaling events.<sup>262, 263</sup> Receptor binding is highly dependent on the structural context of the ligand, and appropriate spacing at the nano level is even critical to retain biological activity.<sup>264-266</sup> Therefore, it is possible that these ligands are oriented improperly and cannot facilitate interactions with cells. While unlikely, it is also possible that higher concentrations of ligand are required to elicit cellular responses; however, such concentrations are limited by material cost and are thus experimentally impractical to pursue.

Additional formulations of microgel particles could be devised using alternative synthesis techniques to create particles of much smaller size, relative to the ligands.<sup>130</sup> Moreover, alternative structures, such as the core-shell microgel system, could be used to incorporate amine groups into the shell for more effective bioconjugation. Instead of tethering ligands, which possibly reduces its bioactivity, such a core-shell system could be employed to incorporate biomolecules within the core structure for controlled release by degradative mechanisms or endogenous stimuli. In this way, the microgel system could be used to deliver anti-inflammatory agents, such as IL-1Ra or angiostatin, to abrogate inflammatory events rather than control cell binding.<sup>185, 259</sup>

The long-term goal of this work is to engineer microgel coatings that dynamically present bioactive ligands in a non-fouling background, creating surfaces that interact with macrophages in order to elicit specific host responses and direct the events of inflammation. Multilayered coatings constructed of an inner microgel core surrounded by an outer microgel shell will support temporally controlled cell adhesion to our

surfaces. Using dynamic and stimuli-responsive interfaces, the presentation of surface-bound moieties can be coordinated with specific stages of inflammation, as directed by endogenous enzymes (**Figure 7.2**).

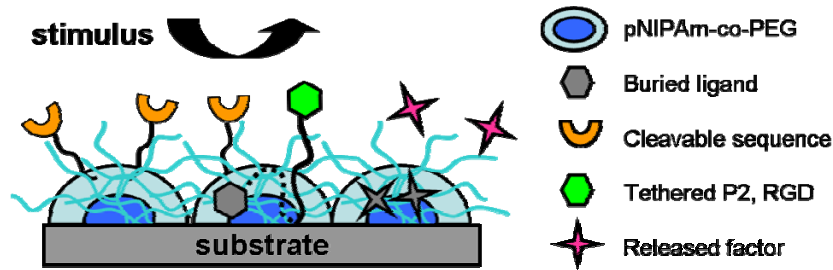


**Figure 7.2: Stimuli-responsive microgel coatings to dynamically present biological molecules targeting inflammatory cells.**

These bioactive approaches may create less inflammatory macrophages and attract wound healing cells. Using this versatile microgel system, we intend to provide insight into the complex interactions of macrophages with biomaterials that may enable more well-designed implants or devices and extend their *in vivo* lifetime. If successful, this microgel technology has the potential to significantly improve device performance by limiting deleterious cellular effects and fibrous encapsulation at the biomaterial-tissue interface. Microgel coatings could then be developed for a wide variety of biomaterials and medical devices, enabling them to reach their full potential *in vivo*.

## APPENDIX A

### COVALENT TETHERING OF FUNCTIONAL MICROGEL FILMS ONTO POLY(ETHYLENE TEREPHTHALATE) SURFACES \*

\* Modified from N Singh, AW Bridges, AJ García, and LA Lyon. Covalent tethering of functional microgel films onto poly(ethylene terephthalate) surfaces. *Biomacromolecules* 8 (2007): 3271-3275.

AW Bridges contributed scientifically to this work, including *in vitro* cell culture and adhesion studies, and fluorescence microscopy (Figure A.5).

#### INTRODUCTION

Recently there has been an increasing interest in developing biotolerant polymeric surfaces that have the ability to support or immobilize biological functionalities tailored for specific biotechnological and medical applications.<sup>267-270</sup> As an important example, it is common to immobilize extracellular-matrix proteins (e.g., collagen, fibronectin) or cell signaling molecules on polymeric surfaces to yield functional biomaterials that have the ability to modulate cell adhesion, proliferation, and differentiation, thus mimicking a natural cellular environment.<sup>269, 271-274</sup>

Another interesting class of polymeric materials with desirable properties for biotechnology is the hydrogel microparticle or microgel. The synthesis, characterization and applications of stimuli-responsive microgels have been extensively studied over the past few years.<sup>38, 225, 231, 275, 276</sup> Recently, Nolan *et al.* investigated the performance of poly(*N*-isopropylacrylamide) (pNIPAm) microgels cross-linked with short poly(ethylene glycol) (PEG) chains, as protein adsorption-resistant films.<sup>89</sup> The PEG cross-linked pNIPAm microgels having poly(acrylic acid) as co-monomer, were assembled electrostatically by spin-coating onto a cationic glass substrate. The results indicated that

glass surfaces coated with microgels showed reduced protein adsorption and cell adhesion *in vitro*, i.e. non-fouling behavior. However, the potential of these microgel films as non-fouling base coatings for future biomedical implants cannot be probed and realized until they are assembled on a more flexible and biocompatible substrate than glass. This motivated our current goal to design a flexible substrate-based microgel film with potential non-fouling and anti-inflammatory behavior for *in vivo* studies. Equally important, we also aim to enhance the stability of the adherent microgel films in comparison with the Coulombically assembled film in biological environments by improvements in the surface chemistry.

For *in vivo* studies of biomaterials, common desirable attributes for a model biomaterial (in this case, a polymer) include good mechanical strength, flexibility, chemical and physical stability in the biological environment, and a surface chemistry/composition that allows for facile biofunctionalization. In view of these properties, poly(ethylene terephthalate) (PET) was chosen as a model biomaterial onto which we could deposit non-fouling microgel coatings in order to enhance its properties. PET has been extensively studied in biomaterial applications such as for sutures, vascular grafts, sewing cuffs for heart valves, and components for percutaneous access devices.<sup>277-</sup>

<sup>280</sup> However, the PET surface is inert and hence not suitable for direct biofunctionalization. Major efforts have therefore been undertaken to introduce various functionalities onto the PET surface, such as amine, carboxyl, and hydroxyl moieties, which can be further employed for the covalent immobilization of biomacromolecules.<sup>271,</sup>  
<sup>281, 282</sup> It is especially desirable that the methods used for the chemical modification are confined to the polymer surface, without affecting the bulk/mechanical properties of the

substrate. A suitable technique in this regard has been the chemical activation of the inert polymer surface by plasma treatment, which has already been employed to render PET surfaces hydrophilic and hence more biocompatible.<sup>283</sup> It is also well known that the exposure of polymeric surfaces to a plasma along with oxygen treatment generates surface-active hydroperoxide species that can be used for the chemical grafting of desired chemical and biological functional groups.<sup>271, 281, 284-288</sup>

Our method of functionalizing the PET with polymeric microgel films (**Figure A.1**) is derived from previous methods based on plasma-induced graft polymerization of poly-acrylic acid (pAAc). Plasma- and ozone-induced graft polymerizations of various monomers on PET films, fibers, and fabrics have been demonstrated.<sup>271, 287, 288</sup> However, in order to make the method more general, and to give the adherent microgel film more stability in biological environments, we introduced onto the PET surface a photo-affinity label, viz., aminobenzophenone. Upon excitation with UV irradiation, molecules of the benzophenone family have the ability to abstract an aliphatic hydrogen atom from any nearby polymer chain forming a covalent carbon-carbon bond.<sup>270, 289, 290</sup> Due to the presence of a microgel in the close vicinity of the benzophenone, it can abstract hydrogen atom from the microgel and hence covalently attach the particles to the PET surface. Essentially, the benzophenone here serves as a glue between the base PET substrate and the microgel film.



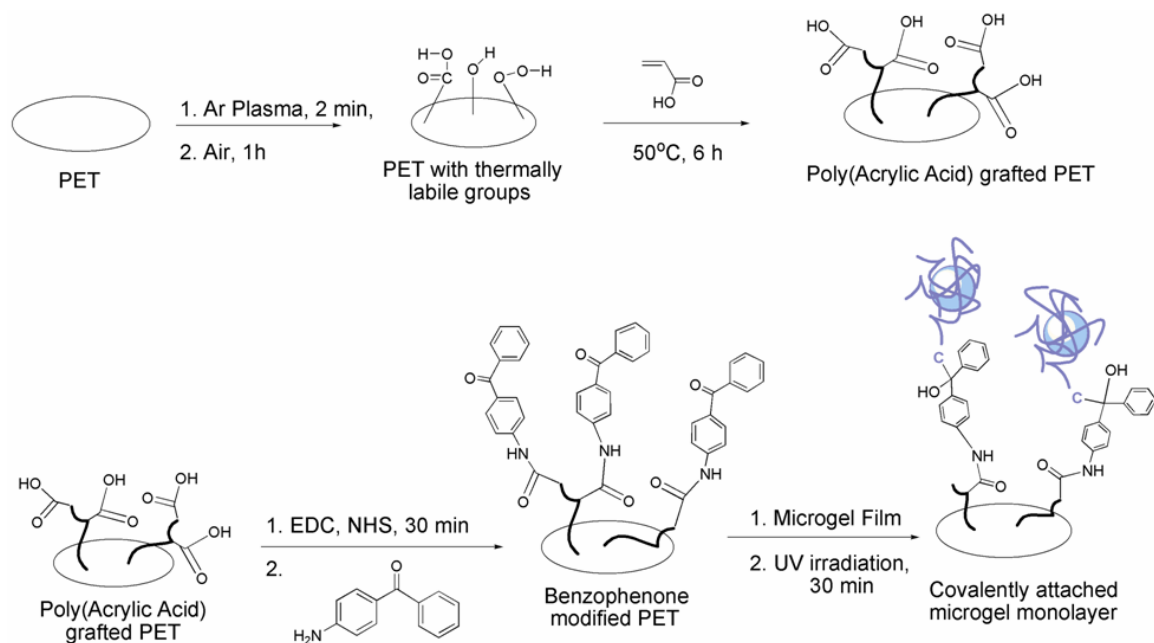


**Figure A.1: Strategy for covalent tethering of microgels onto a poly(ethylene terephthalate) surface.**

## EXPERIMENTAL SECTION

### MATERIALS

All materials were obtained from Sigma Aldrich unless otherwise specified. The monomer NIPAm was recrystallized from hexane obtained from J.T. Baker before use. Poly(ethylene terephthalate) (PET) sheets were obtained from AIN Plastics; Marietta, GA. All other chemicals were used as received. Formate buffer solution (pH 3.47, 10 mM) was prepared from formic acid and NaCl obtained from Fisher Scientific. Poly(ethylene glycol) diacrylate (PEG) (PEG MW 575, Polysciences, Inc.) was used as received. 1-Ethyl-3-(3-dimethylaminopropyl) carbodiimide (EDC) was purchased from Pierce. Dimethyl sulfoxide (DMSO) was obtained from J.T. Baker. Phosphate buffered saline (PBS) solution (pH 7.4, 10 mM) was prepared from NaCl (Fisher), Na<sub>2</sub>HPO<sub>4</sub> (EM Science) and KH<sub>2</sub>PO<sub>4</sub>. Water was distilled and then purified using a Barnstead E-Pure

system to a resistance of 18 M $\Omega$  and finally filtered through 0.2  $\mu$ m membrane filter (Pall Gelman Metrical) before use.

## METHODS

### *Microgel Synthesis*

Poly(*N*-isopropylacrylamide) (pNIPAm) microgel particles (100 mM total monomer concentration) were synthesized with 2 mol % poly (ethylene glycol) (PEG) diacrylate (MW 575) by a free radical precipitation polymerization method. For incorporating functional groups that can be later modified, the microgel particles were synthesized with 10 mol % acrylic acid as a co-monomer. Briefly, 0.4979 g of NIPAm monomer, 0.7011 g of cross-linker PEG-diacrylate, and 0.0025 g of surfactant sodium dodecyl sulfate (SDS) were dissolved in 49 mL distilled, deionized (DI) water, and filtered through a 0.2  $\mu$ m filter. The solution was transferred to and stirred in a three-neck, round-bottom flask, and heated to 70 °C while purging with N<sub>2</sub> gas. After reaching 70 °C and purging for 1 h, 34.3  $\mu$ L of acrylic acid was added, followed by the addition of 0.0114 g (dissolved in 1 mL DI water) of ammonium persulfate (APS) to initiate the reaction. The reaction was kept at 70 °C for 4 h. The synthesized microgels were then filtered and cleaned by five cycles of centrifugation at 15,422 *g* for 45 min. The supernatant was removed, and the particles were redispersed in DI water. The particles were then lyophilized overnight before being used for deposition onto the PET films.

### ***PET Film Functionalization***

PET sheets were cut into 8 mm diameter disks using biopsy punches and briefly rinsed in 70% ethanol to remove contaminants introduced during the manufacturing process. Graft polymerization of acrylic acid (AAc) on 8 mm PET films was done in two steps. PET films were first placed in an 18 W RF Ar plasma (Harrick Scientific) connected to a vacuum pump ( $5 \times 10^{-4}$  mbar) for 2 min. Immediately after the Ar treatment, air was introduced into the plasma chamber and maintained at atmospheric pressure for 1 h to generate peroxide and other oxygen-containing functional groups on the PET surface. The films were immediately transferred to a round bottom flask containing an  $N_2$  purged 25% (v/v) aqueous solution of acrylic acid. The grafting reaction was carried out for 6 h at 50 °C, after which the films were washed in water overnight. The degree of polymer grafting and hence the density of carboxyl groups on the PET surface can be controlled by varying the AAc concentration and reaction time.<sup>286</sup> The pAAc modified PET was further modified with 4-aminobenzophenone (ABP) using carbodiimide coupling.<sup>291</sup> The coupling of 4-aminobenzophenone is done traditionally as a one-step reaction using *N,N'*-dicyclohexylcarbodiimide (DCC) in organic media (DMSO). However, we used an aqueous carbodiimide coupling strategy based on activation of carboxyl groups with *N*-hydroxysuccinimide (NHS) and 1-ethyl-3-(3-dimethylaminopropyl) carbodiimide (EDC) and further reaction with the ABP. This is to avoid the formation of urea precipitate (the by-product in the DCC reaction), which is difficult to remove completely from the surface being modified. The pAAc modified PET films were first activated by incubation in 2 mM EDC and 5 mM NHS in 10 mM 2-(*N*-morpholino)ethanesulfonic acid (MES) buffer solution (pH 6.0) for 30 min at room

temperature. The films were then placed in 20 mM 2-mercaptoethanol solution in DI water to quench the EDC. The activated films were then reacted with ABP in DMSO for 2 h at room temperature. The ABP modified films were washed in DMSO and immersed in 10 mM hydroxylamine solution to quench the reaction. Finally, the films were washed in DI water.

### ***Carboxyl Group Determination***

The amount of pAAc grafting on the PET film surface was characterized by a colorimetric method based on Toluidine Blue O staining.<sup>281</sup> Briefly, the grafted film was placed for 6 h at 30 °C in a 0.5 mM Toluidine Blue O solution prepared at pH 10. The film was then removed and thoroughly washed with NaOH (pH 10) to remove any dye nonspecifically adhered to the surface. The bound dye molecules were then desorbed from the film in a 50% acetic acid solution. The final dye content was determined from the optical density (OD) of the solution at 633 nm using a Shimadzu 1601 UV-visible spectrophotometer.

### ***Particle Deposition***

A spin-coating process was used to deposit a layer of microgel particles onto the functionalized PET films. The PET film was placed onto a glass slide, and the slide was placed onto the spin coater (Specialty Coating Systems) chuck and held in place by vacuum. The rotor speed was maintained at 500 rpm. Dried microgels were dispersed in a 10 mM formate buffer (pH 3.47) solution and one drop of the microgel solution was deposited onto the PET film while spinning. After keeping the film on the spin coater for

100 s, a second drop of the microgel solution was deposited. The PET film was left on the spin coater for additional 100 s and the film was allowed to dry. Finally, another drop of microgel solution was deposited on the PET by the same process and the film was dried after 100 s of spinning. This process was done on both sides of the PET films under dark conditions. Each side of the PET, with the dried microgel film, was irradiated by a 100 W longwave UV lamp (Blak-Ray) for 30 min to covalently attach the microgels onto the PET surface. The microgel-modified PET film was soaked in 10 mM phosphate buffer solution (pH 7.5) for 6 h and then washed with DI water.

### ***Atomic Force Microscopy***

All images were obtained in AC mode on an Asylum Research MFP-3D atomic force microscope (AFM). Spring constants were calculated using the thermal method. Imaging and analysis was performed using the Asylum Research MFP-3D software (written in the IgorPro environment, WaveMetrics, Inc., Lake Oswego, OR). An Olympus AC160 cantilever with  $k = 42 \text{ N/m}$ ,  $f_0 = 300 \text{ kHz}$  was used for imaging.

### ***In vitro cell adhesion***

The IC-21 murine macrophage cell line (ATCC; Manassas, VA) was used to determine the bioresistant properties of the microgel coated PET *in vitro*. Cells were seeded at a density of  $67,000 \text{ cells/cm}^2$  on unmodified PET and microgel-coated PET disks in 24-well tissue culture-treated polystyrene plates in culture media containing 10% fetal bovine serum. After 48 h, adherent cells were fluorescently stained with calcein-

AM (Molecular Probes, Eugene, OR) and imaged using a Nikon TE-300 microscope to determine relative cell numbers and cell spreading on each surface.

## RESULTS AND DISCUSSION

In order to deposit uniform films of microgels, the PET films had to be rendered amenable to robust particle attachment. The approach described above (**Figure A.1**) involves surface activation in an Ar plasma followed by the introduction of air to introduce thermally-labile groups. These thermally-labile groups thermally decompose to form radicals, thus initiating the polymerization of AAc to form pAAc-grafts on the PET surface.<sup>284-286</sup> The carboxyl groups of the pAAc on the PET surface are subsequently used in the functionalization of the surface with photo-affinity label (ABP) using carbodiimide coupling chemistry. We characterized the surface grafting density of pAAc by the Toluidine blue O dye binding assay. **Figure A.2** shows UV-visible absorbance spectra of Toluidine blue O dye arising from various surface treatments. Based on previous methods, by assuming a 1:1 ratio between the dye and the carboxylic acid groups, the OD at 633 nm gives a measure of the degree of grafting.<sup>281, 284</sup> Thus, successful pAAc grafting of the PET surface is evidenced by an increase in the OD from ~0.01 for the bare PET substrate to about 2.02 for the modified surface. The color staining of the dyed films was very uniform across the samples, suggesting relatively uniform coating of the PET (data not shown). For the pAAc grafted PET, we estimate about  $1.4 \times 10^{-7}$  moles of carboxyl groups and following the reaction with ABP, only about  $1.1 \times 10^{-8}$  moles of carboxyl groups are left on the surface. Hence, this suggests that

the benzophenone modification of the PET results in a loss of ~92% of the carboxyl groups due to their conversion into amide groups.

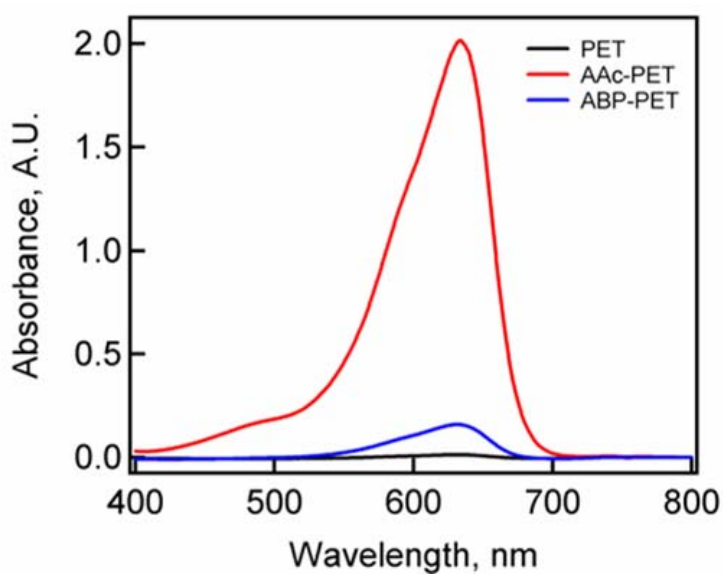


**Figure A.2: Absorption spectra for desorbed Toluidine Blue O dye.** Spectra are shown for bare PET (black), poly(acrylic acid) grafted PET before (red) and after (blue) modification with 4-aminobenzophenone.

Our method of surface functionalization of the PET with photo-affinity labels results in a very efficient surface modification with the microgels. **Figure A.3** shows 3D renderings of AFM images obtained from a representative film. It can be seen from the 50 x 50  $\mu\text{m}$  scan (**Figure A.3b**) that there are no uncoated areas in the interrogated region. The microgels also form a dense conformal monolayer as indicated by the 10x10  $\mu\text{m}$  scan (**Figure A.3c**). The unevenness in the microgel-coated PET is due to the uneven base surface of the PET as seen in **Figure A.3a**.

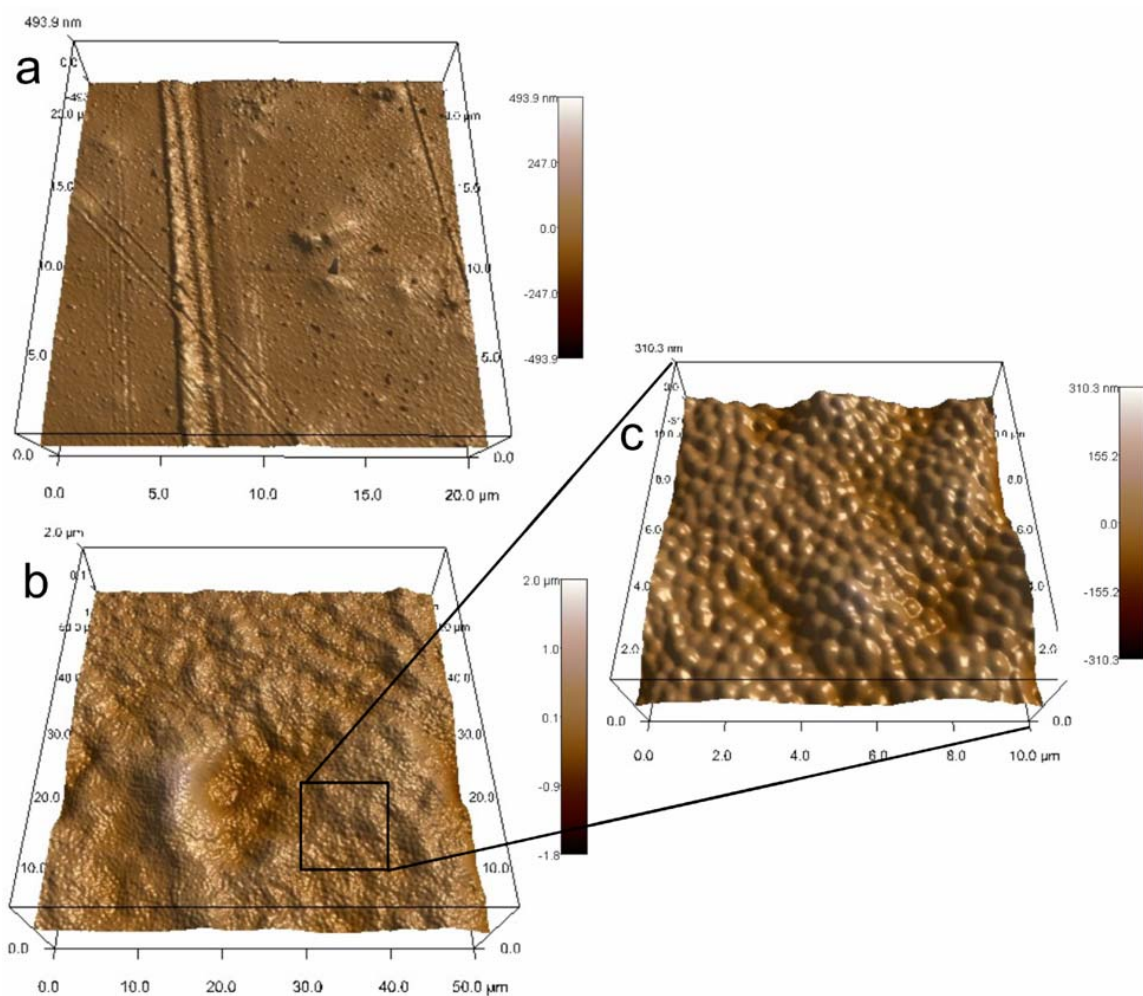


**Figure A.3: 3D rendering of AFM images.** Representative images are shown for (a) bare PET, (b, c) and microgel-modified PET.



The benzophenone modification and photo-crosslinking are critically important steps for obtaining a stable monolayer, as suggested by **Figure A.4**. **Figure A.4a** shows an AFM image of a microgel film that was spin-coated onto pAAc-grafted PET *without* benzophenone modification, followed by extensive washing. It is clear that the coverage is sparse with only a few microgel particles retained on the surface. Since covalent linkages are not possible in the absence of the photo-affinity group, the particles cannot remain adhered to the film during the washing step. This poor coverage is probably also due, in part, to the anionic charge on both the microgels (due to the AAc co-monomers) and the film (due to the pAAc grafts). In the case of benzophenone-modified surface (**Figure A.4b**) slightly more microgels are retained on the PET surface, presumably due to less Coulombic repulsion between the microgels and the modified PET. In this case, the photo-irradiation step is omitted and again, no covalent attachment is possible. However, the best results are found for the pAAc-grafted PET surfaces modified by benzophenone and further photo-irradiated (**Figure A.3b**). The photo-cross-linking is thus shown to provide a microgel film with excellent adhesion to the substrate and hence a presumed stability for use in biological environments.

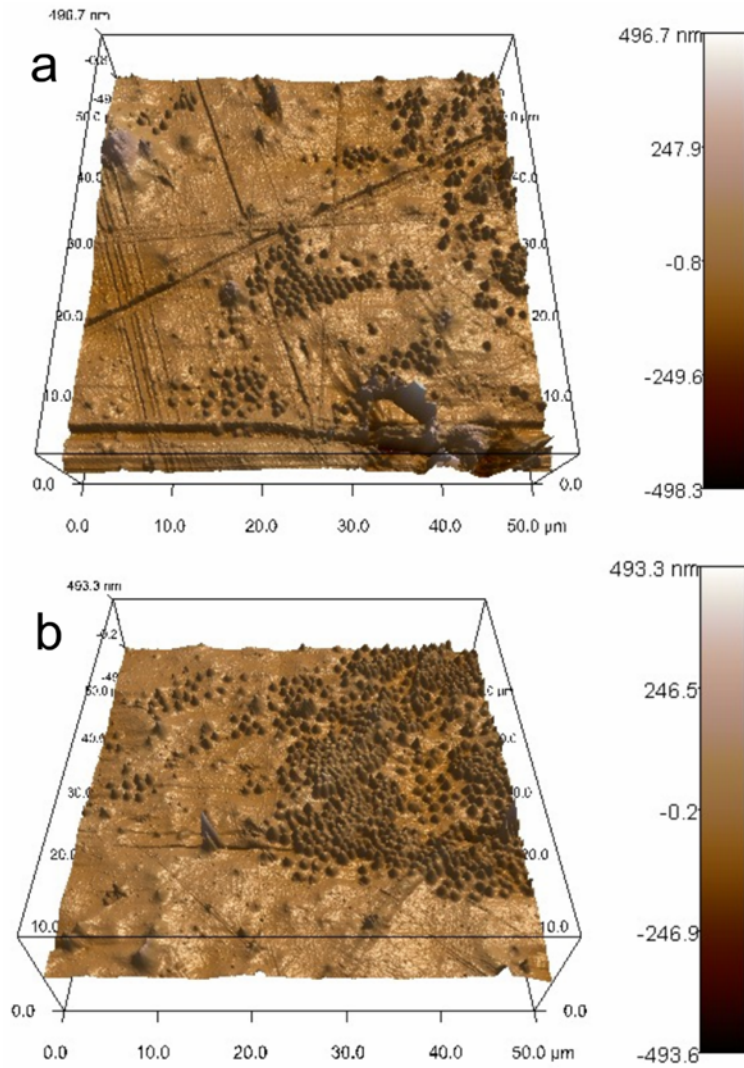


**Figure A.4: Effects of benzophenone modification and photo-crosslinking on microgel functionalization process.** 3D rendering of AFM image of microgels spin coated onto pAAc-grafted PET (a) without benzophenone modification and (b) with benzophenone modification but without UV irradiation.

It is known that one of the key steps in the inflammatory host response to biomaterials is non-specific protein adsorption, which then mediates cell adhesion and spreading.<sup>1</sup> Recent efforts in the field of biomaterials and medical implants have focused on developing non-fouling surface treatments to prevent this non-specific protein adsorption and cell adhesion.<sup>270, 292-294</sup> Our group has previously shown the efficacy of PEG-containing pNIPAm microgels as protein and cell adhesion-resistant materials.<sup>89, 231</sup> In addition to their non-fouling behavior, the facile and well-controlled synthesis of highly monodispersed microgels in a range of sizes, ease of their biofunctionalization using various orthogonal chemical functionalities, and possibility of co-assembling varied microgels onto a single substrate to generate complex bio-interfaces makes them interesting candidates for biomedical implant coatings for modulation of inflammatory response. We take advantage of these attributes to study and produce model biomaterials incorporating microgels that can be tested for their functionality.

Based on the AFM confirmation of a stable uniform monolayer of microgels on the PET surface, we tested the cell adhesion resistance of these surfaces *in vitro*. IC-21 macrophages were plated on substrates in culture media containing 10% serum. This provides a rigorous test for bioresistance as cell adhesive proteins present in serum rapidly adsorb onto synthetic surfaces and mediate cell adhesion and spreading. In contrast to bare PET films, which supported high levels of cell adhesion and spreading, microgel-functionalized PET films exhibited no macrophage adhesion over the 48 h test period (**Figure A.5**), indicating a stable cell adhesion-resistant coating. We attribute the lack of cell adhesion to microgel-functionalized surface to the protein-resistant nature of the PEG cross-linked microgels. The ability of microgel-coated surfaces to resist cell

adhesion and spreading was distributed throughout the entire sample, indicating uniform distribution of bioresistance. The success of this surface functionalization strategy thus allows the study of the non-fouling behavior of the PEG cross-linked pNIPAm microgels *in vivo* and also gives us opportunities to develop more complex biomaterials incorporating multifunctional microgel monolayers.

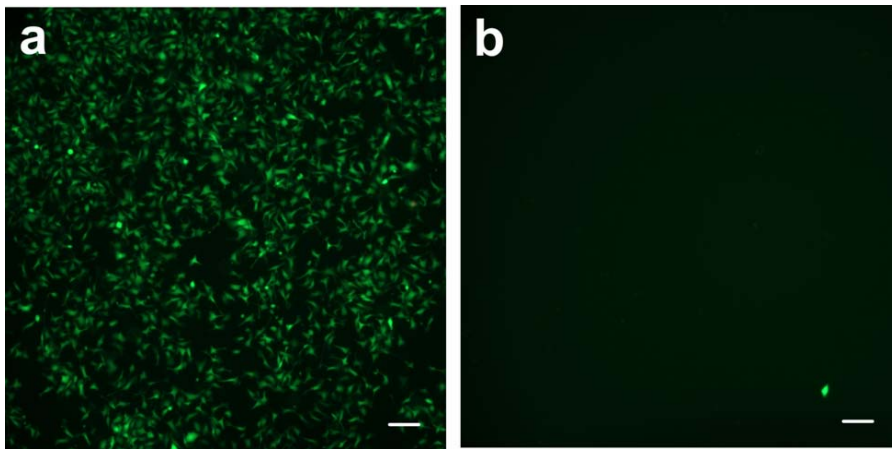


**Figure A.5: Macrophage adhesion to biomaterial surfaces.** Representative images detail macrophage adhesion on samples of (a) bare PET and (b) PET covalently functionalized by microgels. Adherent live cells were stained with calcein-AM (green). Scale bar = 100  $\mu\text{m}$ .

## CONCLUSION

In conclusion, we report a simple, scalable, and reproducible method of functionalizing PET with a conformal, dense film of hydrogel microparticles. The microgel layer is stable due to the covalent attachment of the microgels to the PET surface via a photo-affinity technique. This method can be easily extended for modifying the inert PET surface with any organic species, providing bioactive surfaces possessing

excellent stability. Note that the spin coating deposition method is used here mainly for speed, convenience, and potential scalability. However, it cannot be used to coat substrates with complex geometries and in such cases other deposition techniques must be employed. We are currently evaluating methods for dip-coating of microgels onto complex substrates. Future studies are also geared towards studying the stability and properties of these microgel coatings *in vivo*.

## REFERENCES

1. Anderson JM: Biological responses to materials, *Annu. Rev. Mater. Res.* 2001, 31:81-110
2. Gorbet MB, Sefton MV: Biomaterial-associated thrombosis: roles of coagulation factors, complement, platelets and leukocytes, *Biomaterials* 2004, 25:5681-5703
3. Kottke-Marchant K, Anderson JM, Umemura Y, Marchant RE: Effect of albumin coating on the in vitro blood compatibility of Dacron arterial prostheses, *Biomaterials* 1989, 10:147-155
4. Sutherland K, Mahoney JR, 2nd, Coury AJ, Eaton JW: Degradation of biomaterials by phagocyte-derived oxidants, *J Clin Invest* 1993, 92:2360-2367
5. Zhao Q, Topham N, Anderson JM, Hiltner A, Lodoen G, Payet CR: Foreign-body giant cells and polyurethane biostability: in vivo correlation of cell adhesion and surface cracking, *J Biomed Mater Res* 1991, 25:177-183
6. Destouet JM, Monsees BS, Oser RF, Nemecek JR, Young VL, Pilgram TK: Screening mammography in 350 women with breast implants: prevalence and findings of implant complications, *AJR Am J Roentgenol* 1992, 159:973-978; discussion 979-981
7. Ambrose CG, Clanton TO: Bioabsorbable implants: review of clinical experience in orthopedic surgery, *Ann Biomed Eng* 2004, 32:171-177
8. Voronov I, Santerre JP, Hinek A, Callahan JW, Sandhu J, Boynton EL: Macrophage phagocytosis of polyethylene particulate in vitro, *J Biomed Mater Res* 1998, 39:40-51
9. McGraw J, Hiebert GW, Steeves JD: Modulating astrogliosis after neurotrauma, *J Neurosci Res* 2001, 63:109-115
10. Wisniewski N, Moussy F, Reichert WM: Characterization of implantable biosensor membrane biofouling, *Fresenius Journal of Analytical Chemistry* 2000, 366:611-621
11. Wilson CJ, Clegg RE, Leavesley DI, Percy MJ: Mediation of biomaterial-cell interactions by adsorbed proteins: a review, *Tissue Eng* 2005, 11:1-18
12. Collier TO, Anderson JM: Protein and surface effects on monocyte and macrophage adhesion, maturation, and survival, *J Biomed Mater Res* 2002, 60:487-496

13. Shen M, Garcia I, Maier RV, Horbett TA: Effects of adsorbed proteins and surface chemistry on foreign body giant cell formation, tumor necrosis factor alpha release and procoagulant activity of monocytes, *J Biomed Mater Res A* 2004, 70:533-541
14. Chen EH, Grote E, Mohler W, Vignery A: Cell-cell fusion, *FEBS Lett* 2007, 581:2181-2193
15. Anderson JM, Rodriguez A, Chang DT: Foreign body reaction to biomaterials, *Semin Immunol* 2007,
16. Henson PM: The immunologic release of constituents from neutrophil leukocytes. II. Mechanisms of release during phagocytosis, and adherence to nonphagocytosable surfaces, *J Immunol* 1971, 107:1547-1557
17. Mathur AB, Collier TO, Kao WJ, Wiggins M, Schubert MA, Hiltner A, Anderson JM: In vivo biocompatibility and biostability of modified polyurethanes, *J Biomed Mater Res* 1997, 36:246-257
18. Gilligan BJ, Shults MC, Rhodes RK, Updike SJ: Evaluation of a subcutaneous glucose sensor out to 3 months in a dog model, *Diabetes Care* 1994, 17:882-887
19. Biran R, Martin DC, Tresco PA: Neuronal cell loss accompanies the brain tissue response to chronically implanted silicon microelectrode arrays, *Exp Neurol* 2005, 195:115-126
20. Turner JN, Shain W, Szarowski DH, Andersen M, Martins S, Isaacson M, Craighead H: Cerebral astrocyte response to micromachined silicon implants, *Exp Neurol* 1999, 156:33-49
21. de Groot M, Schuurs TA, van Schilfgaarde R: Causes of limited survival of microencapsulated pancreatic islet grafts, *J Surg Res* 2004, 121:141-150
22. Zekorn TD, Horcher A, Mellert J, Siebers U, Altug T, Emre A, Hahn HJ, Federlin K: Biocompatibility and immunology in the encapsulation of islets of Langerhans (bioartificial pancreas), *Int J Artif Organs* 1996, 19:251-257
23. Peek LJ, Middaugh CR, Berkland C: Nanotechnology in vaccine delivery, *Adv Drug Deliv Rev* 2008, 60:915-928
24. Anderson JM: In-vivo biocompatibility of implantable delivery systems and biomaterials, *European Journal of Pharmaceutics and Biopharmaceutics* 1994, 40:1-8
25. Williams DF: On the mechanisms of biocompatibility, *Biomaterials* 2008, 29:2941-2953

26. Geelhood SJ, Horbett TA, Ward WK, Wood MD, Quinn MJ: Passivating protein coatings for implantable glucose sensors: evaluation of protein retention, *J Biomed Mater Res B Appl Biomater* 2007, 81:251-260
27. Amiji M, Park H, Park K: Study on the prevention of surface-induced platelet activation by albumin coating, *J Biomater Sci Polym Ed* 1992, 3:375-388
28. Prichard HL, Reichert WM, Klitzman B: Adult adipose-derived stem cell attachment to biomaterials, *Biomaterials* 2007, 28:936-946
29. Whitesides GM, Ostuni E, Takayama S, Jiang X, Ingber DE: Soft lithography in biology and biochemistry, *Annu Rev Biomed Eng* 2001, 3:335-373
30. Prime KL, Whitesides GM: Adsorption of proteins onto surfaces containing end-attached oligo(ethylene oxide): a model system using self-assembled monolayers., *J Am Chem Soc* 1993, 115:10714-10721
31. Zhao B, Brittain WJ: Polymer brushes: surface-immobilized macromolecules., *Prog. Polym. Sci.* 2000, 25:677-710
32. Edmondson S, Osborne VL, Huck WT: Polymer brushes via surface-initiated polymerizations, *Chem Soc Rev* 2004, 33:14-22
33. Kopecek J: Hydrogel biomaterials: A smart future?, *Biomaterials* 2007, 28:5185-5192
34. Nath N, Chilkoti A: Creating "Smart" surfaces using stimuli responsive polymers, *Advanced Materials* 2002, 14:1243-+
35. Hoffman AS: Hydrogels for biomedical applications, *Adv Drug Deliv Rev* 2002, 54:3-12
36. Mendelsohn JD, Yang SY, Hiller J, Hochbaum AI, Rubner MF: Rational design of cytophilic and cytophobic polyelectrolyte multilayer thin films, *Biomacromolecules* 2003, 4:96-106
37. Nayak S, Lyon LA: Ligand-functionalized core/shell microgels with permselective shells, *Angew Chem Int Ed Engl* 2004, 43:6706-6709
38. Nayak S, Lyon LA: Soft nanotechnology with soft nanoparticles, *Angew Chem Int Ed Engl* 2005, 44:7686-7708
39. Anderson JM, Miller KM: Biomaterial biocompatibility and the macrophage, *Biomaterials* 1984, 5:5-10



40. Hynes RO: Integrins: bidirectional, allosteric signaling machines, *Cell* 2002, 110:673-687
41. McNally AK, Anderson JM: Beta1 and beta2 integrins mediate adhesion during macrophage fusion and multinucleated foreign body giant cell formation, *Am J Pathol* 2002, 160:621-630
42. Ley K: The role of selectins in inflammation and disease, *Trends Mol Med* 2003, 9:263-268
43. Dinnes DL, Marcal H, Raftery MJ, Labow RS, Mahler SM: The macrophage-biomaterial interface: a proteomic analysis of the conditioned medium environment, *J Chem Technol Biotechnol* 2008, 83:482-495
44. Parker LC, Whyte MK, Dower SK, Sabroe I: The expression and roles of Toll-like receptors in the biology of the human neutrophil, *J Leukoc Biol* 2005, 77:886-892
45. Rabinovitch M: Professional and non-professional phagocytes: an introduction, *Trends Cell Biol* 1995, 5:85-87
46. Thomsen P, Gretzer, C.: Macrophage interactions with modified material surfaces, *Current Opinion in Solid State and Materials Science* 2001, 5:163-176
47. Nathan CF: Secretory products of macrophages, *J Clin Invest* 1987, 79:319-326
48. Gordon S: Alternative activation of macrophages, *Nat Rev Immunol* 2003, 3:23-35
49. Mosser DM: The many faces of macrophage activation, *J Leukoc Biol* 2003, 73:209-212
50. Mills CD, Kincaid K, Alt JM, Heilman MJ, Hill AM: M-1/M-2 macrophages and the Th1/Th2 paradigm, *J Immunol* 2000, 164:6166-6173
51. Henson PM: The immunologic release of constituents from neutrophil leukocytes. I. The role of antibody and complement on nonphagocytosable surfaces or phagocytosable particles, *J Immunol* 1971, 107:1535-1546
52. Hu WJ, Eaton JW, Ugarova TP, Tang L: Molecular basis of biomaterial-mediated foreign body reactions, *Blood* 2001, 98:1231-1238
53. Sun DH, Trindade MC, Nakashima Y, Maloney WJ, Goodman SB, Schurman DJ, Smith RL: Human serum opsonization of orthopedic biomaterial particles: protein-binding and monocyte/macrophage activation in vitro, *J Biomed Mater Res A* 2003, 65:290-298

54. Tang L, Wu Y, Timmons RB: Fibrinogen adsorption and host tissue responses to plasma functionalized surfaces, *J Biomed Mater Res* 1998, 42:156-163
55. Sefton MV, Sawyer A, Gorbet M, Black JP, Cheng E, Gemmell C, Pottinger-Cooper E: Does surface chemistry affect thrombogenicity of surface modified polymers?, *J Biomed Mater Res* 2001, 55:447-459
56. Tang L, Liu L, Elwing HB: Complement activation and inflammation triggered by model biomaterial surfaces, *J Biomed Mater Res* 1998, 41:333-340
57. Tang L, Sheu MS, Chu T, Huang YH: Anti-inflammatory properties of triblock siloxane copolymer-blended materials, *Biomaterials* 1999, 20:1365-1370
58. Vroman L, Adams AL, Klings M: Interactions among human blood proteins at interfaces, *Fed Proc* 1971, 30:1494-1502
59. Xu LC, Siedlecki CA: Effects of surface wettability and contact time on protein adhesion to biomaterial surfaces, *Biomaterials* 2007, 28:3273-3283
60. Horbett TA: Principles underlying the role of adsorbed plasma proteins in blood interactions with foreign materials., *Cardiovasc Pathol* 1993, 2:137S-148S
61. Andrade JD, Hlady V: Protein adsorption and materials biocompatibility - a tutorial review and suggested hypotheses., *Adv Polym Sci* 1986, 79:1-63
62. Kao WJ, Lee D: In vivo modulation of host response and macrophage behavior by polymer networks grafted with fibronectin-derived biomimetic oligopeptides: the role of RGD and PHSRN domains, *Biomaterials* 2001, 22:2901-2909
63. McNally AK, Anderson JM: Complement C3 participation in monocyte adhesion to different surfaces, *Proc Natl Acad Sci U S A* 1994, 91:10119-10123
64. Tang L, Lucas AH, Eaton JW: Inflammatory responses to implanted polymeric biomaterials: role of surface-adsorbed immunoglobulin G, *J Lab Clin Med* 1993, 122:292-300
65. Tang L, Eaton JW: Fibrin(ogen) mediates acute inflammatory responses to biomaterials, *J Exp Med* 1993, 178:2147-2156
66. Wu Y, Simonovsky FI, Ratner BD, Horbett TA: The role of adsorbed fibrinogen in platelet adhesion to polyurethane surfaces: a comparison of surface hydrophobicity, protein adsorption, monoclonal antibody binding, and platelet adhesion, *J Biomed Mater Res A* 2005, 74:722-738

67. Collier TO, Anderson JM, Kikuchi A, Okano T: Adhesion behavior of monocytes, macrophages, and foreign body giant cells on poly (N-isopropylacrylamide) temperature-responsive surfaces, *J Biomed Mater Res* 2002, 59:136-143
68. Garcia AJ: Get a grip: integrins in cell-biomaterial interactions, *Biomaterials* 2005, 26:7525-7529
69. Danen EH, Sonnenberg A: Integrins in regulation of tissue development and function, *J Pathol* 2003, 201:632-641
70. Wehrle-Haller B, Imhof BA: Integrin-dependent pathologies, *J Pathol* 2003, 200:481-487
71. Altieri DC, Plescia J, Plow EF: The structural motif glycine 190-valine 202 of the fibrinogen gamma chain interacts with CD11b/CD18 integrin (alpha M beta 2, Mac-1) and promotes leukocyte adhesion, *J Biol Chem* 1993, 268:1847-1853
72. Flick MJ, Du X, Witte DP, Jirouskova M, Soloviev DA, Busuttill SJ, Plow EF, Degen JL: Leukocyte engagement of fibrin(ogen) via the integrin receptor alphaMbeta2/Mac-1 is critical for host inflammatory response in vivo, *J Clin Invest* 2004, 113:1596-1606
73. Tang L, Ugarova TP, Plow EF, Eaton JW: Molecular determinants of acute inflammatory responses to biomaterials, *J Clin Invest* 1996, 97:1329-1334
74. Forsyth CB, Solovjov DA, Ugarova TP, Plow EF: Integrin alpha(M)beta(2)-mediated cell migration to fibrinogen and its recognition peptides, *J Exp Med* 2001, 193:1123-1133
75. Chapman HA: Plasminogen activators, integrins, and the coordinated regulation of cell adhesion and migration, *Curr Opin Cell Biol* 1997, 9:714-724
76. Erwig LP, Kluth DC, Walsh GM, Rees AJ: Initial cytokine exposure determines function of macrophages and renders them unresponsive to other cytokines, *J Immunol* 1998, 161:1983-1988
77. Stout RD, Jiang C, Matta B, Tietzel I, Watkins SK, Suttles J: Macrophages sequentially change their functional phenotype in response to changes in microenvironmental influences, *J Immunol* 2005, 175:342-349
78. Stout RD, Suttles J: Functional plasticity of macrophages: reversible adaptation to changing microenvironments, *J Leukoc Biol* 2004, 76:509-513
79. Goerdt S, Orfanos CE: Other functions, other genes: alternative activation of antigen-presenting cells, *Immunity* 1999, 10:137-142

80. Warner RL, Bhagavathula N, Nerusu KC, Lateef H, Younkin E, Johnson KJ, Varani J: Matrix metalloproteinases in acute inflammation: induction of MMP-3 and MMP-9 in fibroblasts and epithelial cells following exposure to pro-inflammatory mediators in vitro, *Exp Mol Pathol* 2004, 76:189-195
81. Montaner LJ, da Silva RP, Sun J, Sutterwala S, Hollinshead M, Vaux D, Gordon S: Type 1 and type 2 cytokine regulation of macrophage endocytosis: differential activation by IL-4/IL-13 as opposed to IFN-gamma or IL-10, *J Immunol* 1999, 162:4606-4613
82. Song E, Ouyang N, Horbelt M, Antus B, Wang M, Exton MS: Influence of alternatively and classically activated macrophages on fibrogenic activities of human fibroblasts, *Cell Immunol* 2000, 204:19-28
83. Xia Z, Triffitt JT: A review on macrophage responses to biomaterials, *Biomed Mater* 2006, 1:R1-9
84. McNally AK, Anderson JM: Multinucleated giant cell formation exhibits features of phagocytosis with participation of the endoplasmic reticulum, *Exp Mol Pathol* 2005, 79:126-135
85. McNally AK, Anderson JM: Interleukin-4 induces foreign body giant cells from human monocytes/macrophages. Differential lymphokine regulation of macrophage fusion leads to morphological variants of multinucleated giant cells, *Am J Pathol* 1995, 147:1487-1499
86. Brodbeck WG, Shive MS, Colton E, Ziats NP, Anderson JM: Interleukin-4 inhibits tumor necrosis factor-alpha-induced and spontaneous apoptosis of biomaterial-adherent macrophages, *J Lab Clin Med* 2002, 139:90-100
87. van Luyn MJ, Khouw IM, van Wachem PB, Blaauw EH, Werkmeister JA: Modulation of the tissue reaction to biomaterials. II. The function of T cells in the inflammatory reaction to crosslinked collagen implanted in T-cell-deficient rats, *J Biomed Mater Res* 1998, 39:398-406
88. Chang DT, Colton E, Anderson JM: Paracrine and juxtacrine lymphocyte enhancement of adherent macrophage and foreign body giant cell activation, *J Biomed Mater Res A* 2008,
89. Nolan CM, Reyes CD, Debord JD, Garcia AJ, Lyon LA: Phase transition behavior, protein adsorption, and cell adhesion resistance of poly(ethylene glycol) cross-linked microgel particles, *Biomacromolecules* 2005, 6:2032-2039
90. Morimoto N, Endo T, Iwasaki Y, Akiyoshi K: Design of hybrid hydrogels with self-assembled nanogels as cross-linkers: interaction with proteins and chaperone-like activity, *Biomacromolecules* 2005, 6:1829-1834

91. Hu Z, Xia X, Marquez M, Weng H, Tang L: Controlled release from and tissue response to physically bonded hydrogel nanoparticle assembly., *Macromol Symp* 2005, 227:
92. Weng H, Zhou J, Tang L, Hu Z: Tissue responses to thermally-responsive hydrogel nanoparticles, *J Biomater Sci Polym Ed* 2004, 15:1167-1180
93. Lutolf MP, Hubbell JA: Synthetic biomaterials as instructive extracellular microenvironments for morphogenesis in tissue engineering, *Nat Biotechnol* 2005, 23:47-55
94. West JL, Hubbell JA: Comparison of covalently and physically cross-linked polyethylene glycol-based hydrogels for the prevention of postoperative adhesions in a rat model, *Biomaterials* 1995, 16:1153-1156
95. West JL, Hubbell JA: Photopolymerized hydrogel materials for drug delivery applications., *Reactive Polymers* 1995, 25:139-147
96. Gombotz WR, Wee SF: Protein release from alginate matrices, *Adv Drug Deliv Rev* 1998, 31:267-285
97. Mundargi RC, Babu VR, Rangaswamy V, Patel P, Aminabhavi TM: Nano/micro technologies for delivering macromolecular therapeutics using poly(D,L-lactide-co-glycolide) and its derivatives, *J Control Release* 2008, 125:193-209
98. Han HD, Song CK, Park YS, Noh KH, Kim JH, Hwang T, Kim TW, Shin BC: A chitosan hydrogel-based cancer drug delivery system exhibits synergistic antitumor effects by combining with a vaccinia viral vaccine, *Int J Pharm* 2008, 350:27-34
99. Jain S, Yap WT, Irvine DJ: Synthesis of protein-loaded hydrogel particles in an aqueous two-phase system for coincident antigen and CpG oligonucleotide delivery to antigen-presenting cells, *Biomacromolecules* 2005, 6:2590-2600
100. Prokop A, Kozlov E, Newman GW, Newman MJ: Water-based nanoparticulate polymeric system for protein delivery: permeability control and vaccine application, *Biotechnol Bioeng* 2002, 78:459-466
101. Ehrbar M, Rizzi SC, Schoenmakers RG, Miguel BS, Hubbell JA, Weber FE, Lutolf MP: Biomolecular hydrogels formed and degraded via site-specific enzymatic reactions, *Biomacromolecules* 2007, 8:3000-3007
102. Drumheller PD, Elbert DL, Hubbell JA: Multifunctional poly(ethylene glycol) semi-interpenetrating polymer networks as highly selective adhesive substrates for bioadhesive peptide grafting., *Biotechnol Bioeng* 1994, 43:772-780

103. Khademhosseini A, Langer R, Borenstein J, Vacanti JP: Microscale technologies for tissue engineering and biology, *Proc Natl Acad Sci U S A* 2006, 103:2480-2487
104. West JL, Hubbell JA: Polymeric biomaterials with degradation sites for proteases involved in cell migration., *Macromolecules* 1999, 32:241-244
105. Gerritsen M, Jansen JA, Kros A, Nolte RJ, Lutterman JA: Performance of subcutaneously implanted glucose sensors: a review, *J Invest Surg* 1998, 11:163-174
106. Kyrolainen M, Rigsby P, Eddy S, Vadgama P: Bio-/haemocompatibility: implications and outcomes for sensors?, *Acta Anaesthesiol Scand Suppl* 1995, 104:55-60
107. Wisniewski N, Reichert M: Methods for reducing biosensor membrane biofouling, *Colloids and Surfaces B-Biointerfaces* 2000, 18:197-219
108. National diabetes fact sheet: general information and national estimates on diabetes in the United States., Atlanta, GA: U.S. Department of Health and Human Services, Centers for Disease Control and Prevention. 2005,
109. Updike SJ, Shults MC, Rhodes RK, Gilligan BJ, Luebow JO, von Heimburg D: Enzymatic glucose sensors. Improved long-term performance in vitro and in vivo, *ASAIO J* 1994, 40:157-163
110. Updike SJ, Shults MC, Gilligan BJ, Rhodes RK: A subcutaneous glucose sensor with improved longevity, dynamic range, and stability of calibration, *Diabetes Care* 2000, 23:208-214
111. Luttikhuisen DT, van Amerongen MJ, de Feijter PC, Petersen AH, Harmsen MC, van Luyn MJ: The correlation between difference in foreign body reaction between implant locations and cytokine and MMP expression, *Biomaterials* 2006, 27:5763-5770
112. Andersson M, Suska F, Johansson A, Berglin M, Emanuelsson L, Elwing H, Thomsen P: Effect of molecular mobility of polymeric implants on soft tissue reactions: An in vivo study in rats, *J Biomed Mater Res A* 2007, 84A:652-660
113. Nair A, Zou L, Bhattacharyya D, Timmons RB, Tang L: Species and density of implant surface chemistry affect the extent of foreign body reactions, *Langmuir* 2008, 24:2015-2024
114. Kingshott P, Griesser HJ: Surfaces that resist bioadhesion., *Current Opinion in Solid State and Materials Science* 1999, 4:403-412
115. Unsworth LD, Sheardown H, Brash JL: Polyethylene oxide surfaces of variable chain density by chemisorption of PEO-thiol on gold: adsorption of proteins from plasma studied by radiolabelling and immunoblotting, *Biomaterials* 2005, 26:5927-5933

116. Unsworth LD, Sheardown H, Brash JL: Protein-Resistant Poly(ethylene oxide)-Grafted Surfaces: Chain Density-Dependent Multiple Mechanisms of Action, *Langmuir* 2008, 24:1924-1929
117. Michel R, Pasche S, Textor M, Castner DG: Influence of PEG architecture on protein adsorption and conformation, *Langmuir* 2005, 21:12327-12332
118. Morra M: On the molecular basis of fouling resistance, *J Biomater Sci Polym Ed* 2000, 11:547-569
119. Szleifer I: Protein adsorption on tethered polymer layers: effect of polymer chain architecture and composition., *Physica A* 1997, 244:370-388
120. Szleifer I: Polymers and proteins: interactions at interfaces., *Current Opinion in Solid State and Materials Science* 1997, 2:337-344
121. Wang C, Yu B, Knudsen B, Harmon J, Moussy F, Moussy Y: Synthesis and performance of novel hydrogels coatings for implantable glucose sensors, *Biomacromolecules* 2008, 9:561-567
122. Singh N, Bridges AW, Garcia AJ, Lyon LA: Covalent tethering of functional microgel films onto poly(ethylene terephthalate) surfaces, *Biomacromolecules* 2007, 8:3271-3275
123. Yang Y, Zhang SF, Kingston MA, Jones G, Wright G, Spencer SA: Glucose sensor with improved haemocompatibility, *Biosens Bioelectron* 2000, 15:221-227
124. Iwasaki Y, Ishihara K, Nakabayashi N, Khang G, Jeon JH, Lee JW, Lee HB: Platelet adhesion on the gradient surfaces grafted with phospholipid polymer, *J Biomater Sci Polym Ed* 1998, 9:801-816
125. Kudo H, Sawada T, Kazawa E, Yoshida H, Iwasaki Y, Mitsubayashi K: A flexible and wearable glucose sensor based on functional polymers with soft-MEMS techniques, *Biosens Bioelectron* 2006, 22:558-562
126. Goreish HH, Lewis AL, Rose S, Lloyd AW: The effect of phosphorylcholine-coated materials on the inflammatory response and fibrous capsule formation: in vitro and in vivo observations, *J Biomed Mater Res A* 2004, 68:1-9
127. Luk YY, Kato M, Mrksich M: Self-assembled monolayers of alkanethiolates presenting mannitol groups are inert to protein adsorption and cell attachment., *Langmuir* 2000, 16:9604-9608
128. Holland NB, Qiu Y, Ruegsegger M, Marchant RE: Biomimetic engineering of non-adhesive glycocalyx-like surfaces using oligosaccharide surfactant polymers, *Nature* 1998, 392:799-801

129. Kane RS, Deschatelets P, Whitesides GM: Kosmotropes form the basis of protein-resistant surfaces., *Langmuir* 2003, 19:2388-2391
130. Blackburn WH, Lyon LA: Size-controlled synthesis of monodisperse core/shell nanogels., *Colloid Polym Sci* 2008, 286:563-569
131. Oh JK, Drumright R, Siegwart DJ, Matyjaszewski K: The development of microgels/nanogels for drug delivery applications., *Prog. Polym. Sci.* 2008, 33:448-477
132. Chapman RG, Ostuni E, Liang MN, Meluleni G, Kim E, Yan L, Pier G, Warren HS, Whitesides GM: Polymeric thin films that resist the adsorption of proteins and the adhesion of bacteria., *Langmuir* 2001, 17:1225-1233
133. Zhang F, Kang ET, Neoh KG, Huang W: Modification of gold surface by grafting of poly(ethylene glycol) for reduction in protein adsorption and platelet adhesion, *J Biomater Sci Polym Ed* 2001, 12:515-531
134. Espadas-Torre C, Meyerhoff ME: Thrombogenic properties of untreated and poly(ethylene oxide)-modified polymeric matrices useful for preparing intraarterial ion-selective electrodes, *Anal Chem* 1995, 67:3108-3114
135. Lee JH, Jeong BJ, Lee HB: Plasma protein adsorption and platelet adhesion onto comb-like PEO gradient surfaces, *J Biomed Mater Res* 1997, 34:105-114
136. Du H, Chandaroy P, Hui SW: Grafted poly-(ethylene glycol) on lipid surfaces inhibits protein adsorption and cell adhesion, *Biochim Biophys Acta* 1997, 1326:236-248
137. Zhang M, Desai T, Ferrari M: Proteins and cells on PEG immobilized silicon surfaces, *Biomaterials* 1998, 19:953-960
138. Jenney CR, Anderson JM: Effects of surface-coupled polyethylene oxide on human macrophage adhesion and foreign body giant cell formation in vitro, *J Biomed Mater Res* 1999, 44:206-216
139. Shen M, Pan YV, Wagner MS, Hauch KD, Castner DG, Ratner BD, Horbett TA: Inhibition of monocyte adhesion and fibrinogen adsorption on glow discharge plasma deposited tetraethylene glycol dimethyl ether, *J Biomater Sci Polym Ed* 2001, 12:961-978
140. Otsuka H, Nagasaki Y, Kataoka K: Self-assembly of poly(ethylene glycol)-based block copolymers for biomedical applications., *Current Opinion in Colloid & Interface Science* 2001, 6:3-10
141. Boulmedais F, Frisch B, Etienne O, Lavallo P, Picart C, Ogier J, Voegel JC, Schaaf P, Egles C: Polyelectrolyte multilayer films with pegylated polypeptides as a new type of anti-microbial protection for biomaterials, *Biomaterials* 2004, 25:2003-2011



142. Ma H, Hyun J, Stiller P, Chilkoti A: "Non-fouling" oligo(ethylene glycol)-functionalized polymer brushes synthesized by surface-initiated atom transfer radical polymerization., *Advanced Materials* 2004, 16:338-341
143. Ma H, Li D, Sheng X, Zhao B, Chilkoti A: Protein-resistant polymer coatings on silicon oxide by surface-initiated atom transfer radical polymerization, *Langmuir* 2006, 22:3751-3756
144. Zhou Y, Liedberg B, Gorochovceva N, Makuska R, Dedinaite A, Claesson PM: Chitosan-N-poly(ethylene oxide) brush polymers for reduced nonspecific protein adsorption, *J Colloid Interface Sci* 2007, 305:62-71
145. Waku T, Matsusaki M, Kaneko T, Akashi M: PEG brush peptide nanospheres with stealth properties and chemical functionality., *Macromolecules* 2007, 40:6385-6392
146. Cao L, Chang M, Lee CY, Castner DG, Sukavaneshvar S, Ratner BD, Horbett TA: Plasma-deposited tetraglyme surfaces greatly reduce total blood protein adsorption, contact activation, platelet adhesion, platelet procoagulant activity, and in vitro thrombus deposition, *J Biomed Mater Res A* 2007, 81:827-837
147. Quinn CP, Pathak CP, Heller A, Hubbell JA: Photo-crosslinked copolymers of 2-hydroxyethyl methacrylate, poly(ethylene glycol) tetra-acrylate and ethylene dimethacrylate for improving biocompatibility of biosensors, *Biomaterials* 1995, 16:389-396
148. Quinn CA, Connor RE, Heller A: Biocompatible, glucose-permeable hydrogel for in situ coating of implantable biosensors, *Biomaterials* 1997, 18:1665-1670
149. Collier TO, Anderson JM, Brodbeck WG, Barber T, Healy KE: Inhibition of macrophage development and foreign body giant cell formation by hydrophilic interpenetrating polymer network, *J Biomed Mater Res A* 2004, 69:644-650
150. Yu B, Wang C, Ju YM, West L, Harmon J, Moussy Y, Moussy F: Use of hydrogel coating to improve the performance of implanted glucose sensors, *Biosens Bioelectron* 2007,
151. Benkirane-Jessel N, Lavallo P, Meyer F, Audouin F, Frisch B, Schaaf P, Ogier J, Decher G, Voegel JC: Control of monocyte morphology on and response to model surfaces for implants equipped with anti-inflammatory agents., *Advanced Materials* 2004, 16:1507-1511
152. Schultz P, Vautier D, Richert L, Jessel N, Haikel Y, Schaaf P, Voegel JC, Ogier J, Debry C: Polyelectrolyte multilayers functionalized by a synthetic analogue of an anti-inflammatory peptide, alpha-MSH, for coating a tracheal prosthesis, *Biomaterials* 2005, 26:2621-2630

153. Shive MS, Anderson JM: Biodegradation and biocompatibility of PLA and PLGA microspheres, *Adv Drug Deliv Rev* 1997, 28:5-24
154. Lutolf MP, Raeber GP, Zisch AH, Tirelli N, Hubbell JA: Cell-responsive synthetic hydrogels., *Advanced Materials* 2003, 15:888-892
155. Zisch AH, Lutolf MP, Ehrbar M, Raeber GP, Rizzi SC, Davies N, Schmokel H, Bezuidenhout D, Djonov V, Zilla P, Hubbell JA: Cell-demanded release of VEGF from synthetic, biointeractive cell ingrowth matrices for vascularized tissue growth, *FASEB J* 2003, 17:2260-2262
156. Tauro JR, Gemeinhart RA: Matrix metalloprotease triggered delivery of cancer chemotherapeutics from hydrogel matrixes, *Bioconjug Chem* 2005, 16:1133-1139
157. Bae M, Cho S, Song J, Lee GY, Kim K, Yang J, Cho K, Kim SY, Byun Y: Metalloprotease-specific poly(ethylene glycol) methyl ether-peptide-doxorubicin conjugate for targeting anticancer drug delivery based on angiogenesis, *Drugs Exp Clin Res* 2003, 29:15-23
158. Barnes PJ: Anti-inflammatory actions of glucocorticoids: molecular mechanisms, *Clin Sci (Lond)* 1998, 94:557-572
159. Cupps TR, Fauci AS: Corticosteroid-mediated immunoregulation in man, *Immunol Rev* 1982, 65:133-155
160. Kiefer R, Kreutzberg GW: Effects of dexamethasone on microglial activation in vivo: selective downregulation of major histocompatibility complex class II expression in regenerating facial nucleus, *J Neuroimmunol* 1991, 34:99-108
161. Norton LW, Koschwanez HE, Wisniewski NA, Klitzman B, Reichert WM: Vascular endothelial growth factor and dexamethasone release from nonfouling sensor coatings affect the foreign body response, *J Biomed Mater Res A* 2007, 81:858-869
162. Zhong Y, Bellamkonda RV: Dexamethasone-coated neural probes elicit attenuated inflammatory response and neuronal loss compared to uncoated neural probes, *Brain Res* 2007, 1148:15-27
163. Kim DH, Martin DC: Sustained release of dexamethasone from hydrophilic matrices using PLGA nanoparticles for neural drug delivery, *Biomaterials* 2006, 27:3031-3037
164. Patil SD, Papadimitrakopoulos F, Burgess DJ: Concurrent delivery of dexamethasone and VEGF for localized inflammation control and angiogenesis, *J Control Release* 2007, 117:68-79

165. Wadhwa R, Lagenaur CF, Cui XT: Electrochemically controlled release of dexamethasone from conducting polymer polypyrrole coated electrode, *J Control Release* 2006, 110:531-541
166. Zhong Y, Bellamkonda RV: Controlled release of anti-inflammatory agent alpha-MSH from neural implants, *J Control Release* 2005, 106:309-318
167. He W, McConnell GC, Schneider TM, Bellamkonda RV: A novel anti-inflammatory surface for neural electrodes., *Advanced Materials* 2007, 19:3529-
168. Gerritsen M, Kros A, Sprakel V, Lutterman JA, Nolte RJ, Jansen JA: Biocompatibility evaluation of sol-gel coatings for subcutaneously implantable glucose sensors, *Biomaterials* 2000, 21:71-78
169. Wang XH, Li DP, Wang WJ, Feng QL, Cui FZ, Xu YX, Song XH: Covalent immobilization of chitosan and heparin on PLGA surface, *Int J Biol Macromol* 2003, 33:95-100
170. van Bilsen PH, Popa ER, Brouwer LA, Vincent J, Taylor CE, de Leij LF, Hendriks M, van Luyn MJ: Ongoing foreign body reaction to subcutaneous implanted (heparin) modified Dacron in rats, *J Biomed Mater Res A* 2004, 68:423-427
171. Sung WJ, Na K, Bae YH: Biocompatibility and interference eliminating property of pullulan acetate/polyethylene glycol/heparin membrane for the outer layer of an amperometric glucose sensor., *Sensors and Actuators B* 2004, 99:393-398
172. Fu J, Ji J, Yuan W, Shen J: Construction of anti-adhesive and antibacterial multilayer films via layer-by-layer assembly of heparin and chitosan, *Biomaterials* 2005, 26:6684-6692
173. Rele SM, Cui W, Wang L, Hou S, Barr-Zarse G, Tatton D, Gnanou Y, Esko JD, Chaikof EL: Dendrimer-like PEO glycopolymers exhibit anti-inflammatory properties, *J Am Chem Soc* 2005, 127:10132-10133
174. Tseng PY, Rele SS, Sun XL, Chaikof EL: Membrane-mimetic films containing thrombomodulin and heparin inhibit tissue factor-induced thrombin generation in a flow model, *Biomaterials* 2006, 27:2637-2650
175. Du YJ, Brash JL, McClung G, Berry LR, Klement P, Chan AK: Protein adsorption on polyurethane catheters modified with a novel antithrombin-heparin covalent complex, *J Biomed Mater Res A* 2007, 80:216-225
176. Kim DH, Smith JT, Chilkoti A, Reichert WM: The effect of covalently immobilized rhIL-1ra-ELP fusion protein on the inflammatory profile of LPS-stimulated human monocytes, *Biomaterials* 2007, 28:3369-3377

177. Udipi K, Ornberg RL, Thurmond KB, 2nd, Settle SL, Forster D, Riley D: Modification of inflammatory response to implanted biomedical materials in vivo by surface bound superoxide dismutase mimics, *J Biomed Mater Res* 2000, 51:549-560
178. Nguyen KT, Shaikh N, Shukla KP, Su SH, Eberhart RC, Tang L: Molecular responses of vascular smooth muscle cells and phagocytes to curcumin-eluting bioresorbable stent materials, *Biomaterials* 2004, 25:5333-5346
179. Su SH, Nguyen KT, Satasiya P, Greilich PE, Tang L, Eberhart RC: Curcumin impregnation improves the mechanical properties and reduces the inflammatory response associated with poly(L-lactic acid) fiber, *J Biomater Sci Polym Ed* 2005, 16:353-370
180. Pan Ch J, Tang JJ, Weng YJ, Wang J, Huang N: Preparation, characterization and anticoagulation of curcumin-eluting controlled biodegradable coating stents, *J Control Release* 2006, 116:42-49
181. Hahn SK, Jelacic S, Maier RV, Stayton PS, Hoffman AS: Anti-inflammatory drug delivery from hyaluronic acid hydrogels, *J Biomater Sci Polym Ed* 2004, 15:1111-1119
182. Anastase-Ravion S, Blondin C, Cholley B, Haeffner-Cavaillon N, Castellot JJ, Letourneur D: Heparin inhibits lipopolysaccharide (LPS) binding to leukocytes and LPS-induced cytokine production, *J Biomed Mater Res A* 2003, 66:376-384
183. Ulbrich H, Eriksson EE, Lindbom L: Leukocyte and endothelial cell adhesion molecules as targets for therapeutic interventions in inflammatory disease, *Trends Pharmacol Sci* 2003, 24:640-647
184. Salas A, Sans M, Soriano A, Reverter JC, Anderson DC, Pique JM, Panes J: Heparin attenuates TNF-alpha induced inflammatory response through a CD11b dependent mechanism, *Gut* 2000, 47:88-96
185. Mantovani A, Locati M, Vecchi A, Sozzani S, Allavena P: Decoy receptors: a strategy to regulate inflammatory cytokines and chemokines, *Trends Immunol* 2001, 22:328-336
186. Kao WJ, Liu Y, Gundloori R, Li J, Lee D, Einerson N, Burmania J, Stevens K: Engineering endogenous inflammatory cells as delivery vehicles, *J Control Release* 2002, 78:219-233
187. DeFife KM, Shive MS, Hagen KM, Clapper DL, Anderson JM: Effects of photochemically immobilized polymer coatings on protein adsorption, cell adhesion, and the foreign body reaction to silicone rubber, *J Biomed Mater Res* 1999, 44:298-307
188. Shen M, Martinson L, Wagner MS, Castner DG, Ratner BD, Horbett TA: PEO-like plasma polymerized tetraglyme surface interactions with leukocytes and proteins: in vitro and in vivo studies, *J Biomater Sci Polym Ed* 2002, 13:367-390

189. Mori R, Shaw TJ, Martin P: Molecular mechanisms linking wound inflammation and fibrosis: knockdown of osteopontin leads to rapid repair and reduced scarring, *J Exp Med* 2008, 205:43-51
190. Klueh U, Dorsky DI, Kreutzer DL: Enhancement of implantable glucose sensor function in vivo using gene transfer-induced neovascularization, *Biomaterials* 2005, 26:1155-1163
191. Ratner BD, Bryant SJ: Biomaterials: where we have been and where we are going, *Annu Rev Biomed Eng* 2004, 6:41-75
192. Bauer TW, Schils J: The pathology of total joint arthroplasty.II. Mechanisms of implant failure, *Skeletal Radiol* 1999, 28:483-497
193. Polikov VS, Tresco PA, Reichert WM: Response of brain tissue to chronically implanted neural electrodes, *J Neurosci Methods* 2005, 148:1-18
194. Wu P, Grainger DW: Drug/device combinations for local drug therapies and infection prophylaxis, *Biomaterials* 2006, 27:2450-2467
195. Hynes RO: *Fibronectins*, New York: Springer 1990,
196. George EL, Georges-Labouesse EN, Patel-King RS, Rayburn H, Hynes RO: Defects in mesoderm, neural tube and vascular development in mouse embryos lacking fibronectin, *Development* 1993, 119:1079-1091
197. Sakai T, Larsen M, Yamada KM: Fibronectin requirement in branching morphogenesis, *Nature* 2003, 423:876-881
198. Sakai T, Johnson KJ, Murozono M, Sakai K, Magnuson MA, Wieloch T, Cronberg T, Isshiki A, Erickson HP, Fassler R: Plasma fibronectin supports neuronal survival and reduces brain injury following transient focal cerebral ischemia but is not essential for skin-wound healing and hemostasis, *Nat Med* 2001, 7:324-330
199. Ni H, Yuen PS, Papalia JM, Trevithick JE, Sakai T, Fassler R, Hynes RO, Wagner DD: Plasma fibronectin promotes thrombus growth and stability in injured arterioles, *Proc Natl Acad Sci U S A* 2003, 100:2415-2419
200. Sokal RR, Rohlf FJ: *Biometry: the principles and practice of statistics in biological research.*, W.H. Freeman: New York 1995,
201. Tang L, Jennings TA, Eaton JW: Mast cells mediate acute inflammatory responses to implanted biomaterials, *Proc Natl Acad Sci U S A* 1998, 95:8841-8846

202. Shen M, Horbett TA: The effects of surface chemistry and adsorbed proteins on monocyte/macrophage adhesion to chemically modified polystyrene surfaces, *J Biomed Mater Res* 2001, 57:336-345
203. Velling T, Risteli J, Wennerberg K, Mosher DF, Johansson S: Polymerization of type I and III collagens is dependent on fibronectin and enhanced by integrins alpha 11beta 1 and alpha 2beta 1, *J Biol Chem* 2002, 277:37377-37381
204. Sottile J, Hocking DC: Fibronectin polymerization regulates the composition and stability of extracellular matrix fibrils and cell-matrix adhesions, *Mol Biol Cell* 2002, 13:3546-3559
205. Kao WJ, Lee D, Schense JC, Hubbell JA: Fibronectin modulates macrophage adhesion and FBGC formation: the role of RGD, PHSRN, and PRRARV domains, *J Biomed Mater Res* 2001, 55:79-88
206. Chauhan AK, Moretti FA, Iaconcig A, Baralle FE, Muro AF: Impaired motor coordination in mice lacking the EDA exon of the fibronectin gene, *Behav Brain Res* 2005, 161:31-38
207. Hashimoto-Uoshima M, Yan YZ, Schneider G, Aukhil I: The alternatively spliced domains EIIIB and EIIA of human fibronectin affect cell adhesion and spreading, *J Cell Sci* 1997, 110 ( Pt 18):2271-2280
208. Liao YF, Gotwals PJ, Koteliensky VE, Sheppard D, Van De Water L: The EIIA segment of fibronectin is a ligand for integrins alpha 9beta 1 and alpha 4beta 1 providing a novel mechanism for regulating cell adhesion by alternative splicing, *J Biol Chem* 2002, 277:14467-14474
209. Manabe R, Ohe N, Maeda T, Fukuda T, Sekiguchi K: Modulation of cell-adhesive activity of fibronectin by the alternatively spliced EDA segment, *J Cell Biol* 1997, 139:295-307
210. Kyriakides TR, Leach KJ, Hoffman AS, Ratner BD, Bornstein P: Mice that lack the angiogenesis inhibitor, thrombospondin 2, mount an altered foreign body reaction characterized by increased vascularity, *Proc Natl Acad Sci U S A* 1999, 96:4449-4454
211. Kyriakides TR, Zhu YH, Smith LT, Bain SD, Yang Z, Lin MT, Danielson KG, Iozzo RV, LaMarca M, McKinney CE, Ginns EI, Bornstein P: Mice that lack thrombospondin 2 display connective tissue abnormalities that are associated with disordered collagen fibrillogenesis, an increased vascular density, and a bleeding diathesis, *J Cell Biol* 1998, 140:419-430
212. Keselowsky BG, Collard DM, Garcia AJ: Integrin binding specificity regulates biomaterial surface chemistry effects on cell differentiation, *Proc Natl Acad Sci U S A* 2005, 102:5953-5957

213. Alsberg E, Anderson KW, Albeiruti A, Rowley JA, Mooney DJ: Engineering growing tissues, *Proc Natl Acad Sci U S A* 2002, 99:12025-12030
214. Lutolf MP, Weber FE, Schmoekel HG, Schense JC, Kohler T, Muller R, Hubbell JA: Repair of bone defects using synthetic mimetics of collagenous extracellular matrices, *Nat Biotechnol* 2003, 21:513-518
215. Erli HJ, Ruger M, Ragoss C, Jahnen-Dechent W, Hollander DA, Paar O, von Walter M: The effect of surface modification of a porous TiO<sub>2</sub>/perlite composite on the ingrowth of bone tissue in vivo, *Biomaterials* 2006, 27:1270-1276
216. Crossley GH, Brinker JA, Reynolds D, Spencer W, Johnson WB, Hurd H, Tonder L, Zmijewski M: Steroid elution improves the stimulation threshold in an active-fixation atrial permanent pacing lead. A randomized, controlled study. Model 4068 Investigators, *Circulation* 1995, 92:2935-2939
217. Ma H, Wells M, Beebe TP, Chilkoti A: Surface-initiated atom transfer radical polymerization of oligo(ethylene glycol) for reduction in protein adsorption, *Adv Funct Mater* 2006, 16:640-648
218. Zhang F, Kang ET, Neoh KG, Wang P, Tan KL: Surface modification of stainless steel by grafting of poly(ethylene glycol) for reduction in protein adsorption, *Biomaterials* 2001, 22:1541-1548
219. Lee JH, Kopeckova P, Kopecek J, Andrade JD: Surface properties of copolymers of alkyl methacrylates with methoxy (polyethylene oxide) methacrylates and their application as protein-resistant coatings, *Biomaterials* 1990, 11:455-464
220. Wagner VE, Bryers JD: Monocyte/macrophage interactions with base and linear- and star-like PEG-poly(acrylic acid) co-polymers, *J Biomed Mater Res A* 2003, 66:62-78
221. Hyung Park J, Bae YH: Hydrogels based on poly(ethylene oxide) and poly(tetramethylene oxide) or poly(dimethyl siloxane). III. In vivo biocompatibility and biostability, *J Biomed Mater Res A* 2003, 64:309-319
222. Norton LW, Tegnell E, Toporek SS, Reichert WM: In vitro characterization of vascular endothelial growth factor and dexamethasone releasing hydrogels for implantable probe coatings, *Biomaterials* 2005, 26:3285-3297
223. Tan J, Brash JL: Nonfouling biomaterials based on polyethylene oxide-containing amphiphilic triblock copolymers as surface modifying additives: Adsorption of proteins from human plasma to copolymer/polyurethane blends, *J Biomed Mater Res A* 2008,

224. Ronneberger B, Kao WJ, Anderson JM, Kissel T: In vivo biocompatibility study of ABA triblock copolymers consisting of poly(L-lactic-co-glycolic acid) A blocks attached to central poly(oxyethylene) B blocks, *J Biomed Mater Res* 1996, 30:31-40
225. Pelton R: Temperature-sensitive aqueous microgels, *Adv Colloid Interface Sci* 2000, 85:1-33
226. van der Giessen WJ, Lincoff AM, Schwartz RS, van Beusekom HM, Serruys PW, Holmes DR, Jr., Ellis SG, Topol EJ: Marked inflammatory sequelae to implantation of biodegradable and nonbiodegradable polymers in porcine coronary arteries, *Circulation* 1996, 94:1690-1697
227. Suska F, Esposito M, Gretzer C, Kalltorp M, Tengvall P, Thomsen P: IL-1alpha, IL-1beta and TNF-alpha secretion during in vivo/ex vivo cellular interactions with titanium and copper, *Biomaterials* 2003, 24:461-468
228. Baldwin L, Hunt JA: The in vivo cytokine release profile following implantation, *Cytokine* 2008, 41:217-222
229. Rodriguez A, Meyerson H, Anderson JM: Quantitative in vivo cytokine analysis at synthetic biomaterial implant sites, *J Biomed Mater Res A* 2008,
230. Immunofluorescence and cell sorting. In: Coligan JE, Bierer B, Margulies DH, Shevach EM, Strober W, Coico R, editors. *Current Protocols in Immunology*. New York: John Wiley & Sons, 2007,
231. Gan DJ, Lyon LA: Synthesis and protein adsorption resistance of PEG-modified poly(N-isopropylacrylamide) core/shell microgels, *Macromolecules* 2002, 35:9634-9639
232. Jenney CR, Anderson JM: Adsorbed serum proteins responsible for surface dependent human macrophage behavior, *J Biomed Mater Res* 2000, 49:435-447
233. Unsworth LD, Sheardown H, Brash JL: Protein resistance of surfaces prepared by sorption of end-thiolated poly(ethylene glycol) to gold: effect of surface chain density, *Langmuir* 2005, 21:1036-1041
234. Feng W, Brash JL, Zhu S: Non-biofouling materials prepared by atom transfer radical polymerization grafting of 2-methacryloxyethyl phosphorylcholine: separate effects of graft density and chain length on protein repulsion, *Biomaterials* 2006, 27:847-855
235. Petrie TA, Raynor JE, Reyes CD, Burns KL, Collard DM, Garcia AJ: The effect of integrin-specific bioactive coatings on tissue healing and implant osseointegration, *Biomaterials* 2008, 29:2849-2857



236. Suggs LJ, Shive MS, Garcia CA, Anderson JM, Mikos AG: In vitro cytotoxicity and in vivo biocompatibility of poly(propylene fumarate-co-ethylene glycol) hydrogels, *J Biomed Mater Res* 1999, 46:22-32
237. Milner KR, Snyder AJ, Siedlecki CA: Sub-micron texturing for reducing platelet adhesion to polyurethane biomaterials, *J Biomed Mater Res A* 2006, 76:561-570
238. Bridges AW, Singh N, Burns KL, Babensee JE, Lyon LA, Garcia AJ: Reduced acute inflammatory responses to microgel conformal coatings., Submitted,
239. Capadona JR, Petrie TA, Fears K, Latour R, Collard DM, Garcia AJ: Surface-nucleated assembly of fibrillar extracellular matrices, *Adv Mater* 2005, 17:260-42608
240. US department of health and human services/Food and Drug Administration. Guideline on validation of the limulus amoebocyte lysate test as an end-product endotoxin test for human and animal parental drugs, biological products, and medical devices., 1987, 1-30
241. Khazen W, M'Bika J P, Tomkiewicz C, Benelli C, Chany C, Achour A, Forest C: Expression of macrophage-selective markers in human and rodent adipocytes, *FEBS Lett* 2005, 579:5631-5634
242. Kunz-Schughart LA, Weber A, Rehli M, Gottfried E, Brockhoff G, Krause SW, Andreesen R, Kreutz M: [The "classical" macrophage marker CD68 is strongly expressed in primary human fibroblasts], *Verh Dtsch Ges Pathol* 2003, 87:215-223
243. Moro T, Takatori Y, Ishihara K, Konno T, Takigawa Y, Matsushita T, Chung UI, Nakamura K, Kawaguchi H: Surface grafting of artificial joints with a biocompatible polymer for preventing periprosthetic osteolysis, *Nat Mater* 2004, 3:829-836
244. Lehle K, Lohn S, Reinerth GG, Schubert T, Preuner JG, Birnbaum DE: Cytological evaluation of the tissue-implant reaction associated with subcutaneous implantation of polymers coated with titaniumcarboxonitride in vivo, *Biomaterials* 2004, 25:5457-5466
245. Hasebe T, Shimada A, Suzuki T, Matsuoka Y, Saito T, Yohena S, Kamijo A, Shiraga N, Higuchi M, Kimura K, Yoshimura H, Kuribayashi S: Fluorinated diamond-like carbon as antithrombogenic coating for blood-contacting devices, *J Biomed Mater Res A* 2006, 76:86-94
246. Thevenot P, Hu W, Tang L: Surface chemistry influences implant biocompatibility, *Curr Top Med Chem* 2008, 8:270-280
247. Suska F, Emanuelsson L, Johansson A, Tengvall P, Thomsen P: Fibrous capsule formation around titanium and copper, *J Biomed Mater Res A* 2008, 85:888-896

248. Barbosa JN, Madureira P, Barbosa MA, Aguas AP: The influence of functional groups of self-assembled monolayers on fibrous capsule formation and cell recruitment, *J Biomed Mater Res A* 2006, 76:737-743
249. von Recum AF, van Kooten TG: The influence of micro-topography on cellular response and the implications for silicone implants, *J Biomater Sci Polym Ed* 1995, 7:181-198
250. Ward WK, Slobodzian EP, Tiekotter KL, Wood MD: The effect of microgeometry, implant thickness and polyurethane chemistry on the foreign body response to subcutaneous implants, *Biomaterials* 2002, 23:4185-4192
251. Koschwanez HE, Yap FY, Klitzman B, Reichert WM: In vitro and in vivo characterization of porous poly-L-lactic acid coatings for subcutaneously implanted glucose sensors, *J Biomed Mater Res A* 2008,
252. Dungal P, Long N, Yu B, Moussy Y, Moussy F: Study of the effects of tissue reactions on the function of implanted glucose sensors, *J Biomed Mater Res A* 2008, 85:699-706
253. Yagi M, Miyamoto T, Sawatani Y, Iwamoto K, Hosogane N, Fujita N, Morita K, Ninomiya K, Suzuki T, Miyamoto K, Oike Y, Takeya M, Toyama Y, Suda T: DC-STAMP is essential for cell-cell fusion in osteoclasts and foreign body giant cells, *J Exp Med* 2005, 202:345-351
254. Vignery A: Macrophage fusion: the making of osteoclasts and giant cells, *J Exp Med* 2005, 202:337-340
255. Jiang WW, Su SH, Eberhart RC, Tang L: Phagocyte responses to degradable polymers, *J Biomed Mater Res A* 2007, 82:492-497
256. Berglin M, Andersson M, Sellborn A, Elwing H: The effect of substrate molecular mobility on surface induced immune complement activation and blood plasma coagulation, *Biomaterials* 2004, 25:4581-4590
257. Sperling C, Schweiss RB, Streller U, Werner C: In vitro hemocompatibility of self-assembled monolayers displaying various functional groups, *Biomaterials* 2005, 26:6547-6557
258. Gasque P: Complement: a unique innate immune sensor for danger signals, *Mol Immunol* 2004, 41:1089-1098
259. Chavakis T, Athanasopoulos A, Rhee JS, Orlova V, Schmidt-Woll T, Bierhaus A, May AE, Celik I, Nawroth PP, Preissner KT: Angiostatin is a novel anti-inflammatory factor by inhibiting leukocyte recruitment, *Blood* 2005, 105:1036-1043

260. Tsai AT, Rice J, Scatena M, Liaw L, Ratner BD, Giachelli CM: The role of osteopontin in foreign body giant cell formation, *Biomaterials* 2005, 26:5835-5843
261. Lahiri J, Isaacs L, Tien J, Whitesides GM: A strategy for the generation of surfaces presenting ligands for studies of binding based on an active ester as a common reactive intermediate: a surface plasmon resonance study, *Anal Chem* 1999, 71:777-790
262. Wong JY, Kuhl TL: Dynamics of membrane adhesion: the role of polyethylene glycol spacers, ligand-receptor bond strength, and rupture pathway, *Langmuir* 2008, 24:1225-1231
263. Kuhlman W, Taniguchi I, Griffith LG, Mayes AM: Interplay between PEO tether length and ligand spacing governs cell spreading on RGD-modified PMMA-g-PEO comb copolymers, *Biomacromolecules* 2007, 8:3206-3213
264. Altroff H, Schlinkert R, van der Walle CF, Bernini A, Campbell ID, Werner JM, Mardon HJ: Interdomain tilt angle determines integrin-dependent function of the ninth and tenth FIII domains of human fibronectin, *J Biol Chem* 2004, 279:55995-56003
265. Hersel U, Dahmen C, Kessler H: RGD modified polymers: biomaterials for stimulated cell adhesion and beyond, *Biomaterials* 2003, 24:4385-4415
266. Krammer A, Craig D, Thomas WE, Schulten K, Vogel V: A structural model for force regulated integrin binding to fibronectin's RGD-synergy site, *Matrix Biol* 2002, 21:139-147
267. Langer R, Vacanti JP: Tissue engineering, *Science* 1993, 260:920-926
268. Lavik E, Langer R: Tissue engineering: current state and perspectives, *Appl Microbiol Biotechnol* 2004, 65:1-8
269. Lu ZR, Kopeckova P, Wu Z, Kopecek J: Functionalized semitelechelic poly[N-(2-hydroxypropyl)methacrylamide] for protein modification, *Bioconjug Chem* 1998, 9:793-804
270. Murata H, Chang BJ, Prucker O, Dahm M, Ruhe J: Polymeric coatings for biomedical devices, *Surface Science* 2004, 570:111-118
271. Kulik EA, Kato K, Ivanchenko MI, Ikada Y: Trypsin immobilization on to polymer surface through grafted layer and its reaction with inhibitors, *Biomaterials* 1993, 14:763-769
272. Lavik EB, Klassen H, Warfvinge K, Langer R, Young MJ: Fabrication of degradable polymer scaffolds to direct the integration and differentiation of retinal progenitors, *Biomaterials* 2005, 26:3187-3196

273. Ito Y, Zheng J, Imanishi Y: Enhancement of cell growth on a porous membrane co-immobilized with cell-growth and cell adhesion factors, *Biomaterials* 1997, 18:197-202
274. Kim P, Kim DH, Kim B, Choi SK, Lee SH, Khademhosseini A, Langer R, Suh KY: Fabrication of nanostructures of polyethylene glycol for applications to protein adsorption and cell adhesion, *Nanotechnology* 2005, 16:2420-2426
275. Jones CD, Lyon LA: Synthesis and characterization of multiresponsive core-shell microgels, *Macromolecules* 2000, 33:8301-8306
276. Saunders BR, Vincent B: Microgel particles as model colloids: theory, properties, and applications, *Adv Colloid Interface Sci* 1999, 80:1-25
277. Homsy CA, McDonald KE, Akers WW, Short C, Freeman BS: Surgical suture-canine tissue interaction for six common suture types, *J Biomed Mater Res* 1968, 2:215-230
278. Soares BM, Guidoin RG, Marois Y, Martin L, King MW, Laroche G, Zhang Z, Charara J, Girard JF: In vivo characterization of a fluoropassivated gelatin-impregnated polyester mesh for hernia repair, *J Biomed Mater Res* 1996, 32:293-305
279. Vinard E, Eloy R, Descotes J, Brudon JR, Guidicelli H, Magne JL, Patra P, Berruet R, Huc A, Chauchard J: Stability of performances of vascular prostheses retrospective study of 22 cases of human implanted prostheses, *J Biomed Mater Res* 1988, 22:633-648
280. von Recum AF: Applications and failure modes of percutaneous devices: a review, *J Biomed Mater Res* 1984, 18:323-336
281. Sano S, Kato K, Ikada Y: Introduction of functional groups onto the surface of polyethylene for protein immobilization, *Biomaterials* 1993, 14:817-822
282. Tabata Y, Lonikar SV, Horii F, Ikada Y: Immobilization of collagen onto polymer surfaces having hydroxyl-groups, *Biomaterials* 1986, 7:234-238
283. Piglowski J, Gancarz I, Staniszevska-Kus J, Paluch D, Szymonowicz M, Konieczny A: Influence of plasma modification on biological properties of poly(ethylene terephthalate), *Biomaterials* 1994, 15:909-916
284. Gupta B, Plummer C, Bisson I, Frey P, Hilborn J: Plasma-induced graft polymerization of acrylic acid onto poly(ethylene terephthalate) films: characterization and human smooth muscle cell growth on grafted films, *Biomaterials* 2002, 23:863-871

285. Lee SD, Hsiue GH, Chang PC, Kao CY: Plasma-induced grafted polymerization of acrylic acid and subsequent grafting of collagen onto polymer film as biomaterials, *Biomaterials* 1996, 17:1599-1608
286. Gupta B, Hilborn JG, Bisson I, Frey P: Plasma-induced graft polymerization of acrylic acid onto poly(ethylene terephthalate) films, *J App Polym Sci* 2001, 81:2993-3001
287. Suzuki M, Kishida A, Iwata H, Ikada Y: Graft-copolymerization of acrylamide onto a polyethylene surface pretreated with a glow-discharge, *Macromolecules* 1986, 19:1804-1808
288. Uyama Y, Kato K, Ikada Y: Surface modification of polymers by grafting, *Grafting/Characterization Techniques/Kinetic Modeling* 1998, 137:1-39
289. Dorman G, Prestwich GD: Benzophenone photophores in biochemistry, *Biochemistry* 1994, 33:5661-5673
290. Prucker O, Naumann CA, Ruhe J, Knoll W, Frank CW: Photochemical attachment of polymer films to solid surfaces via monolayers of benzophenone derivatives, *J Am Chem Soc* 1999, 121:8766-8770
291. Hermanson GT: *Bioconjugate Techniques* 1996, Academic Press: San Diego:
292. Dalsin JL, Hu BH, Lee BP, Messersmith PB: Mussel adhesive protein mimetic polymers for the preparation of nonfouling surfaces, *J Am Chem Soc* 2003, 125:4253-4258
293. Lopez GP, Ratner BD, Tidwell CD, Haycox CL, Rapoza RJ, Horbett TA: Glow discharge plasma deposition of tetraethylene glycol dimethyl ether for fouling-resistant biomaterial surfaces, *J Biomed Mater Res* 1992, 26:415-439
294. Tziampazis E, Kohn J, Moghe PV: PEG-variant biomaterials as selectively adhesive protein templates: model surfaces for controlled cell adhesion and migration, *Biomaterials* 2000, 21:511-520